Small Molecule Hsp90 Modulator and Neuregulin-induced Peripheral Demyelination

By

Chengyuan (Chanel) Li

Submitted to the graduate degree program in
Pharmacology and Toxicology and the Graduate Faculty of the
University of Kansas in partial fulfillment of the requirements for
the degree of Doctor of Philosophy.

_____
Rick T. Dobrowsky, Ph.D., Chairperson

_____
Nancy A. Muma, Ph.D.

_____
Alex R. Moise, Ph.D.

_____
Erik A. Lundquist, Ph.D.

_____
Kristi L. Neufeld, Ph.D.

Date Defended: June 27th 2012

The Dissertation Committee for Chengyuan Li
certifies that this is the approved version of the following
dissertation:

Small Molecule Hsp90 Modulator and Neuregulin-induced Peripheral Demyelination

By

Chengyuan (Chanel) Li

_____

Rick T. Dobrowsky, Ph.D., Chairperson

Date Approved: June 27th 2012

Table of Contents

Acknowledgements

This work was supported by the Juvenile Diabetes Research Foundation [1-2008-280, 17-2010-760]; and The National Institutes of Health National Institute of Neurologic Disorders and Stroke [NS054847, NS075311] to RTD.

I would like to start out by saying that I am lucky. I was lucky to be given the chance to receive a graduate education in the Department of Pharmacology and Toxicology at the University of Kansas. For the past five years, I have had the best mentor I could ever find, Dr. Rick T.Dobrowsky, who is also one of the most intelligent and fair-minded scientists I know. I am deeply grateful and forever indebted to him for more than just the knowledge he imparted, but also the inspiration, belief, and numerous opportunities he offered in order for me to push myself and discover my very best potential. I wouldn't have achieved half of the work in this dissertation without his support. He allowed me to pursue questions and projects with freedom in areas where my interests led me, and from time to time "poked" me with sharp sarcasms, "intimidations" and jokes, which have all been great motivation for me to get the work done. The knowledge, insights and abilities you have helped develop in me during my graduate training will for sure resonate profoundly throughout the rest of my career and life.

My committee members have been a great source of help for my past curriculum and experimental endeavors. I am thankful that Dr. Erik Lundquist

gave his valuable time and expertise for the past journal club I presided in PTX. Dr. Kristi Neufeld provided helpful suggestions and encouragement for finalizing my study after the last committee meeting. Dr. Alex Moise has always been a great source of spiritual support through his "in-hallway" advice, support and encouragements. Special thanks also go to Dr. Nancy Muma, who has been extremely generous and helpful by offering valuable scientific advice and insight for my study on estrogen and the qualifying exam. I am particularly indebted to the Muma lab for allowing me to "steal" reagents and materials without chasing me down. Thank you, I am lucky to have had all of you in my committee.

My immunofluorescence analysis would never have been finished without the patient instruction and assistance from Dr. David Moore and Heather Shinogle from the Microscopy lab. Dr. Brian Blagg had generously provided the compound, KU-32, which constituted an essential part of my study and dissertation. I also want to thank Dr. Qian Li, who I sincerely admire as an excellent female scientist and leader in her field. She has been so instrumental to me in every way one could ask for from a mentor, a teacher, and a friend.

One of the most essential pieces of equipment you must have to survive all the hardships in graduate school (experiments not working, car breaking down, getting sick, being yelled at, etc.) is friendship. I am lucky to have a gang of them: all the current and previous Dobrowsky lab members and PTX folks! Thanks to

Thila who helped so much with the DRG-prep. Thanks to Melanie, Mac, Liang, Pan, Vicky, Michael and Kevin for being there to share my problems and listen to my complaints as well as offer priceless help whenever I needed it. Heather Menchen has been a great friend and her encouragement and emotional support has helped me to stay sane in graduate school. I would also never forget the countless help from Neil Barnes during the time of my settling and adjustment to the life in an entirely new country. It is impossible to mention everyone to whom I owe so many thanks, but almost everyone I encountered as a graduate student in KU have collectively made the past five years such a great memory!

Last but never the least, I am lucky to have the most wonderful and loving family in the world. My parents, Haiwu Li and Yongcui Shen, have always believed in my ability, given me strength to pursue my dreams and so selflessly supported me with every possible resource they can find. My aunt, Sally Sobek, has provided tremendous financial and spiritual support throughout my course of graduate education. Finally, I feel like being the luckiest person because I have Daniel Press in my life, from whom I can always find love and support. Thank you for your unconditional faith in me, both academically and personally.

List of Tables and Figures

List of Abbreviations

ADP	Adenosine Diphosphate
AIDP	Acute Inflammatory Demyelinating Polyneuropathy
ANOVA	Analysis of Variances
AP-1	Activator Protein 1
Akt	Protein Kinase B
ARIA	Acetylcholine Receptor-inducing Activity
ATP	Adenosine Triphosphate
BDNF	Brain-derived Neurotrophic Factor
BB/Wor	Biobreeding/Worcester
cAMP	Cyclic AMP
Cav-1	Caveolin-1
CAM	Cell Adhesion Molecule
Caspr	Contactin Associated Protein
CHIP	carboxyl terminus of Hsp70-interacting protein
CMT	Charcot-Marie-Tooth disease type
CNS	Central Nervous System
IP	Immunoprecipitation
CRD	Cystein Rick Domain
CsCl	Caesium chloride
DAPI	4',6-diamidino-2-phenylindole
DF	Degree of Freedom
DMED	Dulbecco's modified Eagle's medium
DMSO	Dimethyl sulfoxide
DNA	Deoxyribonucleic Acid
DPN	Diabetic Peripheral Neuropathy
DN-ErbB	Dominant Negative ErbB Receptor
DRG	Dorsal Root Ganglia
EGF	Epidermal Growth Factor
ER	Endoplasmic Reticulum
ER-α/β	Estrogen Receptor-α/β
E2	β-estradiol
FDA	Food and Drug Administration
GBS	Guillain-Barré syndrome
GGF	Glial Growth Factor
GPCR	G-protein-coupled Receptor
GPI	Glycosyl Phosphatidylinositol

GPR30	G-protein-coupled Receptor 30
GRP75/mMortalin/mtHSP70	Mitochondrial Glucose-regulated Protein75
GRP78/BiP	Glucose-regulated Protein 78
HOP	HSP-organizing Protein
HRP	Horseradish Peroxidase
HSC70/HSP73	Heat Shock Cognate Protein73
HSF-1	Heat Shock Factor-1
HSP	Heat Shock Protein
HSR	Heat Shock Response
Ig	Immunoglobulin
JNK	C-jun N-terminal Kinase
K_v	Voltage-gated Potassium Channel
KO/-/-	Knockout
LM1	$IV^3NeuAc\text{-}nLcOse_4Cer$
MAPK	Mitogen-activated Protein Kinases
MBP/P1	Myelin Basic Protein
Mek/Erk	Mitogen-activated Protein Kinase/Extracellular Signal-Regulated Kinase Kinase
MS	Multiple Sclerosis
Nav	Voltage-gated Sodium Channel
NCV	Nerve Conduction Velocity
NF-κB	Nuclear Factor-κB
NGF	Nerve Growth Factor
NH	Non-Heatshock
NIH	National Institute of Health
NRG1	Neuregulin-1
NT-3	Neurotrophin-3
OLG	Oligodendrocyte
Parp-1	Poly [ADP-ribose] polymerase 1
PBS	Phosphate-buffered Saline
PCR	Polymerase Chain Reaction
PKC	Protein Kinase C
P-TEFb	Positive Transcription Elongation Factor b
PGP-9.5	Protein Gene Product 9.5
PI3K	Phosphatidylinositol 3-Kinase
PMP-22	Peripheral Protein 22
PNS	Peripheral Nervous System
polyQ	Polyglutamine
MPZ/P0	Myelin Protein Zero

NF155	Neurofascin155
RNA	Ribonucleic Acid
SC	Schwann Cell
siRNA/RNAi	silencing RNA
STZ	Streptozotocin
SUMO	Small Ubiquitin-like Modifier
TEM	Transmission Electron Microscopy
UDP	Uridine DiPhosphate
WT	Wildtype

Abstract

Modulating molecular chaperones is emerging as an attractive approach to treat neurodegenerative diseases associated with protein aggregation, diabetic peripheral neuropathy (DPN) and possibly, demyelinating neuropathies. KU-32 is a small molecule inhibitor of heat shock protein 90 (Hsp90) and reverses sensory deficits associated with myelinated fiber dysfunction in DPN. Additionally, KU-32 prevented the loss of myelinated internodes induced by treating myelinated Schwann cell-dorsal root ganglia sensory neuron co-cultures with neuregulin-1 Type 1 (NRG1). Since KU-32 decreased NRG1-induced demyelination in an Hsp70-dependent manner, the goal of the current study was to clarify how Hsp70 may be mechanistically linked to preventing demyelination. The activation of p42/p44 MAPK and induction of the transcription factor c-jun function as negative regulators of myelination. NRG1 activated MAPK, induced c-jun expression and promoted a loss of myelin segments in DRG explants isolated from both wild type and Hsp70 KO mice. Although KU-32 did not block the activation of MAPK, it blocked c-jun induction and protected against a loss of myelinated segments in wildtype (WT) mice. KU-32 did not prevent the NRG1-dependent induction of c-jun and loss of myelin segments in explants from Hsp70 KO mice. Over-expression of Hsp70 in myelinated DRG explants prepared from WT or Hsp70 KO mice was sufficient to block the induction of c-jun and the loss of myelin segments induced by NRG1. Lastly, inhibiting the proteasome prevented KU-32 from decreasing c-jun levels. Collectively, these data support that Hsp70 induction is sufficient to prevent NRG1-induced demyelination by enhancing the proteasomal degradation of c-jun.

Chapter 1: Myelin, Neuregulin-induced Demyelination and Diabetic Peripheral Neuropathy

1.1 The History of Myelin Discovery

The emergence of microscopic and dissection techniques in the eighteenth' century accelerated the development of our knowledge of vertebrate anatomy, including the nervous system. The earliest documentation of nerve myelin can be traced back to the year 1717, when Dutch scientist Leeuwenhoek described a microscopic observation of "nervules surrounded by fatty parts" (Rosenbluth, 1999). More than a century later, Ehrenberg, Remak and Schwann further identified the medullary appearance of myelin, the relative transparency of unmyelinated fibers versus myelinated fibers, and Schwann cells (SCs), respectively (Ehrenberg, 1837; Rosenbluth, 1999). Using hematoxylin stain, Dieters was able to distinguish neuroglia as another component of nervous tissue from neurons, although at this stage these interstitial plexi were predominantly regarded as connective substance (Pasik and Pasik, 2004). Based on the white medulla appearance and early misinterpretation of myelin as an inner deposition of axon, Rudolf Virchow coined the term "myeline" from "*myelos*", the Greek term of marrow (Virchow, 1854). By then myelin was still regarded as a continuous sheath resulting from syncytial network until in 1871 when Louis Antoine Ranvier observed gaps, or "nodes" in the myelin that periodically interrupted the sheath. Soon after that the "Schmidt–Lantermann incisures" were discovered, which mark the spiraling slits traversing the thickness of myelin sheath (Rosenbluth, 1999). After Italian physician and physicist Galvani first described the electroconductive and insulating properties of nerves in 1791 (Clarke and O'Malley, 1968), the role of myelin and nodes of Ranvier in enabling saltatory impulse conduction was first demonstrated by Tasaki in 1939. However, whether myelin derived from axons or glial cells remained a debate until more than two decades later. With the advent of electron microscopy, Betty Ben Geren demonstrated

unequivocally in her study of developing chick peripheral nerve that myelin is a spiral wrapping of SC plasma membrane around the axon (Geren, 1954). Her finding was then confirmed by two independent investigators who showed that similar to SCs in the peripheral nervous system (PNS), the central nervous system (CNS) glia oligodendrocytes synthesize the myelin in the optic nerves (Maturana, 1960; Peters, 1960). Functional and morphological differences between CNS and PNS glia were soon revealed by later studies which suggested that oligodendrocytes myelinate multiple axons simultaneously and rarely form Schmidt-Lantermann incisures, whereas SCs commonly do and give rise to only one myelin segment of an axon (Bunge et al., 1962; Maturana, 1960). Following these discoveries, improvement in fixation techniques and ultrastructural analysis further boosted the characterization of other fine features of myelin, including its domain organization and molecular composition.

1.2 Structural and Functional Significance of Peripheral Nerve Myelination

The above landmark studies led to the unexpected realization that glial cells and myelin are not just sticky accessories of neurons, but instead form an intimate cellular interaction and are perhaps the most spectacular step in the evolution of the vertebrate nervous system architecture. At a topological level, myelin formation initiates with the association and laying of the axon trunk in an invagination of glial cells, namely, SCs in the PNS and interfasicular oligodendrocytes in the CNS. These cells then progressively and repeatedly wrap long axonal segments with a lamellar stack of their extended plasma membrane, which in this case has acquired the name “mesaxon”. Depending on the diameter of the axon being myelinated, the number of myelin wrappings can range from 10-160 (Arbuthnott et al., 1980). Such multilayered sheath of glial membrane is tightly compacted and sealed, defining the structure of myelin internodes that are gapped at regular intervals along an axon by the nodes of Ranvier, where the

axonal membrane is “naked” and comes into contact with extracellular milieu. From an electrophysiological perspective, vertebrate myelin is evolved to perform two tasks: to insulate the axon and to enable saltatory nerve impulse conduction. The latter allows the “jumping” of action potentials from node to node such that the speed of impulse propagation is dramatically increased without the need to expand axon diameter and increase the energy required for depolarizing an entire length of axon membrane, as is necessary for impulse propagation in unmyelinated fibers. This space and energy saving had a tremendous impact on the evolution of larger body size, which in turn allowed the development of complex motion coordination and cognitive abilities of gnathostomata vertebrates (Nave, 2010a). To better appreciate this, in order to transmit an electrical potential for a given length and speed, an unmyelinated squid axon would take 15,000 times more volume and 5,000 times more energy than a myelinated frog axon. Such an extreme example is also exemplified in humans: an unmyelinated axon has a conductivity as low as 0.1 m/s whereas the nerve conduction speed of the thickest myelinated axon can reach as fast as 120 m/s (Trapp and Kidd, 2004).

Most efferent motor nerves in the periphery and projection tracts in brain white matter are myelinated, while somatosensory and autonomic nerves usually contain a mixture of myelinated and unmyelinated axons. Typically, voluntary motor fibers are myelinated; Aα, Aβ sensory fibers that associate with proprioceptors, mechanoreceptors and thermoreceptors as well as preganglionic autonomic fibers. In most cases, sciatic nerves in the PNS and optic nerves in the CNS are studied to characterize the ultrastructure of myelin (Quarles et al., 2006). On the other hand, many fibers are also unmyelinated and include nociceptive C fibers, postganglionic autonomic nerves that are responsible for visceral sensation and involuntary functions, and axons extended from granule cells in hippocampus and cerebellum are unmyelinated.

Table 1.2 List of Mammalian CNS and PNS Neuron Fiber Types

CNS					
Distribution		Neuron Type			Myelin
Retina/Optic Nerve		Ganglion			Yes
Cortex		L5 Pyramidal Cell (Principal Axon)			Yes
Cerebellum		Purkinje Cell (Principal Axon)			Yes
Hippocampus		CA1/CA3 Pyramidal Neurons (Alveus/Fimbria)			Yes
Hippocampus		Dentate Gyrus/Granule Cell (Mossy Fiber)			No
Hippocampus		CA3 Pyramidal Cell (Schaffer Collaterals)			No
Cerebellum		Granule Cell (Parallel Fiber)			No
PNS					
Type/ Erlanger-Gasser Classification	Neuron Type/Distribution	Diameter	Function/Associated Receptor/Fiber	Conduction Velocity	Myelin
α/Aα	Motor/Sciatic Nerve	13-22 μm	Extrafusal Muscle Fibers	70-120 m/s	Yes
γ/Aγ	Motor/Sciatic Nerve	4-8 μm	Intrafusal Muscle Fibers	4-24 m/s	Yes
Ia/Aα	Sensory/Dorsal Root Ganglion	12-20 μm	Muscle Spindle Primary Receptors	70-120 m/s	Yes
Ib/Aα	Sensory/Dorsal Root Ganglion	11-19 μm	Golgi Tendon Organ	66-114 m/s	Yes
II/Aβ	Sensory/Dorsal Root Ganglion	5-6 μm	Muscle Spindle Secondary Receptors; All Cutaneous Mechanoreceptors	33-75 m/s	Yes
III/Aδ	Sensory/Dorsal Root Ganglion	1-5 μm	Crude touch; Pressure; Nociceptors of Neospinothalamic Tract; Cold Thermoreceptors	5-30 m/s	Thin
IV/C	Sensory/Dorsal Root Ganglion	0.4-2 μm	Nociceptors of Paleospinothalamic Tract; Warmth Thermoreceptors	0.5-2 m/s	No
B	Preganglionic Fibers	1-5 μm	-	3-15 m/s	Thin
C	Postganglionic Fibers	0.2-1.5 μm	-	0.5-2.0 m/s	No

Adapted from (Debanne et al., 2011; Narhi, 2010)

In the PNS, these unmyelinated axons are loosely engulfed by a SC with multiple other small-caliber axons in a Remak bundle. Most nerve fascicles in the periphery contain a mixture of myelinated and unmyelinated axons and may bifurcate upon reaching the spinal cord. For example, in dorsal sensory roots, unmyelinated fibers enter through the lateral division while

myelinated fibers enter through the medial division (Crosby et al., 1962). Table 1.2 summarizes the classifications and properties of mammalian myelinated and unmyelinated fibers. Since CNS myelination is beyond the scope of the present study, this dissertation will focus on summarizing our current understanding of myelinated nerves in the PNS. The term "myelin" therefore will only refer to peripheral myelin unless otherwise specified.

1.2.1 Molecular Structure and Composition of Myelinated Fibers

Function is built on structure. The evolution of fast saltatory conduction developed from an appropriate structural support. Since the major task of myelination is to maximize the speed of conduction velocity, a polarized organization would be preferred over a single uniform compartment. Indeed, myelinated fibers display a remarkable longitudinal polarity that is elaborated by a series of structurally distinct domains: the internodes, the paranodal junctions, the juxtaparanodes and the nodes of Ranvier (Fig.1.2.1). In addition to cellular interaction and organization, these domains further differ in their molecular composition and repertoire of organelles (Salzer, 2003; Salzer et al., 2008).

1.2.1a Internodes

The internodal region is where the lamellar layers of myelin are deposited and comprise the largest domain along a myelinated axon. The length of the axon covered by an internode is closely proportional to axon diameter, ranging from 150 μm to 1.5 mm (Geuna et al., 2009; Trapp and Kidd, 2004). As a result of the tight wrapping of the myelin membrane , the intra- and extracellular space of the SC mesaxon becomes so condensed that it appears as a periodic alternating between electron dense lines corresponding to the two fused cytoplasmic surfaces, and the light or intraperiod lines formed by the close apposition of external surfaces. The latter is

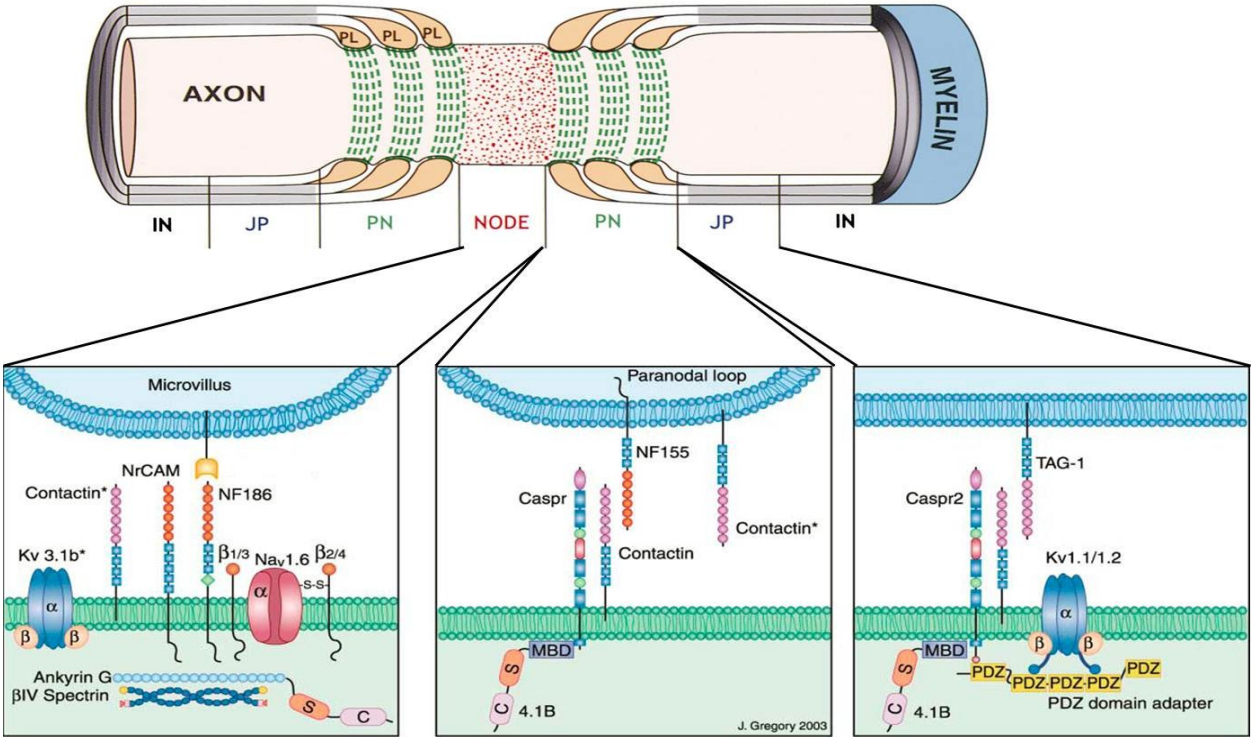

Figure 1.2.1 Schematic representation of the domain structure and composition of a myelinated PNS fiber. Myelinating SCs are in blue. The SC microvillar processes contacting nodal region are not shown. The node of Ranvier (in red dots) is flanked on either side by paranodal (PN) region (in green dashed lines), which are immediately apposed by juxtaparanodes (JP) and internodes (IN). Key components mediating axoglial interaction in each domain are illustrated below. *(adpated from Bhat et al., 2001; Salzer, 2003)*

not fused and displays double lines with a separation of 2.5 nm at higher magnification of the electron micrograph (Figure 1.2.1aC). For this reason the intracellular fusion becomes quite stable whereas the outer faces remain labile (Geuna et al., 2009). Together, these overlaying sheets result in a repeat distance of 12 – 14 nm and makes up the compact myelin (Figure 1.2.1a) (Saher and Simons, 2010; Trapp and Kidd, 2004).

Although myelin originates from the SC plasma membrane, its dehydrated mass contains a significantly higher amount of lipids (approximately 70-85% lipids and 15-30% proteins) compared to most cellular membranes, which are protein-rich. Nature makes the best selection. Lipids are electrically inert and therefore perfect biomolecules to build an insulating barrier of

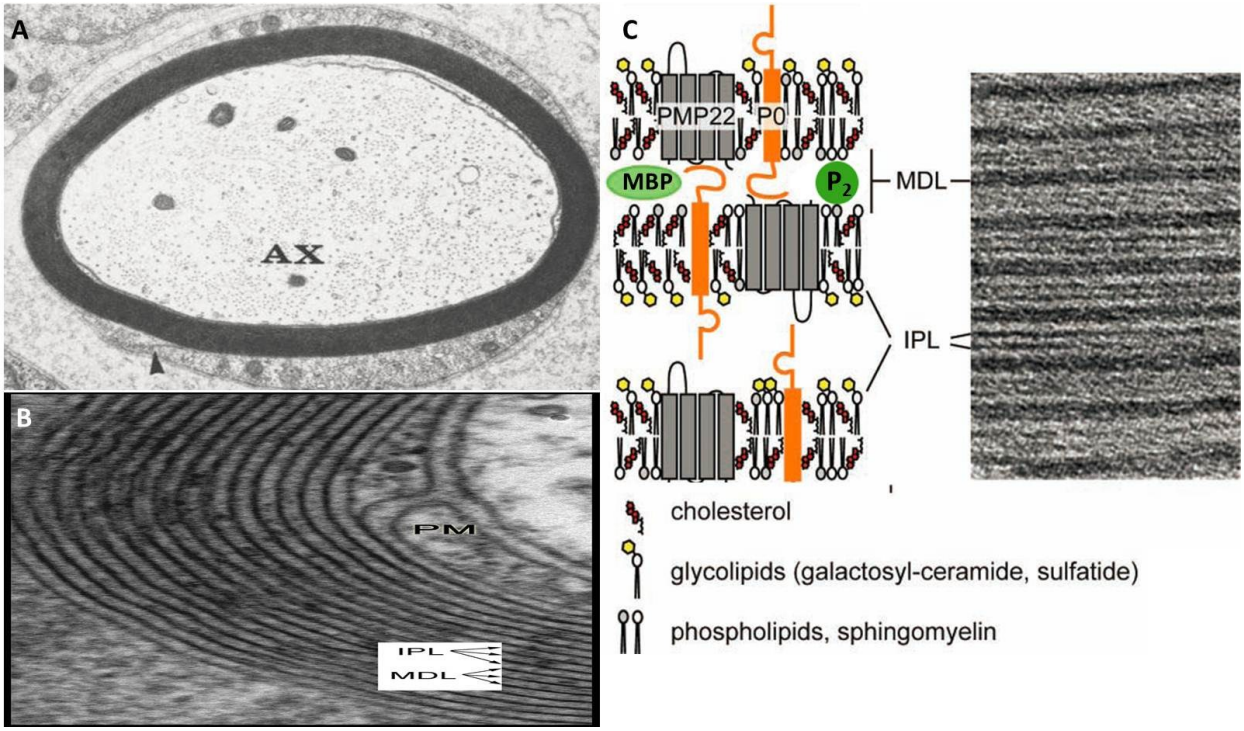

Figure1.2.1a Electromicrographic and schematic depiction of compact myelin. A. Electron micrograph of the cross section of a single peripheral myelinated fiber. AX: axon B. Higher magnification of the compact myelin showing major dense line (MDL) and intraperiod line (IPL). C. Molecular organization of the opposing SC plasma membranes forming the MDL and IPL. The structure and position of major myelin lipids and proteins are schematically demonstrated and corresponded to the MDL and IPL under electron micrograph. *modified from (Garcia-Fresco, 2006; Quarles et al., 2006; Saher et al., 2011)*

myelin. The lipid sheath of myelin is a result of quantitative enrichment of certain amphipathic classes of lipids, including glycolipids, phospholipids and cholesterol (Figure 1.2.1aC) that are commonly found in biological membranes, rather than an invention of myelin-specific lipids (Quarles et al., 2006). More than a quarter of the total lipids are composed by cholesterol, whose synthesis is rate-limiting and essential during myelin assembly (Saher and Simons, 2010). This is suggested by the observation that mice with genetic inactivation of cholesterol biosynthesis or regulation in SCs showed severely delayed and hypo-myelination, correlating with peripheral neuropathic symptoms including tremor and abnormal gait (Saher et al., 2009; Verheijen et al., 2009). Such low tolerance for cholesterol deficiency has been attributed to its crucial function in

stabilizing myelin structure as well as myelin protein trafficking and partitioning into lipid raft microdomains (Saher and Simons, 2010). As an integral component within the compact myelin, cholesterol is primarily enriched in the extracellular leaflet of the membrane. Its hydroxyl head binds the polarized group of glycosphingolipids and phospholipids while its planar steroid backbone is embedded in the membrane lipid bilayer, thereby sealing up the two adjacent lamellar stacks. Also preferentially localized at the extracellular membrane face are galactosylceramide (cerebroside) and its sulfated derivative sulfatide, the major glycosphingolipids that likely contribute to the insulating properties of myelin. Although these galactolipids are of similar abundance to cholesterol, they do not appear to be necessary for myelination and maintenance since UDP-galactose/ceramide galactosyltransferase-null mice that synthesize no galactosylceramide and sulfatides form relatively normal myelin with subtle morphological and conduction abnormalities (Coetzee et al., 1996; Honke et al., 2002; Marcus and Popko, 2002). The most prominent phospholipids in myelin are plasmenyl phosphatidylethanolamine and unlike galactolipids and cholesterol, is expressed mainly at the cytoplasmic side of the membrane. In addition to these common lipids, a minor amount of LM1 ganglioside (sialosyl-lactoneotetraosylceramide) is a characteristic component of peripheral motor and sensory myelin in certain species including humans (Ogawa-Goto et al., 1992). Overall, cholesterol, phospholipids and galactolipids constitute a molar ratio in between 4:3:2 and 4:4:2 and impart a comparatively low intrinsic density to myelin that separates it from other membrane fractions or connective tissues during gradient subfractionation (Quarles et al., 2006).

While there is no myelin-specific lipid, there are proteins that are uniquely expressed or abundant in peripheral nerve myelin. These proteins include myelin protein zero (P0), myelin basic protein (MBP/P_1 protein), peripheral myelin protein-22 (PMP-22) and P_2 protein. In accord

with their biochemical properties and amino acid sequence, P0 and PMP-22 are integral membrane proteins whereas MBP and P_2 are extrinsic membrane proteins (Figure 1.2.1aC). Of these, the transmembrane glycoprotein P0 with an apparent molecular size of 30 kDa accounts for up to 70% of total myelin proteins. P0 associates with cholesterol and connects opposing plasma membranes within the intraperiod lines through homophilic binding of its extracellular domains. Loss of this association results in abnormal spacing of the extracellular leaflets in the compact myelin of P0-null sciatic nerves (Giese et al., 1992). The adhesive property of P0 is further verified in nonadherent cells *in vitro* where cell adhesion was apparently acquired after P0 transfection (D'Urso et al., 1990; Filbin et al., 1990). On the other side, the large cytoplasmic domain of P0 has also been suggested to play a role in maintaining the major dense line. However, this function may not be crucial since no apparent abnormality in intracellular compaction was seen in above mentioned P0-null mice. Unlike P0, MBP locates exclusively at the cytoplasmic face of the major dense line and thus is not detectable by surface probes. It is composed of a heterogeneous group of membrane-bound proteins resulting from alternative splicing of seven exons (Quarles et al., 2006). The most abundant MBP in human or rodent myelin has a molecular weight of about 18.5 kDa. MBP is rich in basic amino acids (and hence the name) and is believed to mediate fusion of the major dense line of compact myelin through interacting with the negatively charged lipid residues, particularly phosphatidylserine. Although this is true in CNS myelin of MBP-deficient shiverer mice, the major dense line in PNS myelin appears unaffected (Privat et al., 1979). Similarly, PMP-22 deficiency in mice has minimal effect on the ultrastructure of PNS myelin (Adlkofer et al., 1995). The fact that significant amount of myelin membrane is produced even in the absence of P0, MBP and PMP-22 indicates that formation of the spiraling multilamellar structure does not depend on these proteins.

Nevertheless, expression of these myelin proteins is required for myelin compaction and alteration in their stoichiometry does have a chronic consequence on the structure and function of myelinated nerves. For example, P0-null mice develop a profound hypomyelination, with non-compacted myelin sheaths and neuropathic symptoms including abnormal motor control (Quarles et al., 2006). Reduced expression of PMP-22 in humans is responsible for the dysmyelination and focal hypermyelination associated with hereditary neuropathy, whereas increased alleles of PMP-22 are a causative factor for Charcot-Marie-Tooth disease type 1A (CMT1A) (Wrabetz et al., 2004b). Of note, mutations in the myelin protein genes may lead to more severe phenotypes than simple loss of gene dosage. Point mutations in the PMP-22 gene that alter its transmembrane domain are causative for the hypomyelination, abnormal SC proliferation and limb paralysis in trembler mice, an animal model of human inherited neuropathies (Quarles et al., 2006). Mutations in MPZ, a gene that encodes for P0, are also associated with Charcot-Marie-Tooth disease (CMT)1B, CMT2, Dejerine-Sottas syndrome and congenital hypomyelination (Shy et al., 2004). P_2 has a structural and functional role that is similar to MBP but is much less abundant in peripheral myelin (5% in human and less than 1% in rodents). Whether or not P_2 is critical for PNS myelination is not known since no P_2-mutants have been generated or identified in rodents or humans (Trapp and Kidd, 2004). Besides the above well-characterized myelin-specific proteins, a recent proteomic analysis identified more than 500 previously unrecognized proteins in purified sciatic nerve myelin, a number that is almost 50 fold of what was detected using conventional gel electrophoretic separation. Surprisingly, P0 and MBP, although still of predominant abundance, constituted only 21% and 8% of total myelin proteins according to mass spectrometric quantification, indicating a previous misestimate of their relative abundance due to technical limitations (Patzig et al., 2011). This

study provides evidence that the molecular composition of myelin is much more complex and facilitates the identification of novel protein candidates for myelin-related disease.

Since the primary function of the compact myelin is to stably insulate the axon, most of its molecules are predicted to have a slow turnover rate. There might be, however, a dynamic metabolic exchange in the non-compact SC cytoplasmic compartments, such as the Schmidt–Lantermann incisures. These funnel-shaped clefts or incisures are loose cytoplasmic openings that spiral through the compact myelin and radially channel through the inner and outer glia soma. It is also important to note that the inner collar (innermost layer) of myelin sheath is not in an immediate contact with the axon, but instead is separated from the axolemma by a 12-14 nm periaxonal space, which is essentially an enclosed extracellular environment (Trapp and Kidd, 2004). The functional significance of periaxonal space is not clear but could involve providing metabolic support for the axon through registering with Schmidt–Lantermann incisures (Nave, 2010b). This is made possible by the gap-junctions contained at the membranes of incisures, which have been documented to mediate radial diffusion of small molecules. Although gap junctions at Schmidt–Lantermann incisures have not been definitively confirmed by ultrastructural study, they do express some of the gap junction proteins including connexin-32 and connexin-29 (Balice-Gordon et al., 1998; Li et al., 2002). Furthermore, pharmacological blockage of gap junctions prevented the radial diffusion across incisures, confirming the presence of functional gap junctions at these sites (Balice-Gordon et al., 1998). Mutations in connexin-32 have been linked to the inherited PNS dysmyelinating neuropathy associated with X-linked CMT disease. Whether the disease pathology involves altered function of Schmidt–Lantermann incisures is unclear. In addition, microtubules, small vesicles and mitochondria may

also be found in this cytoplasmic conduit. They might participate in the motor transport for metabolites, protein or lipids during myelin synthesis or maintenance.

1.2.1b Juxtaparanodes

The length of a juxtaparanode is estimated to be 10-15 nm and is a continuation of the internode on both sides. It is ultrastructurally indistinguishable under transmission electron microscopy (TEM) but can be molecularly differentiated by the juxtaparanodal complex clustered within the axolemma after freeze fracture (Rosenbluth, 1976). Two shaker type delayed rectifying K^+ channels, $K_v1.1$ and $K_v1.2$ as well as their β subunits are enriched in this complex (Salzer, 2003; Wang et al., 1993). These K^+ channels are thought to be important in nodal repolarization and inhibition of membrane hyperexcitation, hence supporting fast, repetitive generation of action potentials (Zhou et al., 1999). K^+ channels clustering and juxtaparanodal complex formation at this site requires expression of several cell adhesion molecules (CAMs), including contactin associated protein 2 (Caspr2) and TAG-1. In particular, Caspr2 associates with $K_v1.1$ and $K_v1.2$ at its carboxyl terminus via an unknown PDZ domain scaffolding protein whereas its cytoplasmic FERM domain anchors Caspr2 to the axon actin cytoskeleton by interacting with the adaptor protein 4.1B. (Poliak et al., 1999; Zoupi et al., 2011). Mice that are deficient in Caspr2 or 4.1B lose the clustering of these complexes in juxtaparanodes and have a diffuse localization of the K^+ channels across the length of internodes (Horresh et al., 2010; Poliak et al., 2003; Traka et al., 2003). On the axonal membrane, Caspr2 forms a *cis* complex with a glycosyl phosphatidylinositol (GPI)-anchored neuronal adhesion molecule, TAG-1, which in turn binds to its glial counterpart through trans homophilic interaction. The importance of this adhesion mediated by TAG-1 is underscored by the failure to form juxtaparanodes in TAG-1 knockout mice. Nonetheless, neither nerve conduction deficiency nor general phenotypic

abnormality has been reported with the absence of Caspr2 or TAG-1 in mice (Poliak et al., 2003; Traka et al., 2003). Therefore, the exact role of the adhesive-junctional specializations of juxtaparanodes remains elusive.

1.2.1c Paranodes

Paranodes lie immediately adjacent to the juxtaparanodes and flank the nodal region. Here, the major dense lines become loose, uncompacted SC cytoplasmic pockets that touch the axonal surface in a fashion reminiscent of the septate junctions found in invertebrates (Salzer, 2003). In doing so, paranodal loops effectively but not completely isolate the periaxonal space from the outside milieu. The paranodal region represents the closest apposition between SC membrane and axolemma; a distance of 2.5-3.0 nm uniformly separates these two (Trapp and Kidd, 2004). Within this gap, adhesive apparatus commonly known as transverse bands are evenly spaced (Peters A et al., 1991). These transverse bands are intramembranous particles integrated by adhesive components contactin, Caspr (also known as paranodin, NCP1) and the 155 kDa neurofascin (NF155) (Salzer, 2003). Contactin associates with Caspr on axonal membrane where they form *cis* complexes, similar to Caspr2 and TAG-1 at juxtaparanodes (Einheber et al., 1997; Menegoz et al., 1997; Rios et al., 2000). Through an as yet unidentified mechanism, this contactin-Caspr complex interacts with NF155 on glial paranodal loops, thereby integrating the axoglial junction (Charles et al., 2002; Gollan et al., 2003). Genetic ablation of any of above components results in loss of transverse bands, disrupted paranodal junctions and electrophysiological deficits (Bhat et al., 2001; Boyle et al., 2001; Pillai et al., 2009; Sherman et al., 2005). In contactin and Caspr deficient mice with normal compact myelin, shaker type K^+ channels are dislocated from juxtaparanodes to paranodes in the absence of gross alteration of Na^+ channel distribution at the nodes, suggesting that paranodal junction specifically affects the

maintenance of juxtaparanodes and may create a lateral diffusion barrier for the spatial segregation of ion channels (Bhat et al., 2001; Boyle et al., 2001). A couple of studies have suggested that paranode formation may be a coordinated effort of both proteins and lipids since gene deletion of the enzymes that make galactosylceramides and sulfatides gave rise to a comparatively similar junctional and conduction defects seen in the Caspr knockouts (Dupree et al., 1998; Honke et al., 2002). Notably, clusters of mitochondria can be found as the surfaces of paranodal bulbs approach the nodes, indicating a metabolic coupling between axon and SC at this region (Berthold, 1968; Landon and Williams, 1963). In agreement, lack of septate-like junctions is associated with aberrant accumulation of mitochondria in the nodal/paranodal regions in sciatic nerves of Caspr knockout mice (Einheber et al., 2006).

1.2.1d Nodes of Ranvier

If the myelin sheath was not interrupted by the nodes of Ranvier, a myelinated fiber would be likened to an electric wire and most likely have continuous impulse transmission, similar to that of an unmyelinated axon. By exposing small stretches of axonal membrane to the extracellular milieu at the nodes, action potentials are biologically restricted to this area, thus enabling energy-efficient saltatory conduction. To generate and regenerate action potentials, myelinated fibers build a battery of ion channels at the nodes. Among these the voltage-gated Na^+ channels are most predominant and carry the ultimate task of nodal depolarization. It is estimated by freeze-fracture electron microscopy that about 1000-1500/μm^2 Na^+ channels are accumulated at the nodal area (Rosenbluth, 1976), a density 25-fold higher than the entire internodal region (Salzer et al., 2008). Specifically, $Na_v1.6$ is the main α-subtype at mature nodes since it requires minimal repriming time and exhibits user-dependent kinetics, befitting the high frequency of activity at this site (Boiko et al., 2001; Herzog et al., 2003). In mouse mutants with motor end plate disease,

depletion of $Na_v1.6$ coincided with delayed nodal maturation and slowed nerve conduction velocity (NCV) (Kearney et al., 2002). Interestingly, ultrastructural studies also revealed apparent paranodal dysmyelination in these mice, which suggests a more complex involvement of $Na_v1.6$ in the organization of myelinated fibers (Rieger et al., 1984). The gating properties of $Na_v1.6$ are further modulated via associating with the transmembrane β subunits, which organize membrane proteins at nodal axolemma (Isom, 2002; Ratcliffe et al., 2001). In addition to sodium channels, Na^+/K^+-ATPase, Na^+/Ca^{2+} antiporters and voltage-gated potassium channels including KCNQ2, KCNQ3 and $K_v3.1b$ have also been localized to certain subsets of nodes, though in much less amount (Salzer, 2003; Zoupi et al., 2011). This channel heterogeneity might reflect a complex regulation of repetitive discharges, for instance by KCNQ2 and KCNQ3, and nodal excitability (Cooper and Jan, 2003). A key feature that discriminates PNS nodes from that of CNS is the contact of nodal axolemma by interdigitating processes projected from the outer collar of adjacent myelinating SCs, termed microvilli. Disorganized and blunted microvilli due to genetic deletion of SC laminin receptor dystroglycan correlated with a reduction in nodal sodium channels and nerve conduction impairment (Saito et al., 2003). Similar to paranodes and juxtaparanodes, establishing axoglial interaction and membrane targeting of ion channels relies on the molecular assembly of multiprotein complexes by adhesion molecules expressed in axonal and glia. $Na_v1.6$ and KCNQs are recruited to this axonodal complex by a multivalent cytoskeletal protein ankyrin G (Lemaillet et al., 2003; Pan et al., 2006). Ankyrin G in turn binds to βIV-spectrin submembranously via which it is tethered to neuronal actin cytoskeleton (Salzer, 2003). Disrupting βIV-spectrin or ankyrin G expression *in vitro* and *in vivo* respectively caused aberrant or abrogated nodal formation (Dzhashiashvili et al., 2007; Yang et al., 2004). This indicates that submembranous cytoskeleton is critically involved in stabilizing the nodal complex. At the

axonodal and microvillar interface, members of the L1-like immunoglobulin superfamily (IgCAMs), NrCAM and the 186 kDa isoform of neurofascin (NF186), provide a bridging interaction that connects axonal cytoskeleton with SC microvilli by binding to glial matrix protein gliomedin (Eshed et al., 2005). This interaction seems to serve as an early SC signal that specifies localization of Na^+ channel-binding CAMs since either of NrCAM, NF186 or gliomedin knockouts display defective clustering at heminodes (early nodal intermediates on each side of adjacent myelin segments) but not mature nodes in myelinated nerves (Feinberg et al., 2010). Based on this evidence, these CAMs are not absolutely required for mature node formation and might have been replaced by other CAMs in these knockouts.

1.3 The Regulation of Peripheral Nerve Myelination and Demyelination by Neuregulin-ErbB Signaling

The precise spatial and functional organization of multiple cell types in the complex nervous system of vertebrates is achieved through ongoing reciprocal interactions between neurons and glia. It has long been recognized that the generation, proliferation and myelin production of SCs are tightly regulated by mitogenic and trophic signals from axons (Friede and Samorajski, 1967). It is also clear that axonal caliber directs whether or not a given axon will be myelinated as well as the subsequent length and thickness of internode formed. The axonal cue transducing this information, however, remained elusive. Recently, a series of elegant studies utilizing transgenic rodent models elucidated that neuregulin-1s (NRG1s), a family of axon-derived gliotrophic factors, are the key molecules dictating SC phenotypes at various stages of development.

1.3.1 NRG1 and ErbB Receptors

More than fifteen membrane-bond and secreted proteins (Esper et al., 2006; Falls, 2003) resulting from alternative promoter usage and RNA splicing (Falls, 2003; Law et al., 2006)

comprise the NRG1 family. They can be subdivided into three major isoforms (I, II, and III) based on their distinct amino terminal sequences (Buonanno and Fischbach, 2001; Garratt et al., 2000a). NRG1 type I (also known as heregulin, neu differentiation factor), NRG1 type II (also known as glial growth factor [GGF]) and NRG1 Type III (also known as acetylcholine receptor-inducing activity [ARIA]) are transmembrane proteins that undergo proteolytic cleavage by metalloproteinases. As a consequence of this cleaving, NRG1 types I and II are shed from the neuronal cell surface and function as paracrine signaling molecules. In contrast, NRG1 type III remains tethered to the membrane through its cysteine rich domain (CRD) and provides a juxtacrine signal (Wang et al., 2001). These three isoforms are the most abundant forms expressed in many projection neurons, most notably spinal motor and dorsal root ganglia (DRG) neurons, but also in glia, including Schwann cells. All NRG1 isoforms contain an epidermal growth factor (EGF)-like signaling domain that is necessary and sufficient for activation of their cognate receptors, members of the ErbB family of tyrosine kinase receptors which includes EGFR (ErbB1), ErbB2, ErbB3 and ErbB4 (Yarden and Sliwkowski, 2001). Despite the structure and sequence homology between EGFR and ErbB receptors, NRG1 selectively binds to ErbB3 and ErbB4 but shows poor affinity to EGFR (Tang and Lippman, 1998). ErbB2 lacks a ligand-binding domain (LBD) and hence cannot bind directly to NRG1. Instead, it acts as a co-receptor with ErbB3, which has a LBD but lacks an active kinase activity. While ErbB2-4 express in various neuronal and glial cell types in the PNS (Pearson and Carroll, 2004), their roles in mediating axon-regulated SC biology are so far the best understood.

NRG1 binds with high affinity to ErbB3 on the SC membrane and leads to its heterodimerization with ErbB2 and subsequent activation of downstream effectors. NRG1-ErbB signaling has a key role at essentially every developmental stage of the Schwann cell lineage

(Garratt et al., 2000a), including promoting gliogenic fate of neural crest cells (Leimeroth et al., 2002; Shah et al., 1994), the migration of Schwann cell precursors and their subsequent proliferation, survival, and maturation (reviewed in Garratt et al., 2000a).

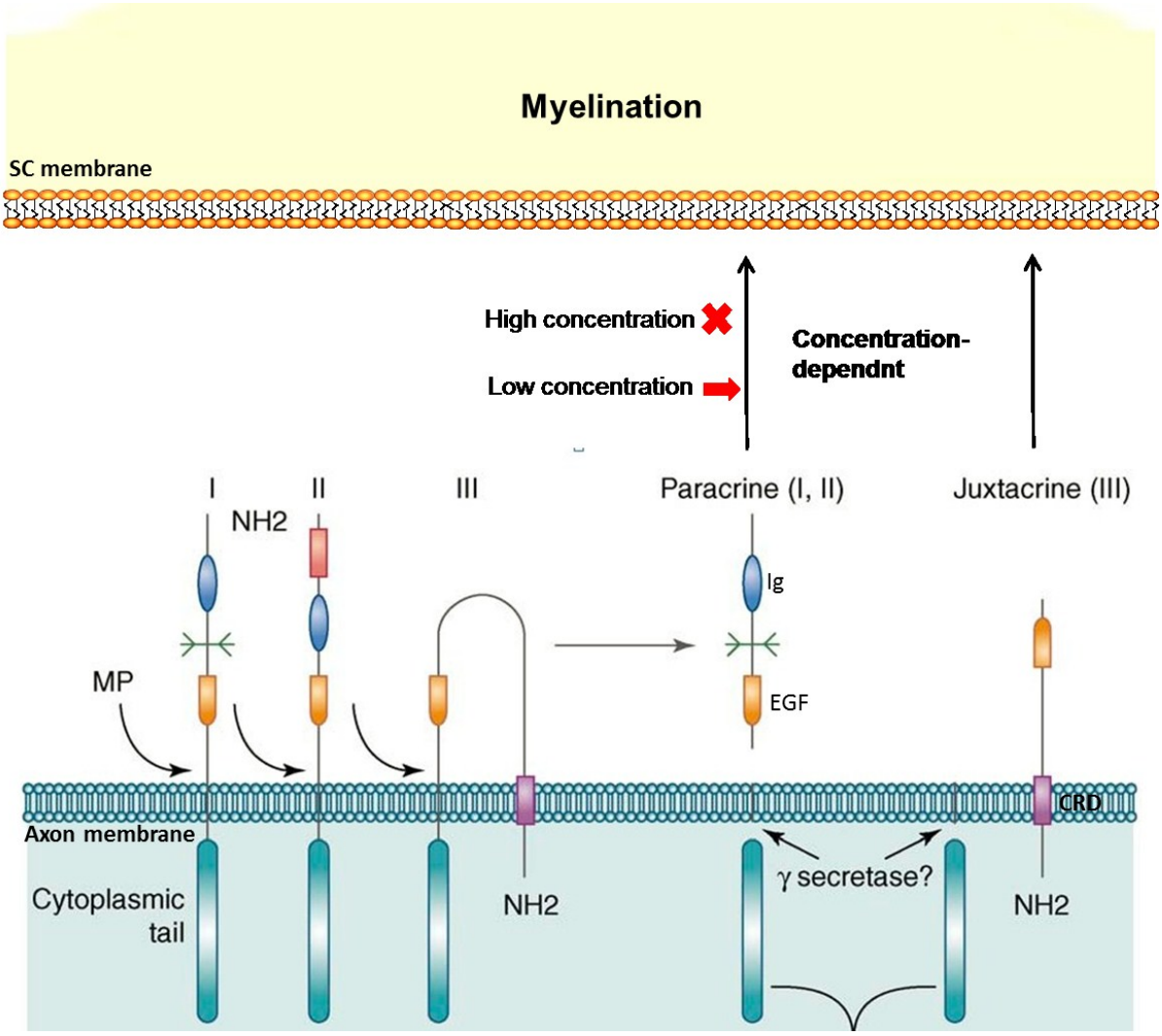

Figure 1.3.1 Differential proteolytic cleavage of NRG1 isoforms and concentration-dependent regulation of SC myelination by NRG1 isoforms. After metalloproteinase (MP) cleavage, type I and type II NRG1 are released from axonal membrane and act as paracrine molecule to ErbB receptors (not shown) on SC membrane. However, type III NRG1 remains tethered to the axolemma due to its cysteine-rich domain (CRD). Regardless of the isoform type, low concentration of soluble NRG1 promotes myelination whereas high concentrations of NRG1 inhibit myelination. EGF: epidermal growth factor. Ig: immunoglobulin. *(adapted from Nave and salzer, 2006)*

In confirmation of NRG1's importance in SC development, mice with targeted disruption of all or certain NRG1 genes and its receptors demonstrate embryonic lethality with severe

deficiencies in multiple cell types, including SCs. (Britsch et al., 1998; Garratt et al., 2000a; Kramer et al., 1996; Meyer and Birchmeier, 1995; Meyer et al., 1997).

1.3.2 Regulation of SC Myelination by NRG1 in Developing Nerves

NRG1 type III is essential for the ensheathment and myelination of axons by SCs as SCs fail to either myelinate or properly ensheath NRG1 type $III^{-/-}$ DRG neurons *in vitro* (Taveggia et al., 2005). Further, genetically enforced expression of NRG1 type III in NRG1 type $III^{-/-}$ neurons substantially rescued myelination to levels similar to those observed in wildtype SC-DRG co-cultures. As indicated previously, levels of NRG1 vary widely on different axon types in a manner correlated with their ensheathment fate: unmyelinated sympathetic neurons express minimal levels of NRG1 type III, whereas BDNF and NT-3-dependent DRG neurons which are more consistently and heavily myelinated express high levels of this NRG isoform (Snider and Wright, 1996). Notably, exogenous expression of NRG1 type III in the post-ganglionic fibers of sympathetic neurons converts these normally unmyelinated and ensheathed fibers to a myelinated fate *in vitro* (Taveggia et al., 2005).

In agreement with the unusually thick myelin sheaths observed upon overexpression of NRG1 type III in SC-DRG co-cultures (Taveggia et al., 2005), transgenic mice overexpressing NRG1 type III in DRG, motor neurons or sciatic nerves become hypermyelinated, as indicated by a decreased g-ratio (measures the ratio between the diameter of the axon cylinder and that of the myelinated axon) (Michailov et al., 2004). This effect appears specific to NRG1 type III since transgenic mice overexpressing the secreted NRG1 type I demonstrate no difference from wild-type. These data suggests that the juxtacrine, but not paracrine stimulation of ErbB by the type III isoform is essential in regulating myelin thickness. By contrast, heterozygous NRG1 type III mice with 50% reduction of NRG1 gene dosage express significantly reduced myelin

protein and transcription factors, correlating with hypomyelination (Taveggia et al., 2005) and decreased NCV (Michailov et al., 2004). Characterization of myelination or later aspects of peripheral nerve development in homozygous NRG1 type III-/- mice are not possible due to embryonic lethality. Despite the fact that these results support isoform-specific effects of NRG1 in instructing SC myelination, another study using DRG/SC co-cultures found that low concentrations of soluble GGF also promoted myelination and high doses of NRG1 type III began to suppress myelination in a MEK/Erk-dependent manner (Syed et al., 2010). Therefore, the binary choice of pro- and contra myelination by NRG1 is concentration-dependent rather than necessarily isoform-specific.

Whereas myelin growth is clearly titrated to the amount of NRG1 available, ErbB2 and ErbB3 are generally expressed at saturating levels throughout development as no decrease in myelination was observed in ErbB2$^{+/-}$ mice (Michailov et al., 2004). However, SC-specific ablation of the ErbB2 gene phenocopies myelination seen in NRG1 type III$^{+/-}$ mice (Garratt et al., 2000b). Likewise, conditional mouse mutants that express a dominant-negative ErbB (DN-ErbB) receptor in SCs had delayed onset of myelination, increased g-ratio and shorter internodal length (Chen et al., 2006). In line with the morphological defects, slower NCV and abnormal mechanical sensitivity were also observed in mice expressing DN-ErbB receptor (Chen et al., 2006). Although NRG1 type III is necessary to induce SC myelination, it is clearly not sufficient since the heterologous, juxtacrine source of NRG1 type III from Chinese hamster ovarian cells failed to stimulate myelin protein expression in rat SCs (Taveggia et al., 2005). Thus, other axonally-derived signals, such as progesterone (Melcangi et al., 2003; Schumacher et al., 2004), BDNF (Chan et al., 2001) and insulin-like growth factor (Cheng et al., 1999), may also be needed to initiate the myelin phenotype. It remains to be addressed however to what extent are

these molecules involved in the relevant processes of myelination, including radial sorting and myelin gene upregulation.

NRG1 type III predominantly activates the phosphatidylinositol 3-kinase (PI3K)-Akt pathway, which is required for SC survival, proliferation and the initial events of myelination (Nave and Salzer, 2006). Inhibition of PI3K with pharmacologic agents or dominant negative gene expression blocks or inhibits myelination *in vitro* (Maurel and Salzer, 2000b; Ogata et al., 2004). On the contrary, overexpression of PI3K or activated Akt promotes myelin protein expression in SC-DRG co-cultures and augmented myelin sheath formation during regeneration of allogenic sciatic nerve grafts (Ogata et al., 2004). Interestingly, GGF also up-regulates PI3K activation in myelinated co-cultures, suggesting an involvement of PI3K in SC dedifferentiation induced by excessive NRG1 stimulation at a later stage (Zanazzi et al., 2001). Consistent with this notion, our group observed a marked elevation in the level of phosphorylated Akt in correlation with enhanced ErbB2 activity and myelin degeneration following heuregulin treatment in myelinated sensory SC-DRG co-cultures (Yu et al., 2008). However, activation of this signaling axis might not be functionally significant in this matter since inhibiting PI3K had no impact on the ability of NRG1 in promoting myelin degeneration in a same co-culture system (Harrisingh et al., 2004).

1.3.3 Regulation of SC Myelination by NRG1 in Mature Nerves

NRG1 and ErbB2 receptor are abundantly expressed in neonatal nerves but decrease in adult nerves (Dobrowsky et al., 2005; Huijbregts et al., 2003), indicating that NRG1-ErbB signaling might be dispensable for the maintenance of mature myelin. Indeed, neither continuous treatment in myelinated co-cultures with a PI3K inhibitor (Maurel and Salzer, 2000b) or ErbB2 gene deletion in adult SCs *in vivo* (Atanasoski et al., 2006) affected myelin integrity or SC

proliferation and survival after nerve injury. It is therefore highly likely that a distinct set of cellular and extracellular factors are employed to maintain and regulate the myelinated SC phenotype. On the other hand, pathological activation of NRG1 signaling in myelinated nerves, triggers SC dedifferentiation and proliferation. This has been repeatedly demonstrated in established myelinated SC-DRGs co-cultures in which addition of exogenous NRG1 such as GGF results in substantial demyelination that progresses from paranodes to internodes (Zanazzi et al., 2001). Such a phenomenon is reminiscent of Wallerian degeneration during nerve injury, which has been shown to display selective induction of GGF (Carroll et al., 1997). The involvement of ErbB2 in this response is somewhat disputable. Although some observed increased ErbB2 activity and blockade of SC proliferative response by ErbB2 inhibitor after sciatic nerve transection (Guertin et al., 2005), others reported that SC proliferation was unaffected in a mouse model of Wallerian degeneration with the conditional ablation of ErbB2 expression (Atanasoski et al., 2006). By contrast, rapid and sustained phosphorylation of extracellular signal-regulated kinase (Erk) is consistently seen subsequent to GGF administration in myelinated cultures or axotomy *in vivo* (Harrisingh et al., 2004; Zanazzi et al., 2001). Erk is a common downstream signal of NRG1 that favors SC proliferation and demyelination. In support of this, selective activation of Raf/Erk independent of NRG1 drives SC dedifferentiation whereas Erk inhibition abrogated demyelination induced by a high concentration of NRG1 (Harrisingh et al., 2004).

Adult SCs retain a striking ability to remodel and this remarkable plasticity is regulated by the transcription factor c-jun (Parkinson et al., 2008). Through a series of elegant studies, Parkinson et al., (2008) demonstrated that c-jun expression and activity is downregulated during myelin differentiation *in vitro* and *in vivo*, but is rapidly upregulated upon nerve injury. In

addition, myelin gene expression was facilitated in c-jun-null SCs and enforced c-jun expression in SCs significantly reduced the number of myelin internodes formed in SC-DRG co-cultures, indicating that c-jun is a negative regulator of myelination. Similarly, absence of c-jun caused a marked delay in the rate of myelin loss both after axon removal and nerve transection. Importantly, exposure of SC DRG/ co-cultures to NRG1 led to a substantial c-jun induction concomitant with extensive myelin fragmentation. These findings provide compelling evidence that c-jun contributes to NRG1-induced demyelination. While transient SC dedifferentiation and proliferation permits axonal regeneration after axotomy, additional or excessive NRG1 signaling outside this context could prolong unwanted or pathological demyelination. For example, transgenic mice overexpressing NRG1 type IIβ3 (GGF β3) specifically in myelinating SCs developed hypertrophic demyelinating peripheral neuropathies and peripheral nerve sheath tumors preceded by SC hyperplagia (Huijbregts et al., 2003).

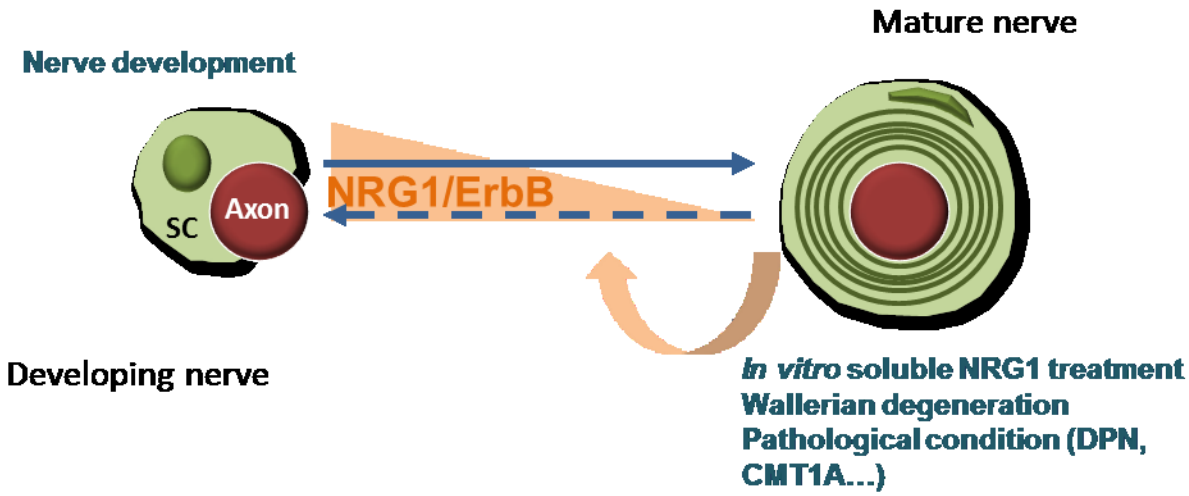

Figure 1.3.3 Regulation of SC myelination and demyelinaton by NRG1/ErbB signaling in developing and mature nerve. Stimulation of ErbB2 receptor by NRG1 during peripheral nerve development encourages SC myelination. In contrast, soluble NRG1 treatment in culture, nerve axotomy and pathological conditions such as diabetic peripheral neuropathy (DPN) deregulates NRG1/ErbB cassette and triggers demyelination.

In a clinical biopsy analysis, overexpression of ErbB2 and ErbB3 receptors in SCs was consistently noted in sural nerves of CMT1A patients (Massa et al., 2006). Upregulation of these receptors were possibly driven by events other than that initiated during axonal denervation and may predict a deregulated and persistent NRG-ErbB activity that contributes to impaired SC differentiation, SC hyperplagia and recurrent demyelination seen in this disease. Marked c-jun immunoreactivity in SC nuclei was also detected in sural, dorsal ulnar nerve and dermal myelinated nerve specimens from subjects with a variety of axonal or demyelinating neuropathies including vasculitic neuropathy, CMT1A and Guillain-Barré syndrome but not healthy controls (Hutton et al., 2011). These observations correlate with the "Wallerian-like degeneration" manifested in some human neuropathies (Griffin and Sheikh, 2004; Wrabetz et al., 2004a; Zochodne et al., 2008) and provide evidence for a mechanism by which altered NRG1 signaling and SC trophism may underlie the phenotypic demyelination in these diseases.

1.4 Myelin-related Disorders

Loss of myelin not only manifests as the pathological hallmark of demyelinating diseases, such as multiple sclerosis and CMT (Bhatheja and Field, 2006; Boyden, 2000; Halliday and McDonald, 1977), but also occurs as a secondary event to a variety of neuropathic and psychiatric disorders, including diabetic neuropathy and schizophrenia (Mitterauer, 2007; Valls-Canals et al., 2002). Regardless of whether it is a causative or secondary event, the consequence of demyelination is the loss of the insulating layer and the electrical properties of the axon, which manifests clinically as slowed NCVs. Since demyelinated axons cannot keep up with the high electric and energy demand required for fast reaction speeds, they progressively lose their integrity. This ultimately incapacitates most motor, sensory and higher functions of the brain at advanced stages of above-mentioned diseases (Franklin and Ffrench-Constant, 2008). Primary

demyelinating neuropathies encompass a heterogeneous group of disorders and depending on the causes, can be subcategorized into hereditary and autoimmune neuropathies. These conditions are characterized by developmental or acquired myelin degeneration resulting from genetic defects or immune assault on various myelin components or regulatory proteins. Diabetic neuropathy also affects myelinated fibers and segmental demyelination has been repeatedly documented in patients with type 1 or type 2 diabetes (Sharma et al., 2002). Since treating diabetes-associated demyelinating neuropathy by inhibiting neuregulin signaling is my primary research interest, I will focus on discussing the clinical features, pathology, pathogenesis and treatment of diabetic neuropathy with a particular emphasis on segmental demyelination while touching briefly on two other common demyelinating disorders.

1.4.1 Charcot-Marie-Tooth Disease

Although myelin generation initiates prenatally in mammals, myelination predominantly occurs after birth and continues throughout maturation of the nervous system (Brodal, 2010). This is why most inherited myelin defects are not disease-causing until after infancy. The complex cellular adaptation of myelinating SC and axon biology predispose myelinated fibers to demyelinating and dysmyelinating neuropathies secondary to a number of gene mutations. Such neuropathologies, when other causes are excluded, are collectively known as Charcot-Marie-Tooth disease (CMT), or hereditary motor and sensory neuropathy. CMT affects approximately 1-8 in every 10,000 individuals and 125,000 total in the US. Because an effective, disease-specific treatment is not available, current management of CMT is limited to symptomatic improvement with physical and orthopedic support.

According to the primary lesion, CMT is further recognized as demyelinating (CMT1) or axonal (CMT2) forms. CMT1 is more common, has an early onset and typically presents with

segmental demyelination and onion bulb formation of degenerating SCs. However, these two forms are often difficult to differentiate by morphological diagnosis as axonal neuropathy often leads to myelin sheath degeneration (Griffin and Hoffman, 1993; Scherer and Salzer, 2001) whereas axonal atrophy may follow demyelination (Sancho et al., 1999). The most widely used clinical criterion, though imperfect, separates CMT1 and CMT2 at a forearm motor conduction velocity of less or greater than 38 m/s, respectively (Wrabetz et al., 2004a). Mutations in proteins of both compact and non-compact myelin are responsible for the diverse disease phenotypes in CMT1. As mentioned earlier, PMP22 gene deletions, duplications as well as mutations are the pathogenetic mechanisms underlying hereditary neuropathy with liability to pressure palsies, CMT1A and Dejerine-Sottas syndrome (Wrabetz et al., 2004a). Mutations in *GJB1*, a gene that encodes connexin 32, are pathogenically involved in the X-linked dominant CMT1X (Bergoffen et al., 1993). Connexin 32 is a gap junction protein localized to adjacent myelin membranes at paranodal loops and Schmidt–Lantermann incisures (Bruzzone et al., 1996; Trapp and Kidd, 2004). Interestingly, biopsies of CMT1X patients revealed a more prominent axonal degeneration than demyelination (Hahn et al., 2001; Vital et al., 2001), indicating a dependency of axonal integrity on functional myelin. Vice versa in CMT2, axonopathy frequently induces Wallerian degeneration, a condition in which myelinating SCs degenerate and revert to a proliferating phenotype (Griffin and Hoffman, 1993; Scherer and Salzer, 2001). This interdependency between myelinating SC and axon physiology is further underscored by the fact that a few mutations identified in MPZ are linked to a CMT2-like phenotype (Frei et al., 1999).

1.4.2 Guillain-Barré Syndrome

Guillain-Barré syndrome (GBS) is a group of acquired demyelinating diseases that affect the PNS by autoimmune attack misdirected toward an antigen on nerve fibers. Clinical

manifestations of GBS start with an ascending paralysis from distal limbs and in severe cases may spread to facial and life-threatening respiratory muscles (Griffin and Sheikh, 2004). More than 90% of GBS occurrences are in the form of acute inflammatory demyelinating polyneuropathy (AIDP) (Emilia-Romagna Study Group on Clinical and Epidemiological Problems in Neurology, 1998); the immunogenic nature of disease pathology is evident from the apparent lymphocytic infiltration throughout the endoneurial space. Affected sensory or motor nerve fibers first demonstrate vacuolization of the myelin sheath, followed by extensive vacuolar myelin degeneration, and subsequently clearance of myelin debris by invading macrophages (Griffin and Sheikh, 2004). The target antigens of AIDP are largely unknown but thought to involve multiple compounds that contain ganglioside-like moieties, which are expressed in high abundance in peripheral nerve tissues. This is derived from the presence of high titers of anti-ganglioside serum antibodies in GBS patients (Oomes et al., 1995; Rees et al., 1995; Sheikh et al., 1998) and the recapitulation of GBS in animal models via ganglioside immunization (Griffin and Sheikh, 2004; Kusunoki et al., 1999). In addition to antibody-induced myelin destruction, activated T-cells may also contribute to breakdown of blood nerve barrier and SC and myelin injury (Asbury et al., 1969; Sivieri et al., 1997). Accordingly, the treatment strategy for GBS is to remove and block the pathogenic antibodies by plasmapheresis and administration of high dose immunoglobulins. Otherwise, breathing aid and supportive care are provided during complications such as respiratory failure.

1.4.3 Diabetic Peripheral Neuropathy and Segmental Demyelination

Diabetes is estimated to affect 347 million people globally as of 2008 (Danaei et al., 2011) and this number is expected to double by 2030 (Wild et al., 2004). Depending on the case definitions used, 30-70% of patients with either type 1 or type 2 diabetes are diagnosed with

some form of peripheral neuropathy (NIDDK, 2009) (National Institutes of Diabetes and Digestive and Kidney Diseases). A distal symmetric sensorimotor polyneuropathy is the most frequent manifestation and affects 90% of patients with Diabetic Peripheral Neuropathy (DPN) (Harati, 2010). Patients with this form of DPN are predisposed to foot ulceration and increased risk of amputation; ulcerative complications from DPN account for approximately 87% of non-traumatic lower extremity amputations. In addition to this traumatic medical event, DPN is also a major contributing factor to the development of joint deformities, limb threatening ischemia as well as other various neurological dysfunctions (Harati, 2010). This greatly reduces the quality of life in people with diabetes through increased disability and is assuming more hospitalizations than all other diabetic complications combined (Mahmood et al., 2009). As a consequence, approximately $15 billion are spent on DPN annually in the US, causing a major drain on healthcare expenditure (Rathmann and Ward, 2003).

1.4.4 Clinical Features and Pathology

DPN encompasses a wide spectrum of clinical and subclinical syndromes differing in their pattern of neurological involvement, anatomic distribution, specific neuropathic alterations, risk covariates and course of development. In distal symmetric sensorimotor polyneuropathy, damage to nerves initially begins with the longest axons, which accounts for the loss of sensation having a “stocking-glove” distribution. Degeneration continues to progress proximally in a dying-back, length-dependent pattern. (Boulton and Malik, 1998). Although post-mortem analysis indicates that all types and sizes of fibers are affected, sensory symptoms predominate over motor deficits at least in the early phase, likely due to the longer (and therefore more susceptible) axons needed to reach the epidermis of the distal limbs. Patients diagnosed with this form of neuropathy often display symptoms such as paradoxical association of numbness with allodynia and dysesthesia

associated with small fiber sensory dysfunction. As DPN advances, large sensory and motor fibers also become impaired. This leads to decreased NCV, loss of vibratory sensation and proprioception, and at advanced stages sensory deafferentation (Habib and Brannagan, 2010; Harati, 2010; Tahrani et al., 2010), all of which are likely to reflect progressive, irreversible loss of myelinated fibers. In particular, segmental demyelination has been a conspicuous finding of pathological change and repeatedly documented in nerve biopsies of patients with DPN (Behse et al., 1977; Thomas and Lascelles, 1965; Viswanath et al., 1974). When assessed in teased fiber preparation, it is characterized by breakdown or loss of single or few continuous myelin internodes (Mizisin and Powell, 2003). Other reports from electron microscopic analysis of diabetic sural nerves described granular and vesicular disintegration of myelin sheath as well as SC membrane hyperplasia (Yagihashi and Matsunaga, 1979). This patho-morphological pattern also manifested in peripheral motor nerves of WBN/Kob rats with spontaneous and long-lasting diabetes, which exhibited myelin blebbing and distention following vesicle and granule accumulation within myelin lamella (Ozaki et al., 1996).

For a long time there has been considerable dispute over whether axonopathy or Schwannopathy is the primary lesion leading to segmental demyelination and peripheral nerve injury in diabetes; evidence supporting both views has been derived from clinical and experimental analysis of DPN. Based on sural nerve biopses, Chopra *et al.* reported segmental demyelination in the absence of significant axonal abnormality prior to the onset of DPN and confirmed this in teased fibers of streptozotocin-induced diabetic monkeys (Chopra et al., 1969; Chopra et al., 1977). In contrast Dyck *et al.* concluded that axon loss was predominant and the degenerating myelin had a clustered distribution characteristic of secondary demyelination (Dyck et al., 1986). The latter finding was aligned with an earlier observation that some fibers

underwent axonal atrophy without concordant decrease in internodal length (Lascelles and Thomas, 1966). Others have also suggested that the dying-back progressive fiber loss is in fact an initial consequence of the primary degeneration in spinal motor and dorsal sensory roots (Couers and Hildebrand, 1965; Greenbaum et al., 1964; Olsson et al., 1968). The majority of evidence, however, supports a co-existence of SC demyelination and axonal degeneration, either in connection or independently (Behse et al., 1977; Lascelles and Thomas, 1966). In agreement, both primary segmental demyelination and demyelination secondary to axon degeneration were identified in the same sural nerve biopsies from diabetic patients afflicted with severe sensory neuropathy (Said et al., 1983). Based on these findings and given the systemic metabolic disturbances in diabetes mellitus, it seems more plausible that a widespread pathology of diverse cell types would occur and contribute to DPN.

1.4.5 Pathogenesis and Treatment

With years of ongoing efforts, a number of biochemical events have been established as important mediators linking hyperglycemic stress to the development of DPN: increased oxidative stress, formation of advanced glycation end-products (AGEs), overflux of glucose through polyol and hexosamine pathways, abnormal activity of mitogen-activated protein kinases (MAPKs) and nuclear factor-κB (NF-κB), neuroinflammation as well as impaired neurotrophic support. Unfortunately, none of the compounds developed against these targets has shown unequivocal effectiveness in preventing, reversing, or even slowing the neuropathic process in humans (Mahmood et al., 2009; Obrosova, 2009; Tahrani et al., 2010). A principal reason to explain these failures is the complexity of the pathogenesis of DPN since this array of molecular targets and pathways do not contribute to its pathophysiological progression in a temporally and/or biochemically uniform fashion. Instead, the relative importance of these

biochemical insults varies upon diabetes duration, genetic heterogeneity and additional pathological conditions. To date, the only effective strategy and gold standard method for preventing and treating DPN remains aggressive glycemic control, supplemented by FDA-approved medications providing pain relief (Tahrani et al., 2010). However, many patients struggle to maintain normoglycemia and the already established neuropathic syndromes necessitate the development of therapies that directly address the underlying nerve damage and repair. The difficulty in pursuing such therapies begins with the fact that we do not even know, at a molecular signaling level, how these metabolic disturbances are coupled to the many functional and morphological changes observed in clinical biopsies, such as segmental demyelination. In this regard, establishing or re-establishing appropriate neuron-glia phenotypes is directed by the molecular signals, typically growth factors, that are operative in reciprocal axoglial interplay (Dobrowsky et al., 2005). Although there is no doubt that impaired neurotrophic support pathogenically contributes to the degeneration of diabetic nerves (Anand et al., 1996; Hellweg and Hartung, 1990; Hellweg et al., 1994; Jakobsen et al., 1981), nerve growth factor supplementation failed to demonstrate definitive efficacy in improving symptoms of DPN at tolerated doses in clinical trials (Apfel, 2002). Among the explanations for this failure is the alarming possibility of altered growth factor responses and signaling in hyperglycemically-stressed neurons and glia (Dobrowsky et al., 2005). Evidence from our group supports that this is likely to be the case for NRG1 signaling in demyelinated nerves in diabetes. As discussed earlier, increased NRG1-ErbB activity is sufficient to induce demyelination and neuropathic change in the peripheral nerve independent of diabetes (Huijbregts et al., 2003). Of note, the “onion bulbs” that are indicative of SC hyperproliferation in GGF β3-induced hypertrophic demyelinating neuropathies, are also frequently observed in diabetic nerve biopsies. We have previously shown

that hyperglycemia enhanced ErbB2 phosphorylation in sciatic nerves of streptozotocin (STZ)-induced diabetic animals (Dobrowsky et al., 2005) and augmented neuregulin-induced demyelination in myelinated SC-DRG neuron co-cultures, possibly through downregulation of an endogenous ErbB2 tyrosine kinase inhibitor protein (Yu et al., 2008). Treatment of diabetic mice that had developed motor and sensory nerve deficits with an ErbB2 inhibitor corrected motor conduction velocity deficits and mechanical hypoalgesia, but only elicited an insignificant trend of improvement in unmyelinated sensory fibers, indicating that myelinated fibers are particularly affected by increased ErbB2 activation (McGuire et al., 2009). Indeed, expression of constitutively active ErbB2 specifically in myelinating SCs was sufficient to cause defects in motor conduction and mechanical insensitivity, which was restored by ErbB2 inhibition. More recently, our biochemical analysis of diabetic mice revealed that diabetes differentially affects the levels of NRG1 isoforms in sciatic, sural and tibial nerves, with the most notable change being that sural nerves exhibit significant increases in NRG1 type I and decreases in NRG1 type III (unpublished observation). However, similar to most other reports, we identified no difference in the g-ratio in sciatic nerves between diabetic and nondiabetic mice (McGuire et al., 2009). While this could be intriguing, it has been widely recognized that rodents are notorious for not reproducing the segmental demyelination associated with human DPN (Mizisin et al., 2007). In addition, most clinical observations of segmental demyelination come from sural nerve biopsies (Behse et al., 1977; Dyck et al., 1986), which agree with our result. Thus, our data suggest a role for pathological induction of NRG1-ErbB in diabetes-induced demyelination and neurological dysfunction of myelinated fibers. Although ErbB2 inhibitors showed effectiveness against neuropathic development in myelinated nerves, diabetes-induced alterations in growth factor signaling can be rather heterogeneous in terms of isoform and fiber type and non-specific

suppression of ErbB signaling undermines survival of unmyelinated axons (Chen et al., 2003). A parallel approach to treat diabetic complications such as DPN is to upregulate the endogenous reparative potential of cells to circumvent the temporal and biochemical heterogeneity of the pathogenic mechanisms which underly the development of DPN. Such a therapeutic "paradigm" may be achieved through modulating the function of molecular chaperones. Along this line, we have identified a small molecule that through inducing neuroprotective molecular chaperones, conferred promising therapeutic efficacy in reversing multiple phenotypes associated with the degeneration of unmyelinated and myelinated nerves, including NRG1-induced demyelination. The remainder of this chapter will review briefly the functions of heat shock proteins and their therapeutic implication in DPN and NRG1-induced demyelination.

1.5 Heat Shock Proteins and Stress Response

Throughout phylogeny, cells have conserved a genetic program for the rapid and robust expression of a special set of proteins - heat shock proteins (HSPs), in response to obnoxious environmental stimuli. This increased synthesis of HSPs is accompanied by a marked inhibition of the synthesis of almost all other proteins and is crucial for cellular protection and recovery from "life-threatening" insults. For example, a prior mild heat exposure increased the survival of cells after an otherwise lethal hyperthermic stress (Li and Werb, 1982; Lindquist, 1986). As the name "heat shock" suggests, this phenomenon is first and best characterized in the setting of heat stimuli (Ritossa, 1962). However, exposure to ischemic, hypoxic, chemical, inflammatory, oxidative and mechanical stress have also been reported to potently elicit the protective effect of the heat shock response (HSR) (Jaattela and Wissing, 1992). The generality of this response can be explained by the fact that there is a greater demand for the chaperone function of HSPs as a

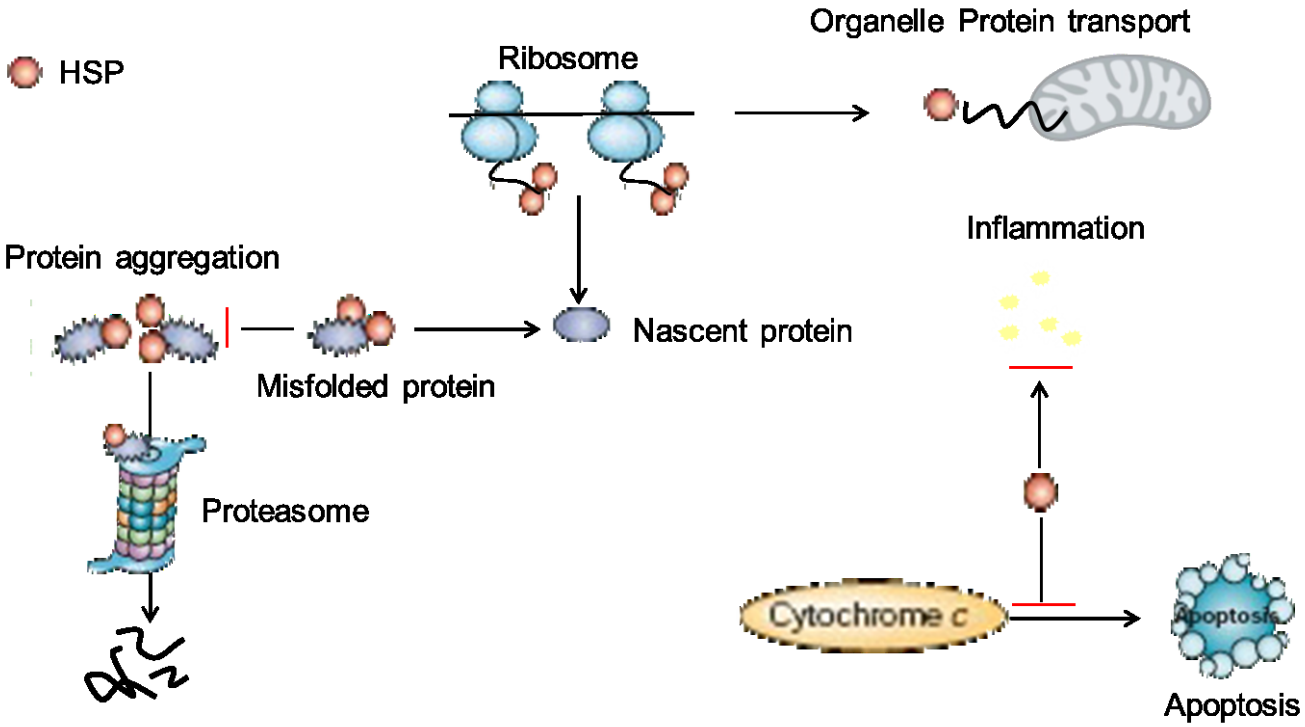

Edited from Muchowski and Wacker,. Nature Reviews 2005

Figure 1.5 Heat shock proteins perform both regular "housekeeping" duty and regulation of signal transduction.

result of an increased amount of protein damage caused by these various forms of internal and external cellular stresses. In fact, most HSPs are better described as molecular chaperones. With the aid of ATP hydrolysis, molecular chaperones perform such housekeeping functions as: aiding in the correct folding and transport of nascent polypeptides during protein biogenesis. Under conditions of stress, chaperones prevent and solubilize protein aggregates by assisting in their refolding or aid the proteasomal or lysosomal clearance of denatured and/or damaged proteins (Ellis, 1987; Muchowski and Wacker, 2005). Although much less is understood compared to their chaperoning function, the involvement of HSPs in signal transduction is being uncovered by an increasing body of evidence. For instance, HSP70 and HSP27 have been shown to inhibit apoptotic and inflammatory responses through suppression of c-jun N-terminal kinase (JNK) and inhibitor of nuclear factor κB kinase-β, respectively (Li and Dobrowsky, 2012).

HSPs are classically categorized by their approximate molecular mass (in kilo-dalton, kDa) into families of HSP100, HSP90, HSP70, HSP60, HSP40 and the small HSPs, although they may also be further described based on different intracellular localization, patterns of expression and functions. Specific Hsps that are particularly implicated in the pharmacological intervention of DPN and demyelination are briefly discussed below.

1.5.1 Hsp70 - Potent "Neuroprotectant"

The HSP70 family is the most abundant and evolutionarily conserved chaperone with human HSP70 sharing 72% and 47% sequence identity with fruit fly HSP70 and the *Escherichia coli* homologue of HSP70 - dnaK, respectively (Hunt and Morimoto, 1985). In mammalian cells, four members of the HSP70 family have been identified: the constitutively expressed cytosolic heat shock cognate 70 (HSC70/HSP73), the stress-inducible cytosolic HSP70/HSP72, the endoplasmic-reticulum (ER)-localized glucose-regulated protein 78 (GRP78/BiP) and the mitochondrial glucose-regulated protein Grp75/mortalin/mtHSP70. Chaperones rarely work alone, and usually associate with each other and/or other co-factors to carry out distinct functions. For example, binding of Hsp40 co-chaperone to Hsp70 often facilitates substrate folding and refolding (Michels et al., 1997; Minami et al., 1996) whereas association of Hsp70 with Hsp90 via Hsp-organizing protein (HOP) typically targets proteins towards proteasomal degradation (Sajjad et al., 2010).

Notably, while most other HSPs are abundantly distributed in the nerve, the inducible form of HSP70 is only weakly expressed and its induction typically represents a cellular protective program adopted by neurons and glia in response to stress (Manzerra et al., 1993; Pavlik and Aneja, 2007; Pavlik et al., 2003). Loss of this protection due to Hsp70 deficiency or dysfunction has been linked to susceptibility to numerous neuropathic changes (Mir et al., 2009; Muchowski

and Wacker, 2005). By the same token, this adaptive response apparently has great therapeutic utility since its recapitulation using physical or pharmacological means confers potent neuroprotection in a variety of pathologies including DPN. For example, increasing HSP70 has shown promising therapeutic effects in a number of neurodegenerative disorders, including Alzheimer's, Parkinson's and polyglutamine (polyQ) expansion diseases (Muchowski and Wacker, 2005). A large part of this protection was attributed to the ability of Hsp70 to decrease toxic protein aggregates through refolding or targeted degradation (Cuervo et al., 2004; Klucken et al., 2004; Shimura et al., 2004). Apart from chaperone function, both heat-shock preconditioning and transgenic overexpression of Hsp70 improved neuronal survival in mice following focal or global cerebral ischemia (Kelly and Yenari, 2002); this protection was linked to Hsp70 interfering with inflammatory and apoptotic signaling pathways. Indeed, virally-directed (Bienemann et al., 2008) or compound-induced expression (Salehi et al., 2006) of Hsp70 suppressed JNK activity and subsequent apoptosis in cultured sympathetic neurons.

With particular implication to DPN, the heat shock factor-1 (HSF-1, Hsp70 gene transcription factor) activators bimoclomol and its analogue BRX-220 improved wound healing and nerve conduction deficits in diabetic rats, respectively (Kurthy et al., 2002; Vigh et al., 1997). As the potential effectiveness of α-lipoic acid in treating DPN has already been noted, Hsp70 levels were decreased in a cohort of type 1 diabetics with DPN and were normalized following α-lipoic acid therapy (Strokov et al., 2000). Studies in our laboratory demonstrated that Hsp70 was central to the efficacy of a pharmacological correction of diabetes-induced myelinated and unmyelinated nerve dysfunction in STZ-mice (Urban et al., 2010). Since no obvious improvement in plasma glucose or insulin levels was observed in treated mice, the protection likely resulted from a direct chaperone effect in the nerves. Although the etiology of DPN is not

associated with the accumulation of a specific misfolded or aggregated protein, our study strongly supports that Hsp70 intersects with the molecular and cellular disturbances underlying nerve dysfunction. While these results do not yield much information regarding whether and how Hsp70 directly influences myelin, another study found improved myelination following pharmacological induction of SC Hsp70 in DRG explants established from a rodent model of hereditary demyelinating neuropathies (Rangaraju et al., 2008). An *in vitro* examination of oligodendrocyte differentiation also revealed that Hsc/Hsp70 but not Hsp25 and Grp78 are required for MBP synthesis (Aquino et al., 1998). In spite of these salient findings, current knowledge of the role of Hsp70 in myelination is rather limited and has received scant attention.

1.5.2 HSP Expression and DPN: An Impaired Defense Against Stress?

Chronic hyperglycemia imposes a multitude of ischemic, hypoxic, oxidative and apoptotic stresses leading to widespread oxidative damage to proteins, cells and tissues (Akude et al., 2010; Obrosova, 2009; Tomlinson and Gardiner, 2008). Neural cells and myelin are especially vulnerable to stress-induced protein denaturation and damage because they do not undergo cell division and are not able to attenuate harmful protein species through mitosis. As the majority of myelin proteins have a slow turnover rate, any glycative and oxidative modifications of myelin proteins and/or lipids would have prolonged and accumulating biochemical consequences towards irreversible damage of myelinated nerves (Brown et al., 1979; Spritz et al., 1975; Sugimoto et al., 2008). Therefore, survival of highly-differentiated neural tissues would rely largely on the endogenous protective and reparative potential of molecular chaperones. Indeed, diabetic nerves that exhibit neuropathological changes often have a reduced expression of HSPs. In spontaneous diabetic Biobreeding/Worcester (BB/Wor) rats, a close model of human type 1 diabetes, 10 months of hyperglycemia markedly reduced HSP70 level in dorsal root ganglia

(DRG), which correlated with a development of advanced polyneuropathy characterized by loss of neurotrophic components and myelinated and unmyelinated fibers (Kamiya et al., 2006). It is difficult to extract from the current limited data on this topic whether diabetes-associated segmental demyelination is directly linked to altered HSP expression. However, decreased HSP function, if it indeed occurs in diabetic nerves, would impair the cytoprotective response and accelerate the pathogenetic insults that lead to myelin degeneration in DPN. Inversely, physically or pharmacologically increasing HSP expression could and has been shown to confer protection against neuropathic changes associated with diabetes. For example, patients with non-insulin-dependent diabetes reduced their blood glucose concentration and symptomatic neuropathy after receiving regular hot-tub hyperthermic treatment (Hooper, 1999; 2003). In diabetic rats, the effectiveness of the HSP co-inducers bimoclomol and its analogue BRX-220 in DPN has already been mentioned (Kurthy et al., 2002; Vigh et al., 1997). The effectiveness of α-lipoic acid in preventing and treating DPN in a cohort of type 1 diabetics with polyneuropathy correlated with the normalization of HSP70 level, which had dropped significantly in these patients (Strokov et al., 2000). While these studies provide tantalizing correlations, they do not differentiate whether the therapeutic benefits are afforded through a systemic influence or a nerve-specific protection or both by HSP induction. Studies in our laboratory address this question and provide evidence that the therapeutic benefits of Hsp70 induction in DPN do not seem to hinge on a metabolic correction and may be relatively nerve-specific (Urban et al., 2010; Urban et al., 2012). Furthermore, we show in the present data that enhanced Hsp70 expression also prevents NRG1-induced demyelination in an Hsp70-dependent fashion.

1.5.3 Hsp90 - Seeking Effective Pharmacological "Heat-shock Therapy"

Notwithstanding its prominent neuroprotective action, direct targeting of Hsp70 as a pharmacological objective has been complicated by its high conservation and ubiquitous expression patterns. On the other hand, Hsp90 has emerged as attractive target for the induction of chaperone protection. Similar to HSP70, HSP90 is highly conserved in its structure and function among species and is plentifully expressed in eukaryotes (comprises up to 2% of total cellular proteins). HSP90 also has different paralogs distributed in several subcellular compartments including cytosol (HSP90α and HSP90β), ER (GRP94) and mitochondria (Hsp75/TRAP-1) of which HSP90β is particularly important for cell survival since mice lacking this isoform die embryonically (Voss et al., 2000). All Hsp90s are highly conserved evolutionarily in their structures and share an N-terminal ATPase domain, a connective linker region and a middle domain involved in binding substrates (client proteins). Hsp90 also has a C-terminal domain that is responsible for interactions with various partner proteins and co-chaperones which provide a coordinate regulation over its diversified functions (Peterson and Blagg, 2009; Soti et al., 2002). Because numerous Hsp90 client proteins are involved in cell growth, differentiation, and survival, inhibitors directed against the Hsp90 N-terminal ATP binding domain induce simultaneous degradation of a wide variety of client proteins and are potent chemotherapeutic agents in cancer (Peterson and Blagg, 2009; Soti et al., 2005). An important aspect of N-terminal Hsp90 inhibitors in treating malignant phenotypes is that the drugs preferentially inhibit Hsp90 and induce client protein degradation in malignant versus normal cells (Luo et al., 2008). This selectivity may be due to the upregulation of Hsp90 to accommodate the malignant cell's dependency on overexpressed oncogenic client proteins (Chiosis et al., 2003) and/or an increased affinity of N-terminal inhibitors for Hsp90-oncoprotein complexes in cancer cells (Kamal et al., 2003). Although this selectivity aids in the clinical

efficacy of N-terminal Hsp90 inhibitors, enthusiasm for their use has been hampered since induction of client protein degradation and cytotoxicity occurs at drug concentrations that also activate an antagonistic aspect of Hsp90 biology, the promotion of the cytoprotective HSR. This is because as a core chaperone in the autoregulatory loop, Hsp90 also represses HSP expression through sequestration of HSF-1 in the cytosol and preventing it from being activated unless being competitively occupied by stress-induced misfolded proteins. This opens possibilities of inducing HSR with limited toxicity through compounds that exhibit mild inhibition or modulation of Hsp90 in cells where increased chaperone expression is needed to confer cellular protection and repair. For instance, since N-terminal Hsp90 inhibitors promote the HSR and decrease protein aggregation, they also have been used in experimental studies to treat neurodegenerative diseases associated with protein misfolding. In this regard, N-terminal Hsp90 inhibitors decrease tau protein aggregation in Alzheimer disease models (Dickey et al., 2007; Luo et al., 2007) and improve motor function in spinal and bulbar muscular atrophy (Waza et al., 2005). Although a similar selectivity exists for the use of N-terminal inhibitors in treating neurodegeneration (Dickey et al., 2007), this selectivity does not circumvent the issue related to dissociating client protein degradation from induction of the HSR. Now, the inverse caveat exists; despite being neuroprotective, induction of client protein degradation may produce cytotoxicity. Thus, developing a highly effective Hsp90 inhibitor for treating neurodegeneration requires establishing a sufficient therapeutic window that avoids increased

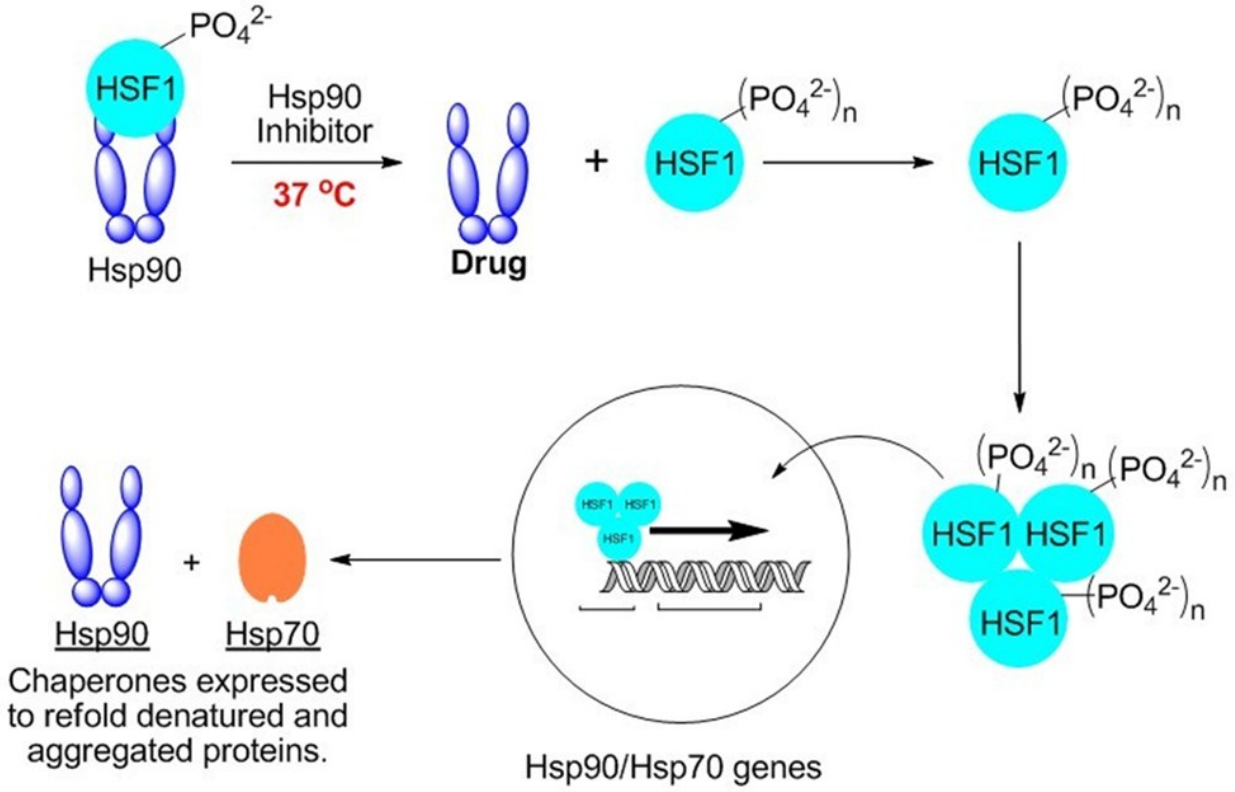

Figure 1.5.2a Inducing heat shock response through inhibiting Hsp90. In non-stressed cells, Hsp90 binds to HSF-1 and this interaction keeps HSF-1 in an inact state in the cytosol. Cellular stress (such as heat shock, not shown) or drug inhibition of Hsp90 can disrupt this association and release HSF-1 from Hsp90-HSF-1 complex. Freed HSF-1 will then undergo trimerization, phosphorylation and subsequent translocation into the nucleus wherein it activates HSE and HSP gene transcription. Upregulation of HSP in nerves executes cytoprotective response and hence neuroprotection.

client protein degradation that may antagonize a cytoprotective HSR. Using a synthetic small molecule Hsp90 N-terminal inhibitor, Rangaraju *et al*. (2010) induced significant Hsp70, Hsp27 and αB-crystallin expression and ameliorated defects in SC myelin formation in a PMP22 mutant mouse model of CMT1A with limited toxicity. The improved myelination was attributed to chaperone-mediated inhibition of the pathological mis-folding and aggregation of PMP22.

Hsp90 also contains a C-terminus ATP binding domain that weakly binds the antibiotic novobiocin. Similar to N-terminal inhibitors, novobiocin can promote client protein degradation and induce a HSR. Through systematic modification of the coumarin ring pharmacophore of

novobiocin, KU-32 was identified as a lead compound that exhibits at least a 500-fold divergence of client protein degradation from induction of Hsp70 (Urban et al., 2010). This divergence provides an excellent therapeutic window to promote neuroprotection in the absence of toxicity. Thus, non-selective uptake and off-target toxicity is not a confounding issue as discussed above. In support of this safety, administering 400 mg/kg of KU-32 to mice (20X > our typical dose) did not induce overt toxicity or histopathological changes on any of the organs examined. Moreover, weekly administration of KU-32 to STZ-diabetic mice rescued pre-existing mechanical and thermal hypoalgesia in addition to an improved motor and sensory nerve conduction velocity (NCV). However, mice with genetic ablation of the inducible HSP70 that developed similar diabetes-associated neurodysfunction failed to respond to KU-32. This suggests that HSP70 is essential in the mechanism of action of this compound. Of note, the neuroprotection in wild type mice occurred without a significant metabolic correction. Instead, *in vitro* assessments demonstrated that KU-32 directly protects unmyelinated and myelinated nerves against DPN-associated neuropathic changes. In particular, KU-32 dose-dependently prevented NRG1-induced myelin degeneration in myelinated sensory neuron/SC co-cultures, indicating a chaperone-mediated intervention of aberrant growth factor signaling (Urban et al., 2010). Since altered neuregulinism contributes to DPN in myelinated nerves, we sought to determine whether the requirement of Hsp70 in motor and sensory recovery by KU-32 correlates with the necessity of Hsp70 in protecting against NRG1-induced demyelination. To further test the hypothesis that Hsp70 may help tolerate and/or counteract otherwise pathogenic consequences of growth factor signaling, the present study also investigated the sufficiency of Hsp70 in inhibiting demyelination and the signaling events downstream of NRG1. In addition, the mechanism of Hsp70 induction by KU-32 is also explored.

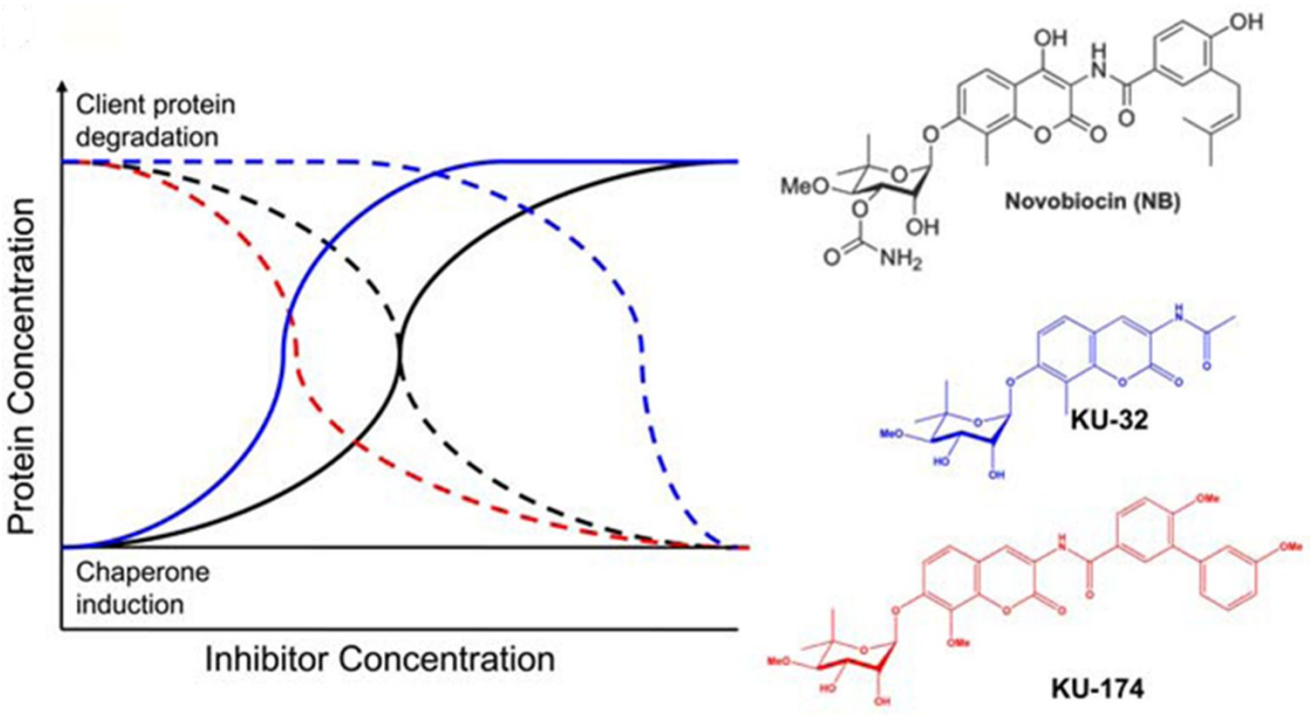

Figure 1.5.2b Structure-activity relationships of Novobiocin analogs in cytotoxicity vs. cytoprotection. Chemical structure of novobiocin compounds and schematic demonstration of dose effects in client protein degradation (dotted lines) and chaperone induction (solid lines) for novobiocin (black), KU-32 (blue) and KU-174.

Chapter 2: Materials and Methods

2.1 Materials

2.1.1 Animals

Breeding colonies of wildtype C57Bl/6 (WT) and Hsp70.1/70.3 double knockout (Hsp70 KO) mice on a C57Bl/6 background (B6;129S7-Hspa1a/Hspa1btm1Dix/Mmcd) (Hunt et al., 2004) were maintained with mice initially purchased from Harlan Laboratories (Indianapolis, IN) and the Mutant Mouse Resource Center (San Diego, CA), respectively. Absence of Hsp70.1 and 70.3 was confirmed by genotyping of genomic DNA and corroborated by lack of inducible Hsp70 protein expression as determined by immunoblot analysis. WT primers (forward-GTACACTTTAAACTCCCTCC; reverse-CTGCTTCTCTTGTCTTCG) amplified a 450 bp band while primers against the neo cassette (forward-ATGGGATCGGCCATTGA-ACAAG; reverse-ACTCGTCAAGAAGGCGATAGAAGG) amplified a 650bp band. The PCR conditions were (94^{o}C-5 min; 35 cycles of 94^{o}C-40 sec; 65^{o}C-1 min; 72^{o}C-40 sec; 72^{o}C- 5min) using KlenTaq polymerase (DNA Polymerase Technology, St Louis, MO) and 200-300 ng DNA template. Cav-1 double knockout mice were obtained from Jackson Laboratories (Bar Harbor, ME). Genetic deletion of Cav-1 and other phenotypic presentations in this strain have been characterized elsewhere by Razani *et al*.(2001).

All animals were housed at the Animal Care Unit at the University of Kansas in a 12hr light/dark cycle at 70ºF and 70% humidity, and given ad libitum access to Purina Diet 5001 Rodent Chow and water. Tissue isolation and animal euthanasia procedures were performed in accordance with protocols approved by the Institutional Animal Care and Use Committee in the University of Kansas and conformed to standards and regulations for the care and use of laboratory rodents set by the National Institutes of Health.

2.1.2 Antibodies

Table 2.1.3 List of Primary and Secondary Antibodies Utilized in the Study

Name	Provider	Catalog No.
Hsp70 (C92F3A-5)	Stressgen (now Enzo Life Sciences), Ann Arbor, MI, U.S.A.	SPA-810
Hsc70		SPA-815
Hsp90		SPA-830
Hsp40		
Hsp27 (C-20)	Santa Cruz Biotechnology, Santa Cruz, CA, U.S.A.	sc-1048
JNK (FL)		sc-571
phospho-JNK (G-7)		sc-6254
c-jun (N)		sc-45
phospho-c-jun	Cell Signaling Technology, Beverly, MA, U.S.A.	54B3
Erk	Cell Signaling Technology, Beverly, MA, U.S.A.	
phosphor-Erk	Cell Signaling Technology, Beverly, MA, U.S.A.	
S100β	DakoCytomation, Glostrup, Denmark	
MBP	Covance, Princeton, NJ, U.S.A.	SMI-94R
PGP9.5	Chemicon, Temecula, CA, U.S.A.	AB1761
Grp78 (H-129)	Santa Cruz Biotechnology, Santa Cruz, CA, U.S.A.	sc-13968
Grp94 (H-212)		sc-11402
Parp-1 (C-20)	Trevigen, Gaithersburg, MD, U.S.A.	4338-MC-50
GPR30	Novus Biologicals, Littleton, CO, U.S.A.	NLS4271
Cav-1 (N-20)	Santa Cruz Biotechnology, Santa Cruz, CA, U.S.A.	Sc-894
P0	Chemicon, Temecula, CA, U.S.A.	AB9352
FLAG (M2)	Stratagene	200472
Lamin A/C	Cell Signaling Technology, Beverly, MA, U.S.A.	2032
LDH	Abcam®, Cambridge, MA, U.S.A.	AB7639-1
sumo-2/3 (18H8)	Cell Signaling Technology, Beverly, MA, U.S.A.	49715
normal mouse IgG	Santa Cruz Biotechnology, Santa Cruz, CA, U.S.A.	sc-2025
horseradish peroxidase (HRP)-conjugated goat secondary antibodies	Santa Cruz Biotechnology, Santa Cruz, CA, U.S.A.	sc-2004; sc-2005
Alexa Fluor ® - conjugated goat/donkey secondary antibodies	Molecular Probes, Eugene, OR, U.S.A.	A11008;

2.1.3 Reagents

The synthesis and structural property of KU-32 was described previously (Burlison et al., 2006; Donnelly et al., 2008). For *in vitro* pharmacological treatment, KU-32 was dissolved in DMSO and diluted in cell medium to a working concentration of 1μM (0.05% DMSO as vehicle correspondingly). Dulbecco's modified Eagle's medium (DMEM) was obtained from Mediatech

(Manassas, VA). MG132 was purchased from Tocris (Ellisville, MO, U.S.A.). Ascorbic acid and collagen were both from Sigma (St.Louis, MO, U.S.A.). Neurobasal medium was obtained from GIBCO (Grand Island, NY, U.S.A.). Nuclear extract kit was purchased from Active Motif (Carlsbad, CA, U.S.A.). Two compounds, 17β-estradiol 3-benzoate and G-1, used in estrogen study were obtained from Sigma-Aldrich (St.Louis, MO, U.S.A.) and TOCRIS (Elliesville, MO, U.S.A.), respectively.

2.2 Methods

2.2.1 Preparation of Purified DRG Neurons, Unmyelinated and Myelinated DRG/SC Explants

DRG neurons were removed from C57Bl/6, Hsp70.1/70.3 double knockout or caveolin-1 double knockout mice (pups born at day 0 (P0) into L15 medium (Yu et al., 2008). Following dissociation of tissues using 0.25% trypsin and 0.5% collagenase at 37ºC for 30min, cells were collected by centrifugation for 5 min at 1,000 g and resuspended in DMEM containing 25mM glucose, 10% fetal calf serum (Atlas Biologicals, Fort Collins, CO, U.S.A.), triturated, counted with hematocytometer and seeded onto collagen-coated glass coverslips or dishes at a density of $6\text{-}7\times10^4$. The cultures were maintained in DMEM maintenance medium containing 100 U/mL penicillin, 100μg/mL streptomycin (Thermoscientific, Logan, UT, U.S.A.), 50μM gentamycin (MP Biologicals, Solon, OH, U.S.A.) and 50ng/mL nerve growth factor (Harlan Biosciences, Indianapolis, IN, U.S.A.). Fast-growing fibroblasts were removed by treating the cells with 10μM cytosine β-D-arabinoside for 2 days and cultures were maintained in regular medium for one week to allow SC proliferation and association with axons. Myelination was then initiated by addition of 50μg/ml ascorbic acid (to induce basal lamina formation) and allowed to myelinate for 18-21 days in culture with medium replenished every 2-3 days. 150-200ng/ml NRG1 (R&D Systems, Minneapolis, MN, U.S.A.) were administered to induce demyelination. To examine the

effect of KU-32 on preventing demyelination, the cells were incubated for 16hr with 0.05% DMSO (vehicle) or 1μM KU-32 prior to adding NRG1; demyelination was assessed 48 hr after adding NRG1. In instances where purified DRG sensory neurons were desired, the cells were treated with 10μM each of cytosine β-D-arabinoside and fluorodeoxyuridine for 2-3 days to eliminate proliferating cells in the culture. For the estrogen studies, cultures were allowed to myelinate for 14 days with the treatment of ascorbic acid, β-estradiol or G1 at the indicated concentrations.

2.2.2 Heat Shock Treatment

For heat-shock treatment, cell culture plates were sealed and floated in an enclosed water bath chamber with the temperature stabilized at 43-44ºC for 30min. Depending on the treatment paradigm, cells were either immediately collected or returned to the tissue culture incubator for additional treatments or recovery before cell lysis.

2.2.3 Biochemical Analysis

2.2.3a Immunoblotting

In preparing for immunoblot assessment, cells were rinsed with PBS, scraped off from plates with lysis buffer containing 50 mM Tris-HCl, pH 7.4, 150 mM NaCl, 1 mM EDTA, 1% NP-40, 1% deoxycholate, 0.1% SDS, 0.5 mM sodium orthovandate, 40 mM NaF, 10 mM b-glycerophosphate, and 1× ®Complete Protease Inhibitors (Roche Diagnostics) and homogenized by sonication. Soluble proteins were collected in the supernatant after centrifuging the crude cell lysates at 10,000g for 10 min at 4ºC; total protein concentration was determined using the Bio-Rad protein assay. Approximately 30-35μg of proteins were mixed with deionized water and loading buffer for separation by SDS-PAGE and transferred to nitrocellulose membrane (Bio-Rad Laboratories, Germany). Membranes were then incubated with 5% non-fat dry milk in

phosphate buffered saline for 1-2hr at room temperature (RT, 25ºC) and probed with primary antibodies recognizing Hsp70, Hsc70, Hsp90, Hsp40, Hsp27, c-jun, phosphor-c-jun, JNK or phospho-JNK at 4ºC overnight. β-actin was also probed as a loading control. For detection of phosphorylated protein, 5% non-fat dry milk was substituted with 5% bovine serum albumin to avoid non-specific blocking of the phosphoepitope. After primary antibody incubation, membranes were washed and further incubated with HRP-conjugated anti-mouse, anti-rabbit, anti-chicken or anti-goat secondary antibodies. Immunoreactivity for each protein was visualized using an enhanced chemiluminescence detection kit (GE Healthcare Life Sciences, Little Chalfont, Buckinghamshire, U.K.) and exposed to X-ray film, which was then digitally scanned and densitometrically analyzed using ImageJ (NIH) software.

2.2.3b Immunoprecipitation

In certain studies, coimmunoprecipitation assay was performed in order to determine specific protein-protein binding or post-translational protein modification. Briefly, cell or tissue lysates were pre-incubated with Protein G/A agarose beads to minimize non-specific interactions prior to antibody incubation at 4ºC overnight. Immune complexes were then collected via reincubation for 3hr at 4ºC with Protein G (Invitrogen, Carlsbad, CA, U.S.A.) or A (RepliGEn Corporation, Waltham, MA, U.S.A.) agarose beads. Beads were chosen according to the primary antibody species. After centrifugation, supernatant was removed and beads were washed 5 times with lysis buffer (NP40 or mRIPA buffer). Bound-proteins were then eluted with sample buffer and prepared for western blotting. In some cases the antibody was replaced by IgG to examine non-specific reaction of antibody with the protein of interest.

2.2.3c Nuclear Fractionation

HEK-293 cells were grown to confluence, rinsed and resuspended in PBS/phosphatase inhibitors. Cell pellets were then collected by centrifuging the cell suspension for 5min at 500 rpm 4ºC. After discarding the supernatant, pellets were resuspended in and incubated with hypotonic buffer on ice for 15min. Cells were fractionated by intensive vortexing with detergent for 10sec, followed by centrifugation at 14,000×g for 30sec at 4ºC. The supernatant was then collected as the cytoplasmic fraction. Nuclear pellets were resuspended in complete lysis buffer, vortexed and incubated for 30min on ice while rocking on a platform at 150rpm. After incubation, the suspension was vortex again for 30sec and centrifuged for 10min at 14,000×g at 4ºC. The solubilized nuclear fraction was then obtained by collecting the supernatant.

2.2.4 siRNA knockdown

MCF-7 cells were plated in 12-well plates at a density of 4×10^4 in complete medium (DMEM containing serum and antibiotics) and subjected to either of the following treatments: untransected, non-targeting siRNA (negative control) (Non-targeting #2) and Hsp90 siRNA (desired) (Hsp90AA1 3320, Hsp90AB1 3326, Dharmacon RNAi technologies, Thermo Scientific, Lafayette, CO, U.S.A.). Each treatment group was prepared in triplicate. 2hr prior to siRNA transection, cells were placed into OPTI-MEM®I reduced serum medium (antibiotic-free) (GIBCO, Grand Island, NY, U.S.A.) 20μM siRNA (stocking solution, in 1× siRNA buffer) was diluted into 1× siRNA buffer to obtain 5μM siRNA solution. To prepare for the transfection medium, 5μM siRNA and DharmaFECT®3 (Thermoscientific Dharmacon, Lafayette, CO, U.S.A.) transfection reagent were mixed with OPTI-MEM®I reduced serum medium in separate tubes and incubated for 5min at room temperature. siRNA were then mixed and incubated with DharmaFECT (in OPTI-MEM®I reduced serum medium) for 20min at room temperature. The mix was then combined with additional OPTI-MEM®I reduced serum medium to obtain the

transfection medium with a final siRNA concentration of 75nM. Previous cell media was removed and replaced with the transfection medium. Cells were then returned to tissue culture incubator (37ºC, 5% CO_2) and incubated for 72hr. If subsequent pharmacological treatments were desired, transfection medium was then replaced with complete medium containing treatments. Otherwise, cells were scraped and lysed for biochemical analysis. The specificity and efficiency of Hsp90 siRNA knockdown was assessed via immunoblotting for Hsp90 protein.

2.2.5 Immunoflourescence Analysis

2.2.5a Immunocytochemistry

After the indicated treatment, promyelinating or myelinated DRG/SC explants grown on glass coverslips were rinsed with PBS and fixed in 4% paraformaldehyde for 20 min at RT. The cells were permeabilized by incubating with cold methanol at -20ºC for 15 min, then blocked with 10% normal goat serum (Invitrogen, Carlsbad, CA) containing 0.3% Triton X-100 (Fisher Sientific, Fair Lawn, NJ, U.S.A.) for 15 min at RT. Primary antibodies against MBP (1:500), PGP9.5 (1:500), Hsp70 (1:80) and/or S100β (1:1000) were diluted in blocking buffer and incubated with cells overnight at 4ºC in a humidified chamber. The next day the cells were washed with PBS and incubated with the secondary antibody: Alexa Fluor 568, Alexa Fluor 488 or Alexa Fluor 647-conjugated goat anti-mouse IgG, goat anti-rabbit IgG, goat anti-donkey IgG or goat anti-chicken IgG. Coverslips were mounted on microscope slides (Fisher Scientific) with the aid of Prolong Antifade kit with or without DAPI (4',6-diamidino-2-phenylindole) counterstain. Slides were imaged using an Olympus/3I Spinning Disk Confocal/TIRF Inverted Microscope and 6-8 random fields per coverslip were captured using the imaging software, SlideBook 5.0 (Intelligent Imaging Innovations, Inc., Denver, CO, U.S.A.).

For demyelination assessment, MBP-positive segments were counted as internodes and the percent of broken versus total internodes was calculated and expressed as a percent of degenerated segments for each picture frame. Changes in internodal length were quantified utilizing an open source imaging software-CellProfiler (http://www.cellprofiler.org). Individual myelin internodes with a length within the range of 20-200 microns were identified through Otsu's method (Otsu, 1979) for thresholding and segmentation (Figure 2.2.5a). Throughout image processing, visual inspection and manual editing were performed during internode identification in cases of errors or regions where segments intersect or touch the border. Major axis length for each identified segment were then computed to represent length of the internodes and included in the average of the population of segments surveyed. For immunofluorescent quantification of Hsp70 expression in premyelinating cultures, intensity was set as the thresholding factor for subject identification instead of length. Hsp70 expression was computed as area × intensity in fluorescence units and normalized to PGP9.5 immunoreactivity. Colocalization of fluorescent channels was achieved using ImageJ (NIH).

In the estrogen studies, a random microscope area of $24x10^6$ micron² in each coverslip was selected and montage image generated using SlideBook 4.0. Myelinated segments were visually identified and manually selected. Total number of segments in each montage image was manually counted whereas the internodal length was automatically computed by SlideBook 4.0 for each segment and expressed as the longest cord length.

A.

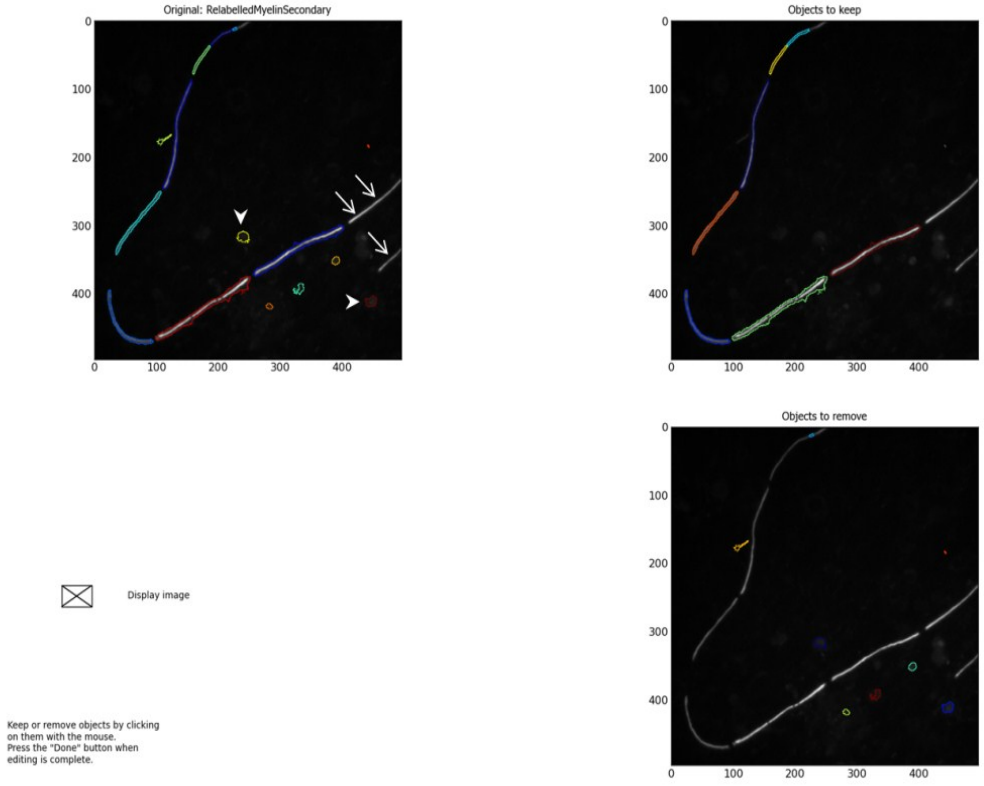
Original: RelabelledMyelinSecondary
Objects to keep
Objects to remove
Display image
Keep or remove objects by clicking
on them with the mouse.
Press the "Done" button when
editing is complete.

B.

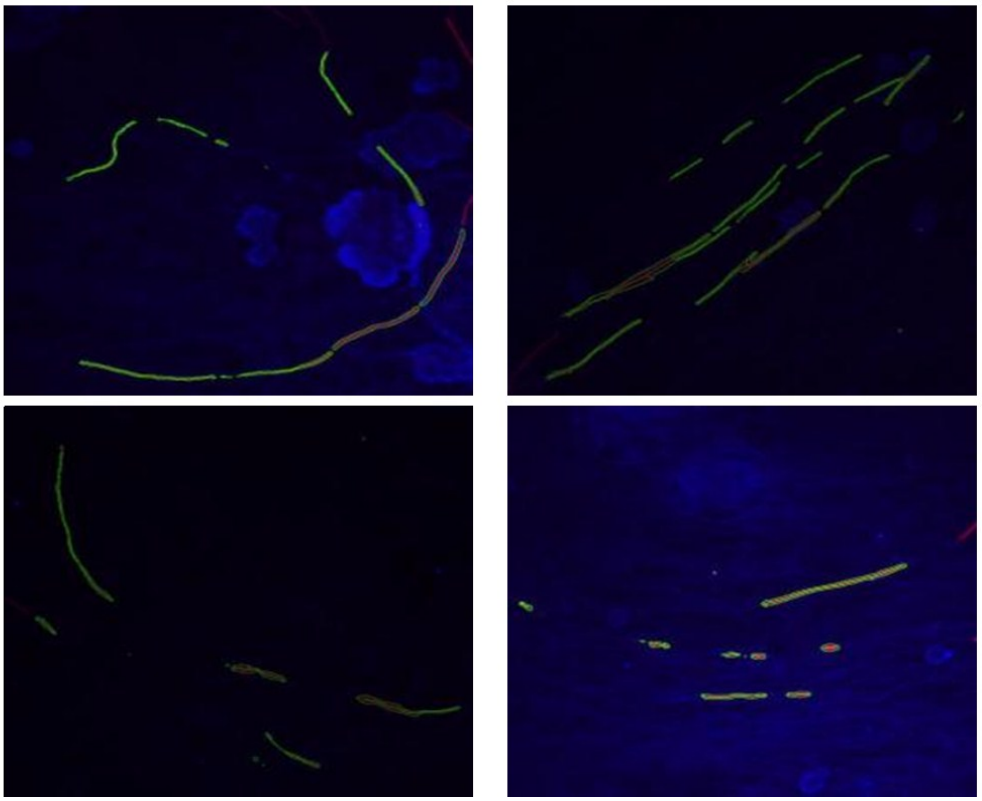

Figure 2.2.5a Identification of MBP segments by CellProfiler. A) An example showing how MBP segments were identified through a combination of automatic identification and manual editing using CellProfiler. In a given input image (e.g., MBP-stained internodes), fluorescent fragments with a major axis length between 20-200μM were identified by CellProfiler and treated as individual objects. Segments touching the borders (arrows) or crossing were automatically excluded from the surveying pool. Some of the MBP-positive cells that are not internodes (arrowheads) were visually inspected and manually edited out if identified by the program. **B)** Following object identification, CellProfiler computed the major axis length and area occupied by each segment identified in each image. Values for average length and area of internodes (delineated in green) were normalized to the corresponding PGP9.5 area after matching the MBP and PGP9.5 fluorescent channels (aritificially assigned green and blue during image processing).

2.2.6 Sciatic Nerve Cross/longitudinal sections

Sciatic nerves were dissected from approximately one month old C57Bl6 mice immediately after euthanasia and fixed in Zamboni's fixative (3% paraformaldehyde, 15% picric acid) (Newcomer Supply, Middleton, WI) RT for 1hr. Tissues were then washed 5 min with PBS containing sodium azide for 3 times before placed into 30% sucrose (in PBS) overnight for cryoprotection. Upon sectioning, nerves were embedded in Tissue-Tek optimal cutting temperature compound (OCT) on dry ice (Sakura USA, Torrence, CA). Frozen nerves were kept at -20ºC in cryostat while sectioned transversely or longitudinally at 10 or 8 micron onto Fisherbrand Superfrost Plus microscope slides (Fisher Scientific, Pittsburgh, PA), respectively. Slides were allowed to warm up to RT prior to immunolabeling as described above.

2.2.7 Recombinant Adenovirus Preparation and Infection

2.2.7a Hsp70 Sense Adenovirus

The cDNA sequence of Homo sapiens heat shock 70kDa protein 1A (HSPA1A) in pcDNA5 vector was amplified by PCR reaction with a forward primer containing a BamHI site (AGCTTGGATCCGAATTCACCATGGCC), and a reverse primer containing a SalI site (GACAAGTCGACATCTACCTCCTCAAT). The PCR product was subsequently digested and cloned into the p-Shuttle-IRES-hrGFP-1 vector between the Bgl II and Sal I site to add an in-

frame C-terminal FLAG tag. The integrity of the sequence was verified by DNA sequencing. The p-Shuttle-IRES-hrGFP-1 plasmid containing the Hsp70 insert was linearized with PmeI. The DNA was phenol-chloroform extracted after digestion. The PmeI digested plasmid was then transformed into electrocompetent E. coli BJ5183 cells containing the pAdEasy-1 adenovirus backbone vector using the pAdEasy kit as per the manufacturer's directions (Agilent Technologies, LaJolla, CA). Recombinant adenoviral plasmid was digested with PacI, ethanol precipitated and resuspended in sterile water. 12μg digested plasmid was tranfected into one T-75 flask of 293 cells with standard transfection using Lipofectamine 2000. Cells were collected 14 days after transfection and lysed through four freeze/thaw/vortex cycles; the supernatants were used to infect ten more confluent T-75 flask of 293 cells. The cells were collected 5 days post infection, and lysed as described above. The virus supernatant was concentrated by a CsCl gradient ultracentrifuge. Virus fraction was collected and mixed with equal volume 2X storage buffer (10mM Tris, pH8.0, 100mM NaCl, 0.1% BSA, and 50% glycerol, filter sterilized), and stored at -80ºC in aliquots. To infect myelinated neuronal cultures, concentrated viral particles were diluted in cell medium to appropriate concentration. 16hr after infection, cell medium was replaced by fresh non-viral medium for NRG1 treatment. Recombinant expression of Hsp70 was confirmed by antibodies against Hsp70 and the C-terminal FLAG epitope.

2.2.7b GPR30 siRNA adenovirus

GPR30 siRNA adenovirus was generated and evaluated as described previously (McAllister et al., 2012). In brief, GPR30 siRNA sequences were: GPR30-737 (sense: AGCCTGTGCTATTCCCTCATTTTT, antisense: AATGAGGGAATAGCACAGGCTTTT); GPR30-1135 (sense: AACGGAGCAGTCAGATGTCAAGTTCATTTT, antisense: ATGAACTTGACATCTGACTGCTCCGTTTTT); GPR30-402 (sense:

AGGACGAGCAGTATTACGATTTTT, antisense: AATCGTAATACTGCTCGTCCTTTT); and GPR30-272 (sense: AGCAACATCCTCATCTTGGTGGTGAATTTT, antisense: ATTCACCACCAAGATGAGGATGTTGCTTTT). The mismatch sequences were GPR30-1135mis (sense: AACGGACGGACTTGTAGAACTAGTCATTTT, antisense: ATGACTAGTTCTACAAGTCCGTCCGTTTTT) and GPR30-402mis (sense: AGGAACGATATGCATGCGATTTTT, antisense: AATCGCATGCATATCGTTCCTTTT). Target sequences were cloned into pSES-HUS vector, which is a shuttle vector for adenovirus and contains a red fluorescent protein (RFP). Expression of RFP was used to indicate the level of GPR30 siRNA expression.

2.2.8 Calcein AM Cell Viability Assay

Fresh isolated DRG explants were seeded at a density of 25,000-30,000/well in Neurobasal medium with 1 × B-27 supplements, 2mM glutamate, 100 U/mL penicillin, 100μg/mL streptomycin and 50ng/ml NGF in black-walled 96-well microplates. The next day, 10μM cytosine β-D-arabinoside was added to the medium for 24hr to remove fibroblasts. The cells were then switched to the maintenance medium (Neurobasal medium, 50ng/ml NGF, 1×B-27 supplements) and treated with 1μM KU-32 overnight. The 3-day-old cells were then stressed with 45mM glucose for 4hr and the media supplement was replaced with 50μl PBS plus 50μl freshly prepared 2X Calcein AM (2μM working concentration) (Invitrogen, Eugene, Oregon, U.S.A.) for a 30-min incubation at normal culture conditions. Calcein fluorescence was then recorded using a 490nm excitation filter and a 520nm emission filter. Since only live cells maintain the activity of intracellular esterase which hydrolyzes non-fluorescent Calcein AM into the strongly-fluorescent Calcein (Figure 2.2.8), the fluorescence intensity is proportional to the

number of viable cells. To control for cell population variability, results were expressed as fluorescence readings divided by protein concentration in each well.

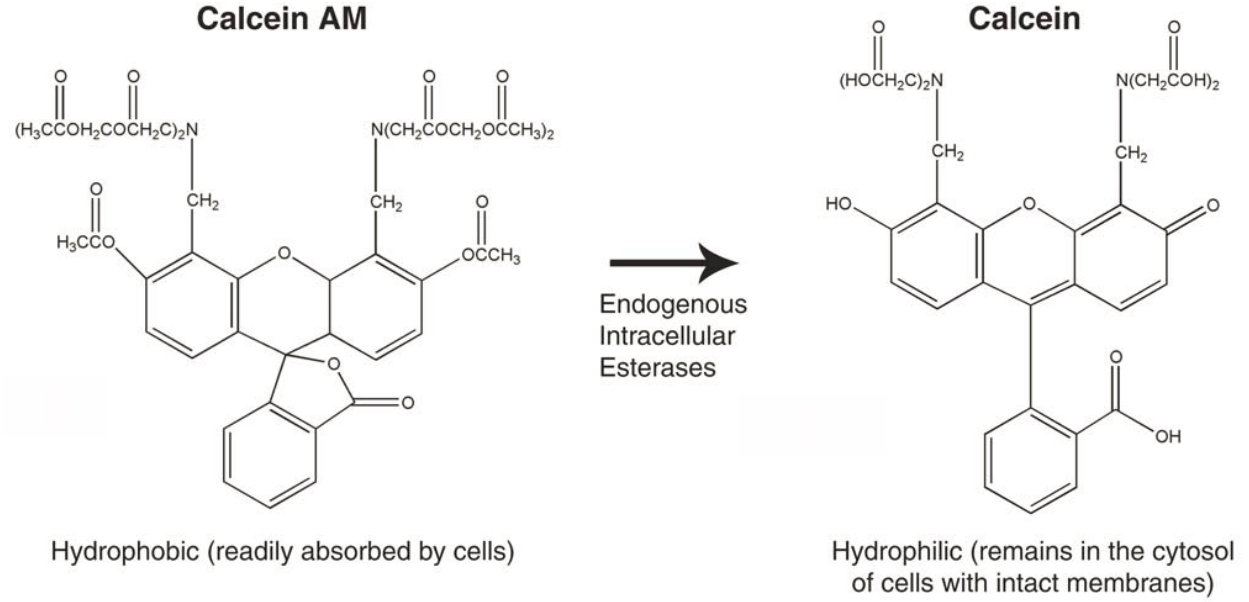

Figure 2.2.8 Hydrolysis of Calcein AM to Calcein. The acetomethoxy derivate of calcein (Calcein AM) is a non-fluorescent, hydrophobic compound that can easily permeate through the cellular membrane of intact, live cells where it is hydrolyzed to calcein through removal of acetomethoxy group by intracellular esterases. Calcein is a hydrophilic compound that is well-retained in cell cytoplasm with intact plasma membranes and produces strong green fluorescence.

2.2.9 Statistical Analysis

Data sets subjected to statistical analysis were presented as arithmetic mean±S.E.M unless otherwise specified. Equality of variances and one-way ANOVA were verified and performed using Systat 12 (Systat Software, Chicago, IL). Differences among treatment groups were considered statistically significant when $p<0.05$, which is determined by Tukey's Honestly-Significant-Difference-Test. To further denote degree of significance, * = $p<0.05$; ** = $p<0.01$; *** = $p<0.001$.

Chapter 3: Inhibition of NRG1-induced Peripheral Demyelination by Small Molecule Hsp90 Modulator

3.1 KU-32 induces HSP expression in an Hsp90-dependent manner

KU-32 is a novobiocin analogue that presumably binds to the nucleotide-binding site at Hsp90 C-terminal domain, which facilitates ATP/ADP exchange at the N-terminus (Peterson and Blagg, 2009). Occupation of this site by coumarin antibiotics such as novobiocin disrupts this function and inhibits Hsp90 activity. Such mechanism of inhibition is distinct from that of conventional N-terminal Hsp90 inhibitors but has produced similar effects in increasing HSP transcription and neuroprotection (Ansar et al., 2007). To verify the specific interaction of KU-32 with Hsp90 in inducing HSP, we examined the expression of a group of HSP after KU-32 treatment with or without Hsp90 silencing. If KU-32 activates chaperone induction through Hsp90 modulation, downregulation of Hsp90 should diminish HSP induction by KU-32. Consistent with this hypothesis, KU-32 led to a 30% increase in Hsp70 and Hsp40 expression in MCF-7 cells, whereas previous transfection of siRNAs directed against Hsp90α,β but not off-sequence control siRNAs mitigated this induction (Figure 3.1.1). Of note, neither Hsp90 knockdown nor non-targeted transfection affected the steady-state levels of these HSPs (Figure 3.1.2). This indicates that inhibition of KU-32-induced HSR was not the result of a broad cellular HSP downregulation. Therefore, Hsp90 plays a central role in KU-32-mediated chaperone upregulation. Interestingly, siRNA-mediated knockdown of Hsp90 did not reduce Hsp27 expression in response to KU-32, suggesting that other molecular targets might be involved in Hsp27 induction by this compound.

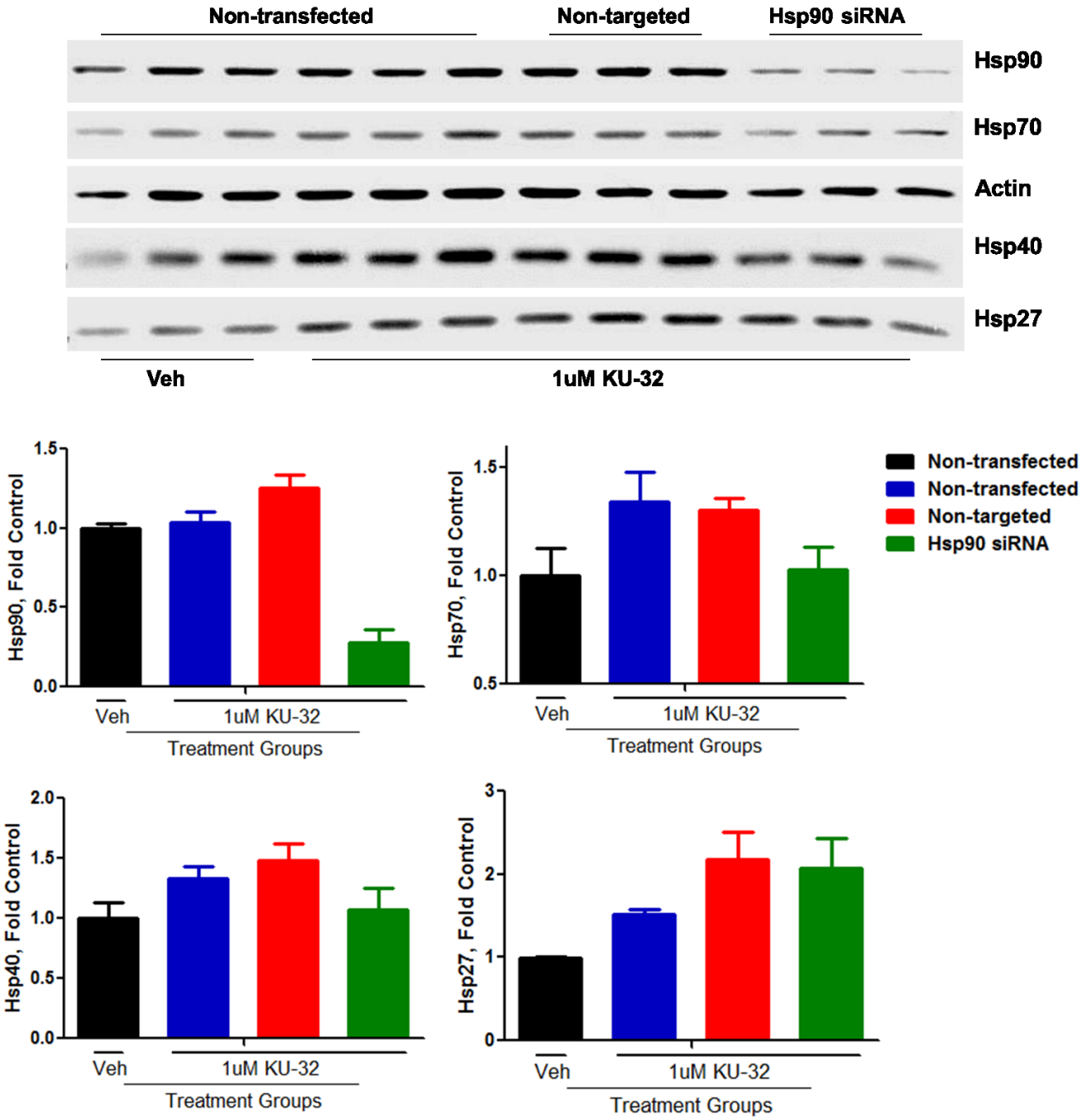

Figure 3.1.1 Hsp90 silencing mitigates KU-32-induced Hsp70 and Hsp40 expression. MCF-7 cells were transfected with non-targeted siRNAs or siRNAs directed against Hsp90α and β isoforms in the presence or absence of 1μM KU-32. Hsp90, Hsp70, Hsp40 and Hsp27 protein expression were then determined by immunoblotting and compared to untransfected control. β-actin level was used to normalize the chaperone expression.

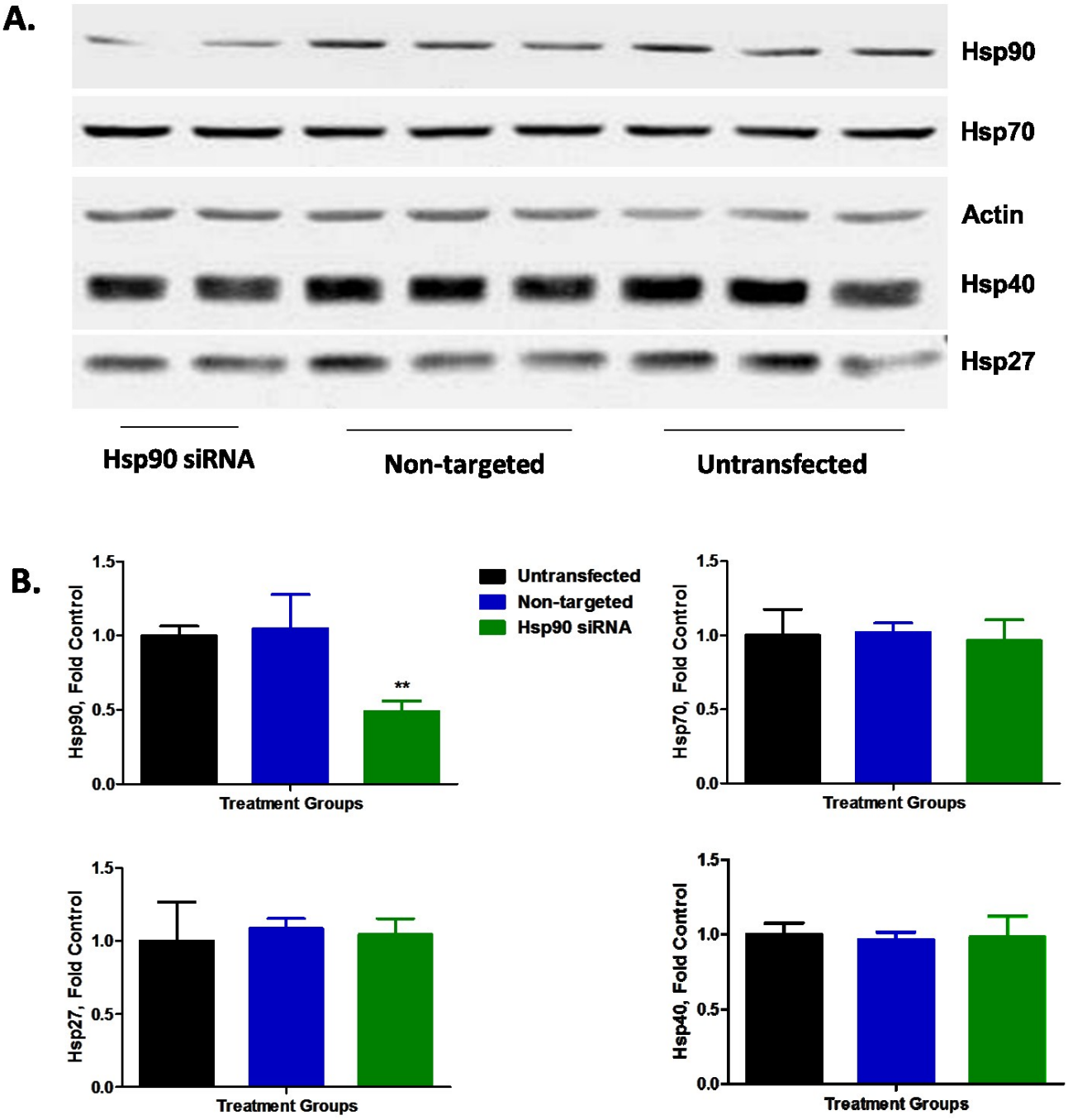

Figure 3.1.2 Hsp90 knockdown does not alter steady-state HSP expression. As above, MCF-7 cells were transfected with Hsp90-specific or off-sequence siRNAs, or left untransfected. **A)** HSP protein levels were assessed using immunoblotting. **B)** Graph quantitation represents average of 3 independent experiments. One-way ANOVA indicates a significant difference for Hsp90 [$F_{(2, 23)}$=10.902; p<0.01] but no difference for Hsp70 [$F_{(2, 23)}$=0.934; p=0.771], Hsp40 [$F_{(2, 23)}$=0.763; p=0.82] and Hsp27 [$F_{(2, 23)}$=1.374; p=0.369]. Tukey's Posthoc Test indicates **p<0.01 for Hsp90 siRNA *vs.* Untransfected. n=6-9. Degree of freedom (df) =2.

3.2 KU-32 Selectively Induces Hsp70 Expression in Myelinating Sensory Nerves

While an array of Hsp90 inhibitors have demonstrated potent HSR induction in pure neuron or glial cell cultures, scant attention has been given to characterize HSP and HSR expression in a population of mixed neurons and glia despite the physiological relevance of this system. Indeed, profound changes can occur in cellular phenotype as well as the pool of gene expression upon axoglial association (Mitchell et al., 1990; Parkinson et al., 2008). We have previously shown that KU-32 inhibited NRG1-induced demyelination in an Hsp70-dependent manner but it remained unclear if neuroprotection may also be associated with the induction of other chaperones. Immunoblot analysis of unmyelinated DRG explant cultures treated with 1μM KU-32 for 4-24 hr indicated that Hsp70 was the primary chaperone upregulated by KU-32 (Fig. 3.1.3). Though Hsp90 and Hsp40 can be induced in response to heat shock, KU-32 did not significantly increase their expression. Similarly, the drug did not alter the level of the constitutively expressed Hsp70 paralog, Hsc70 (Figure 3.3.1B). Although KU-32 did tend to increase the expression of Hsp27, a small Hsp that may be involved in transiently stabilizing mis-folded or damaged proteins until their interaction with Hsp70/Hsp40 (Muchowski and Wacker, 2005), this did not quite reach significance. Since vehicle itself did not change any of the protein levels within the experiment time, induction of HSP by KU-32 was compared to24 hr vehicle-treated cultures. Of note, the basal protein expression of inducible Hsp70 was almost undetectable but increased in response to KU-32 in a time-dependent manner and reached an approximately 4-fold induction at 24 hr of KU-32 treatment (Figure 3.2.1A,C). On the contrary, Hsc70 (Figure 3.3.1B), Hsp90 and Hsp40 that did not respond to KU-32 are abundantly expressed in the nerves. This agrees with our previous observation that KU-32 only weakly

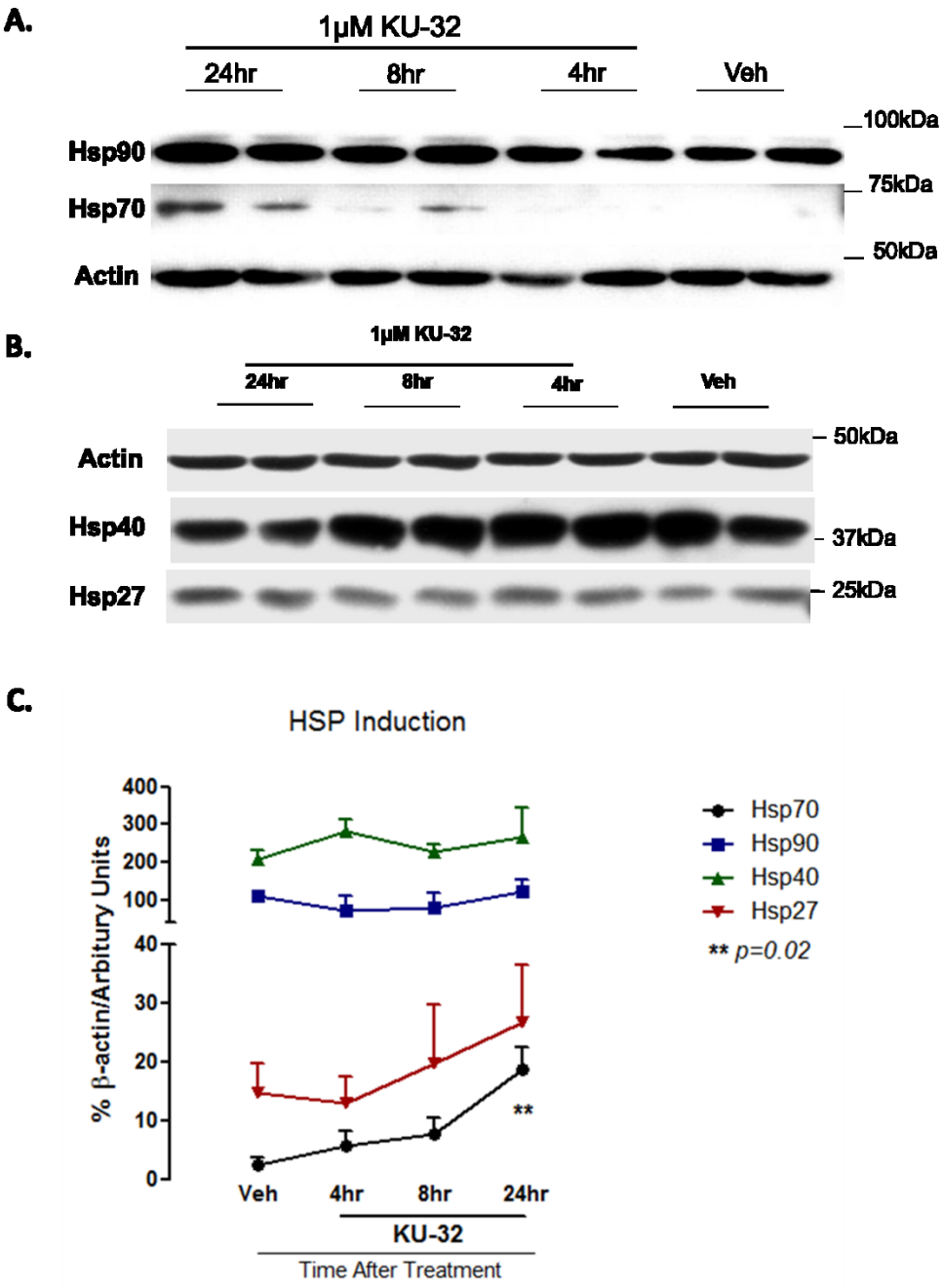

Figure 3.2.1 The steady state protein expression of the inducible Hsp70 is minimal in sensory explants but is increased by KU-32. Primary neonatal mouse DRG explants from either C57Bl6 were isolated and grown in culture for 1 week while fibroblasts were eliminated with antimitotics (Urban et al., 2010). Cultures were treated with 1μM KU-32 or vehicle (0.05% DMSO in deionized water). Cell lysates were collected at 4, 8 or 24hr and immunoblotted for Hsp90, 70, 40 and 27 contents. HSP levels were normalized to β-actin (loading control) for each time point and compared to that of 24hr vehicle treatment. (n=3-6 at each time point) ***p=0.02* for KU-32 vs. veh. Blotting procedure, conditions and exposure time were kept consistent for each protein. Due to the stronger sensitivity of Hsp40 antibody as compared to β-actin, Hsp40 vs. β-actin ratio was around 200%.

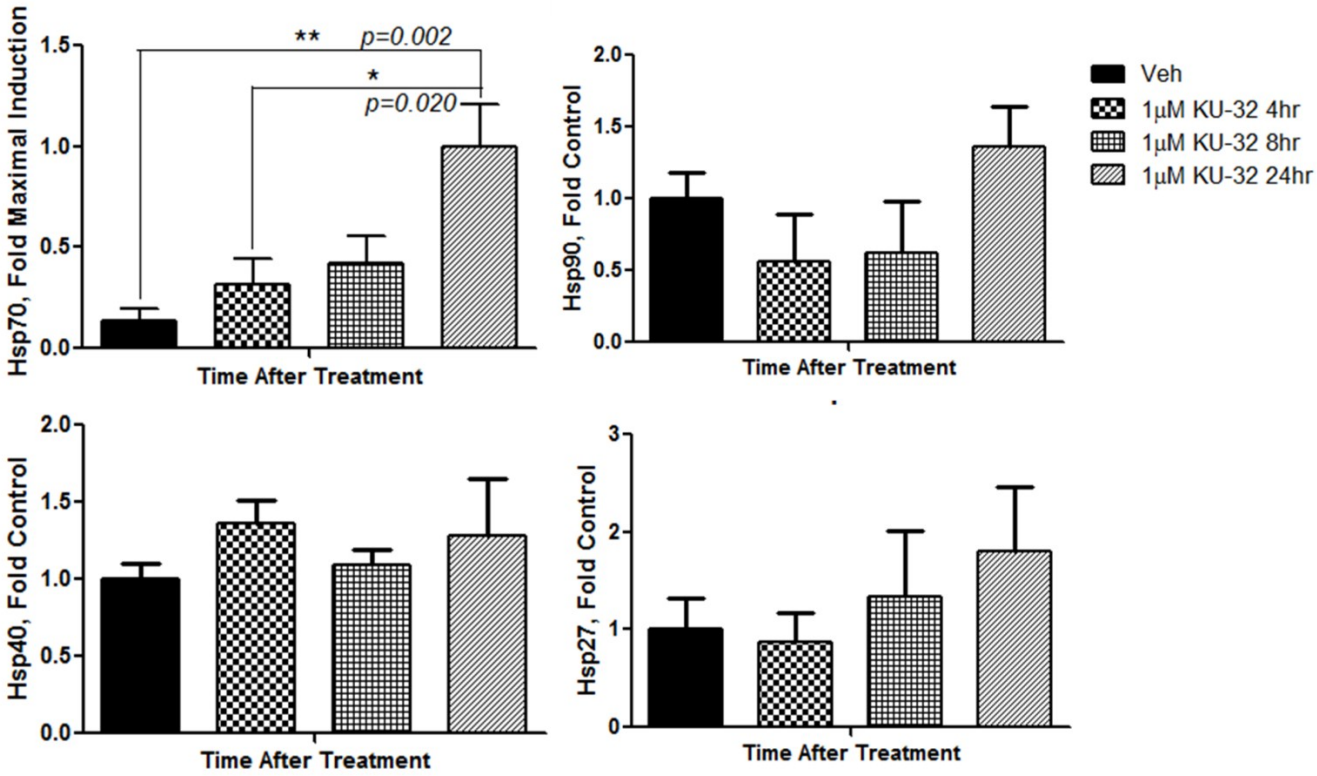

Figure 3.2.2 KU-32 specifically induces Hsp70 but not other HSP expression in DRG explants. Protein expressed as fold control (vehicle treated). One-way ANOVA analysis indicates a significant difference for Hsp70 expression [$F_{(3,18)}$= 6.970; p<0.01], but no difference for Hsp90 [$F_{(3,18)}$=1.697; p=0.206], Hsp40 [$F_{(3,18)}$= 0.581; p=0.637] and Hsp27 [$F_{(3,18)}$=0.678; p=0.576] expression. Tukey's post-hoc honestly-significant test indicates **p<0.01 for 24hr KU-32 vs. veh. *$p<0.05$ for 24hr KU-32 vs. 4hr KU-32 for Hsp70 expression. df=3.

activates heat shock elements as compared to the prototypical Hsp90 N-terminal inhibitor geldanamycin in an Hsp70 promoter-driven luciferase reporter assay (Farmer et al., 2012).

Though these data indicate that Hsp70 is the primary chaperone whose expression is modulated by KU-32, immunoblot analysis of the unmyelinated DRG explants did not allow us to assess whether induction of Hsp70 was occurring within sensory neurons or Schwann cells. We next examined whether the induction of Hsp70 by KU-32 is a result of neuronal or glial influence or both. DRG explants from C57Bl/6 mice were treated with either vehicle or KU-32 for 4hr and processed for immunostaining. A 30-min heat-shock (HS) followed by 1hr recovery was applied to a parallel set of cultures and served as a positive control.

To characterize Hsp70 expression in the mixed culture, cells were double-immunolabeled with antibodies against Hsp70 and neuronal (PGP9.5) or the SC marker (S100β) following. As shown in Fig. 3.2.2A, a low basal level of Hsp70 fluorescence co-localized with PGP9.5 but this was limited to the cell body and was not observed within axons. Subsequent to KU-32 treatment, Hsp70 staining was increased but this signal did not co-localize with PGP9.5. Short term HS also increased Hsp70 expression and this occurred in neurons and the glial cells. Co-staining of Hsp70 and S100β in the explants indicated a prominent expression of Hsp70 in cells labeled with the SC marker S100β, further verifying that KU-32 was increasing Hsp70 within SCs (Fig. 3.2.3). Notably, both 1μM KU-32 and HS plus recovery increased the localization of Hsp70 in the extending processes of SCs. Such increases correlated with a total of ~50% and ~150% induction of Hsp70 by KU-32 and HS versus vehicle, respectively. (Hsp70 fluorescence in these images was quantified by area×intensity) (Figure 3.2.2B). Next, to corroborate this distinct Hsp70 staining in neurons and glia by biochemical analysis, a more enriched sensory neuron culture was prepared by depleting the SCs from the explants using anti-mitotics (Figure 3.2.4A,B). Compared to explants that were not subjected to intensive anti-mitotics, Hsp70 basal expression was decreased in the more purified sensory neurons and its expression was not enhanced by KU-32. In contrast, the presence of SCs in the cultures increased basal level of Hsp70 and KU-32 treatment increased its expression. In addition, Hsp90 also appears to preferentially express in SCs as purified DRGs contained significantly lower Hsp90 compared to a similar population of mixed cultures. On the other hand, expression of Hsp40 and Hsp27 do not seem to differ in terms of treatment or neuron-glial population. Diminution of SC population in DRG explants was verified by significantly reduced S100β immunoreactivity from DRG lysates receiving intensive treatment of mitotic inhibitors (Figure 3.2.5). To further confirm this differential cellular

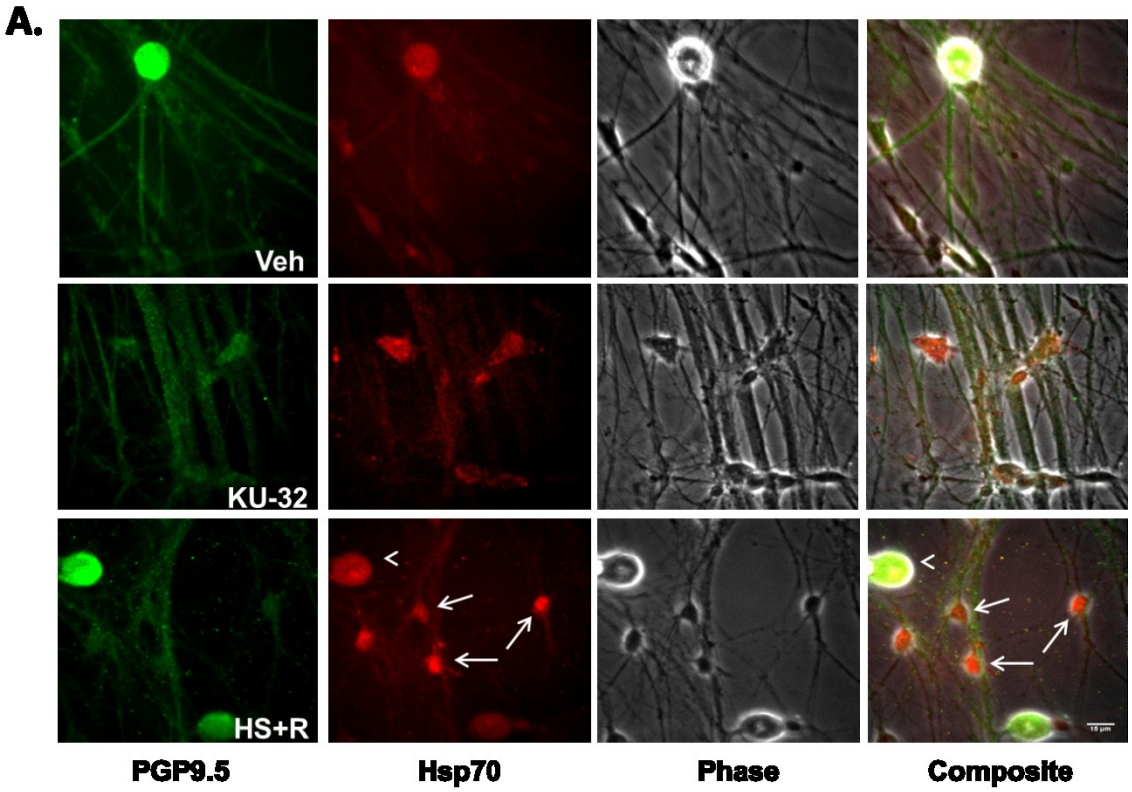

Figure 3.2.3 Inducible Hsp70 is primarily localized to neuronal cell bodies and SCs but not axons in peripheral nerves. A) Primary neonatal mouse sensory neurons were extracted from C57Bl6 mice and maintained in culture for 1 week. Cells were then treated with vehicle or 1μM KU-32 for 4hr, or subjected to 30min HS plus 1hr chase. Cellular localization of Hsp70 expression or induction was achieved by double-fluorescence labeling using antibodies against Hsp70 (red) and PGP9.5 (green). Confocal images were taken under a 40X objective and colocalization of Hsp70 with either PGP9.5 or S100β was performed using ImageJ. **B)** Overall Hsp70 fluorescence was quantified using CellProfiler as an indication of the gross abundance of protein expression. Arrowhead indicates the neuron cell body; arrow indicates increased Hsp70 in SCs. One-way ANOVA analysis indicates a significant difference among groups [$F_{(2,6)}$=12.369; p<0.01]. Tukey's post-hoc test indicates **p<0.01 for HS vs. Control, n=3, df=2.

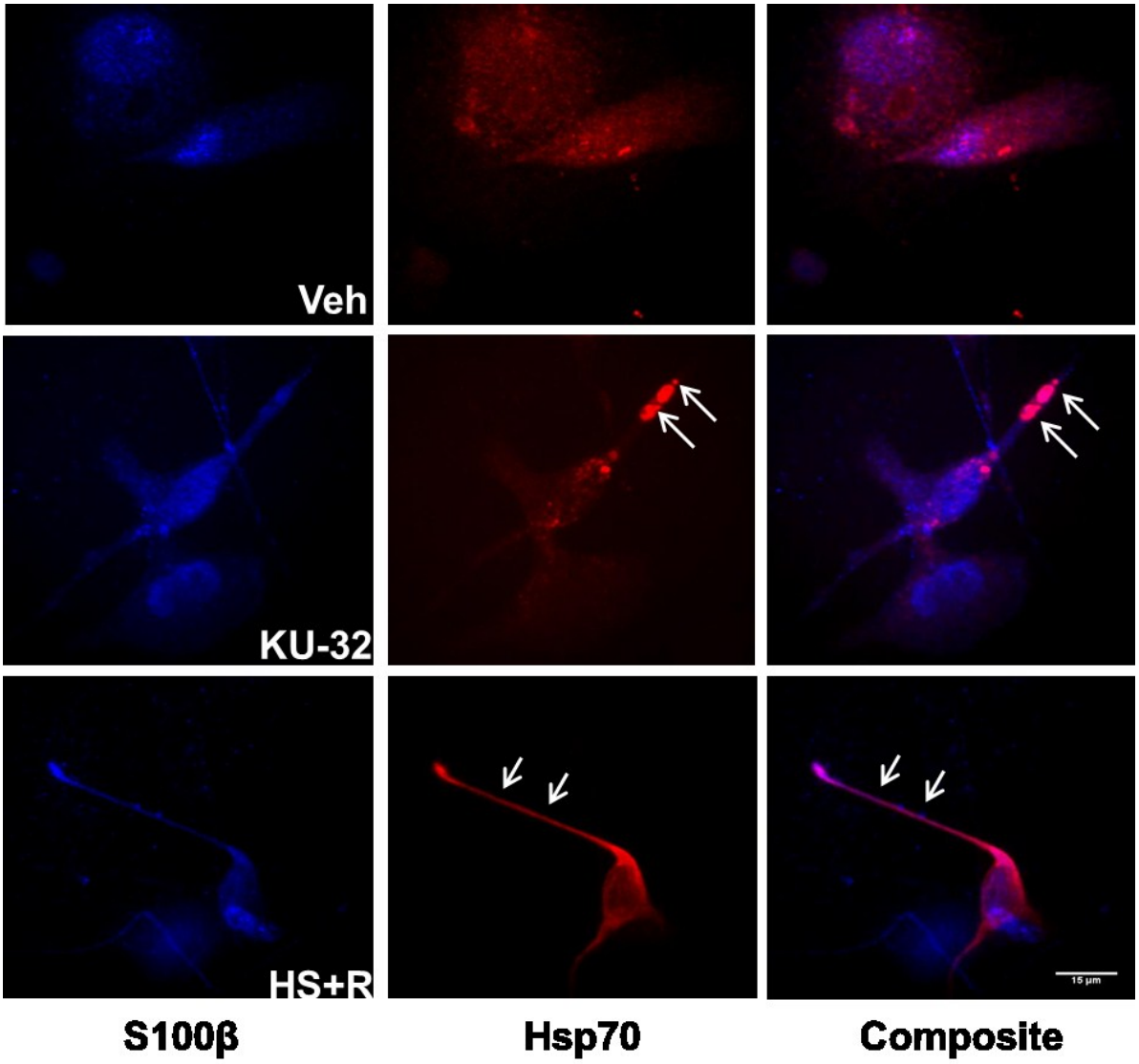

Figure 3.2.4 KU-32 or HS enhances Hsp70 expression in SC processes. Similar to described in Figure 3.1.2, 1 week old C57Bl/6 DRG/SC mixed cultures were immunostained with S100β (blue) and Hsp70 (red) antibodies following exposure to vehicle, KU-32 or HS. Both drug treatment and HS enhanced the immunofluorescent distribution of Hsp70 in SC processes. Experiments were performed twice.

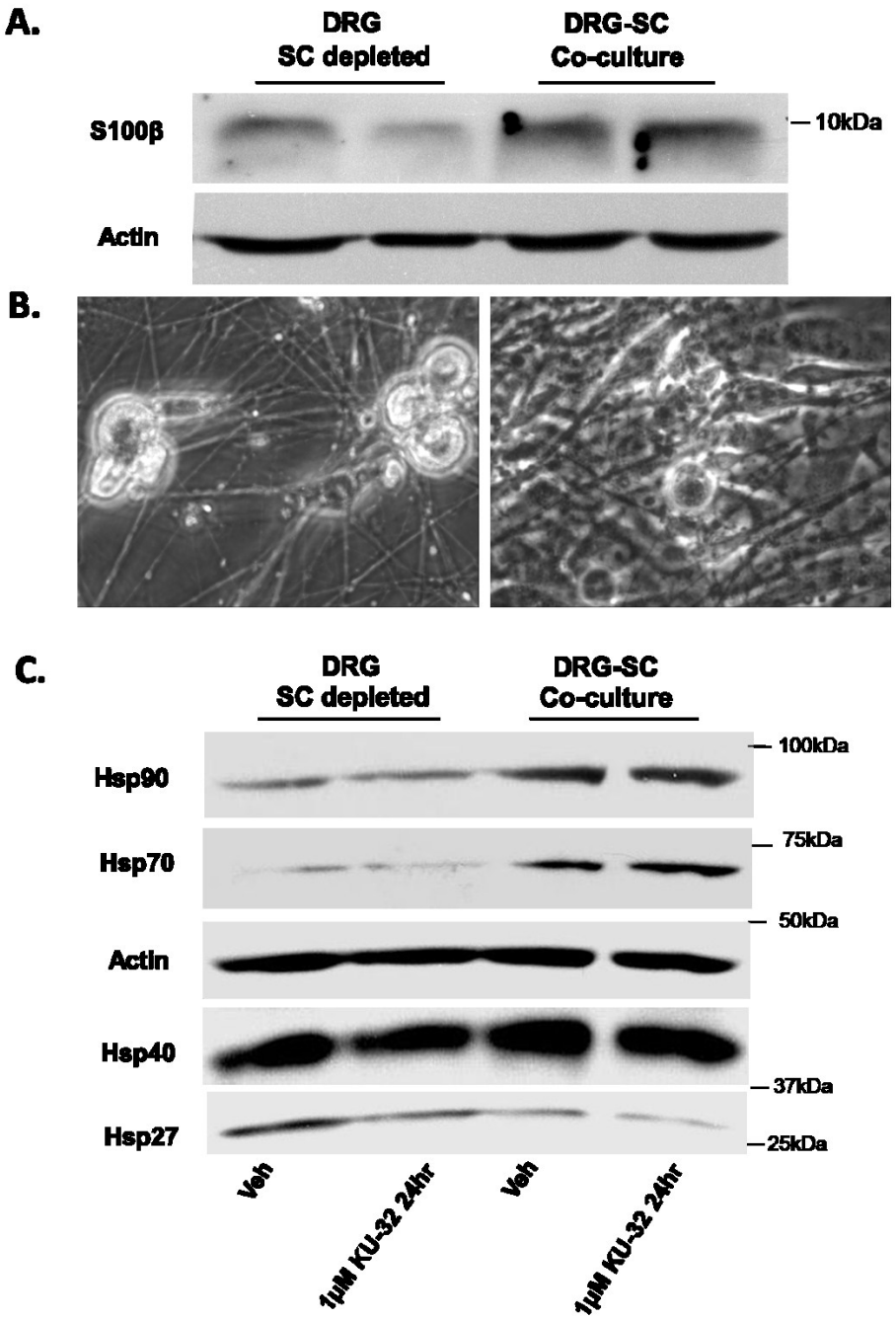

Figure 3.2.5 SC depletion attenuates basal and KU-32-induced Hsp70 expression in DRG explants. SC-free DRG cultures were obtained through prolonged (2-3days) treatment of excised sensory explants with double antimitotics (cytosine β-D-arabinoside and fluorodeoxyuridine). **A)** SC content and depletion of SCs in DRG cultures was verified and assessed using immunoblotting for SC-specific marker S100β. **B)** Phase-contrast images of SC-depleted and mixed DRG cultures. **C)** Expression of Hsp70, Hsp90, Hsp40 and Hsp27 in these purified neurons was examined and compared to mixed DRG/SC explants in the presence or absence of KU-32. Blots shown are representatives of two independent experiments.

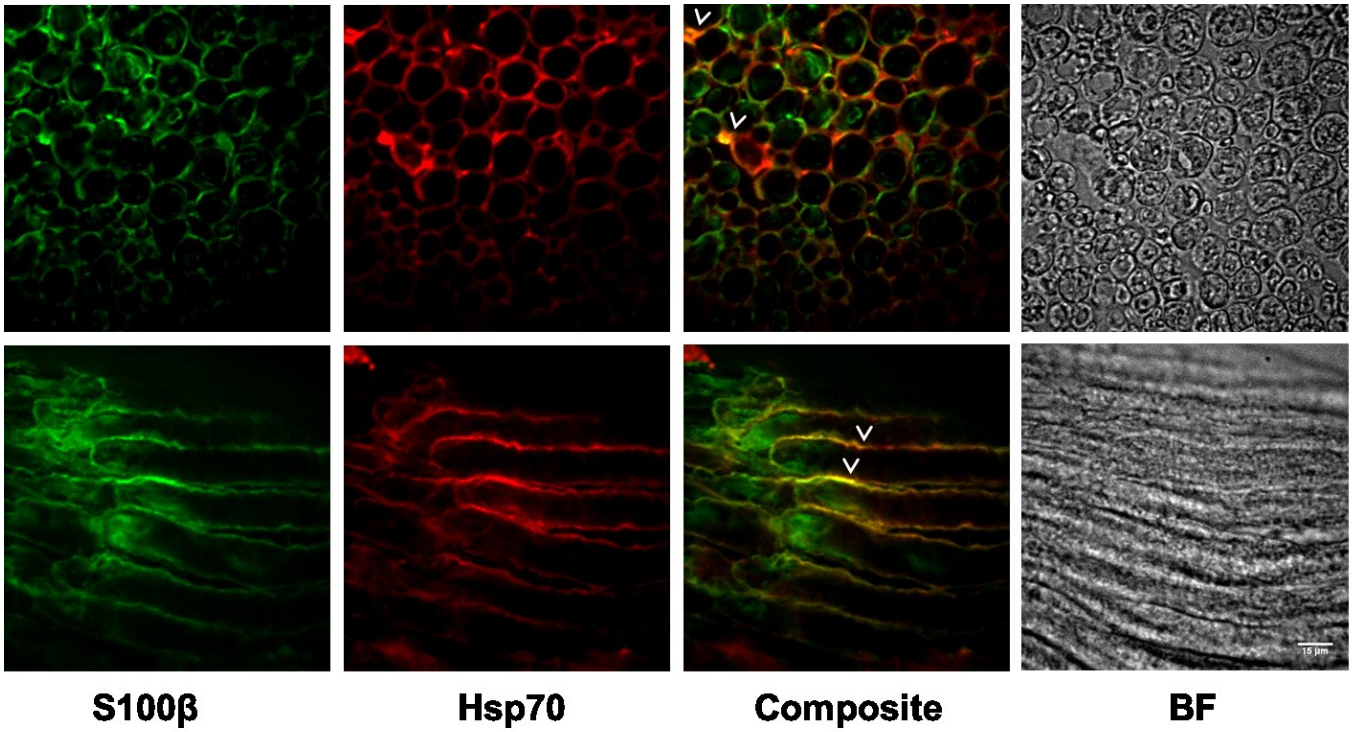

Figure 3.2.6 Hsp70 co-localizes with S100β in mice sciatic nerves. Sciatic nerves were removed from ~1 month-old C57Bl (WT) mice and fixed using 4% paraformaldehyde and cryoprotected using 30% sucrose before embedded into tissue tek for freeze-sectioning (cross-section [10-micron]: upper panel; longitudinal section [8-micron]: lower panel). Sections were then labeled with S100β (green) and Hsp70 (red). Arrowheads indicate co-localization of protein expression. BF denotes bright field.

distribution of Hsp70 *in vivo*, cross- or longitudinal sections were prepared from sciatic nerves from C57Bl6 mice and immunostained for Hsp70 expression. In both longitudinal and crosssections, Hsp70 immunoreactivity significantly overlapped with that of S100β in tissues surrounding axons, indicating that Hsp70 is primarily located in axon-ensheathing SCs in the nerves (Figure 3.3.5). Together, these data provide evidence that KU-32 elicits a weak HSR that is primarily of glia origin in the peripheral nerve.

3.3 Hsp70 is necessary for KU-32 to protect against NRG1-induced demyelination

To assess whether induction of Hsp70 expression by KU-32 is critical to the myelin protection against pathological NRG1 signaling, we prepared myelinated DRG explants from neonatal C57Bl/6 (wildtype) and Hsp70.1/70.3 double knockout ($Hsp70^{-/-}$) mice as described in the methods. Deletion of these two genes resulted in the abrogation of the inducible Hsp70 without affecting the constitutively expressed Hsc70 in knockouts. This absence was verified by genotyping and further confirmed by the inability of heat-shock to elicit Hsp70 expression in cultured explants (Figure 3.3.1).

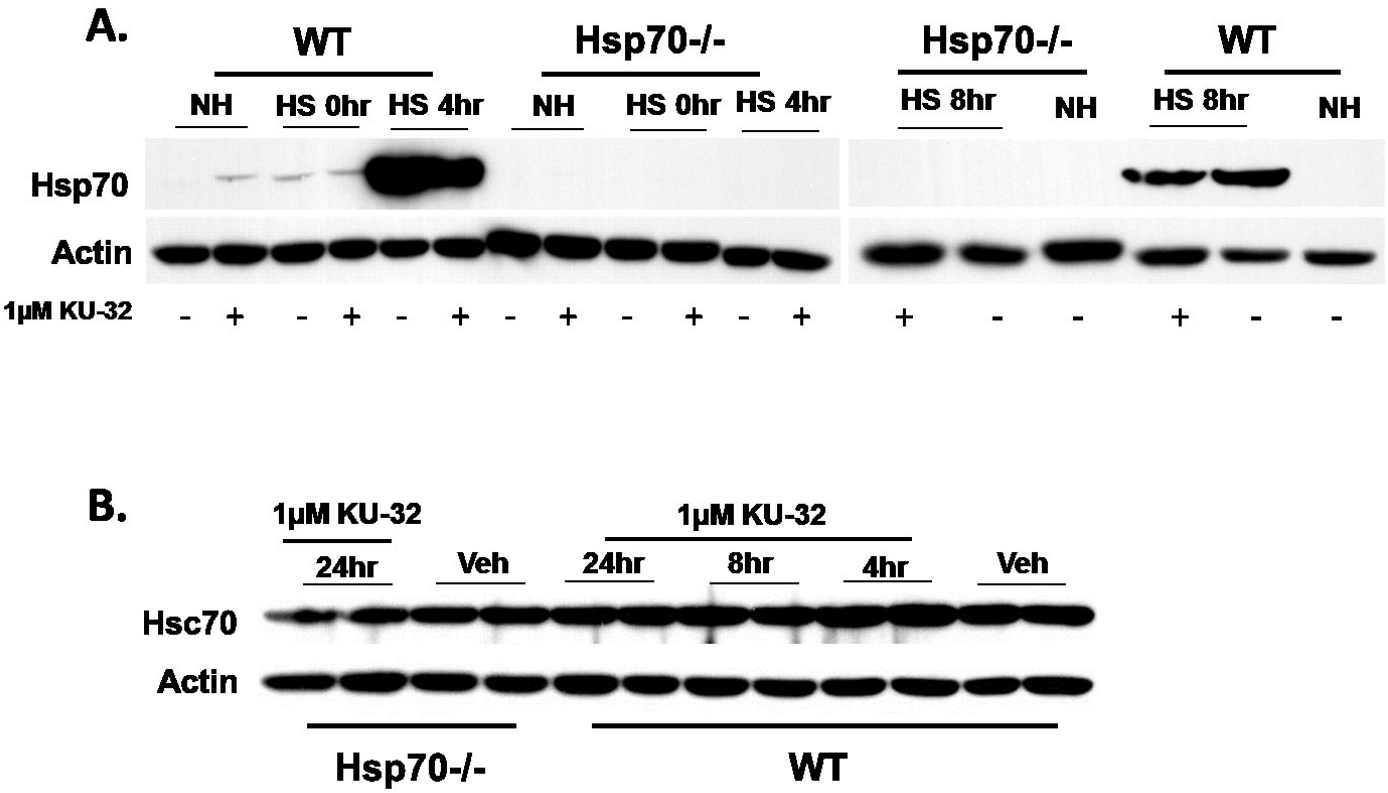

Figure 3.3.1 Absence of the inducible Hsp70 but not Hsc70 in Hsp70.1/70.3 double knockout mice. A) 1 week old neonatal mouse DRG explants from either WT or Hsp70-/- were treated with vehicle or 1μM KU-32 for 24hr in the absence or presence of heat shock (HS, 30 mins at 42°C) or HS plus 0-8 hr recovery time. Cell lysates were prepared and the expression of Hsp70 was determined by immunoblot analysis. **B)** Primary neonatal mouse sensory neurons were isolated, grown in culture for 1 week and treated for the indicated time with vehicle or 1μM KU-32. Cell lysates were prepared and Hsc70 levels were determined. Blots shown are representative of two experiments. NH: Non Heat-shock.

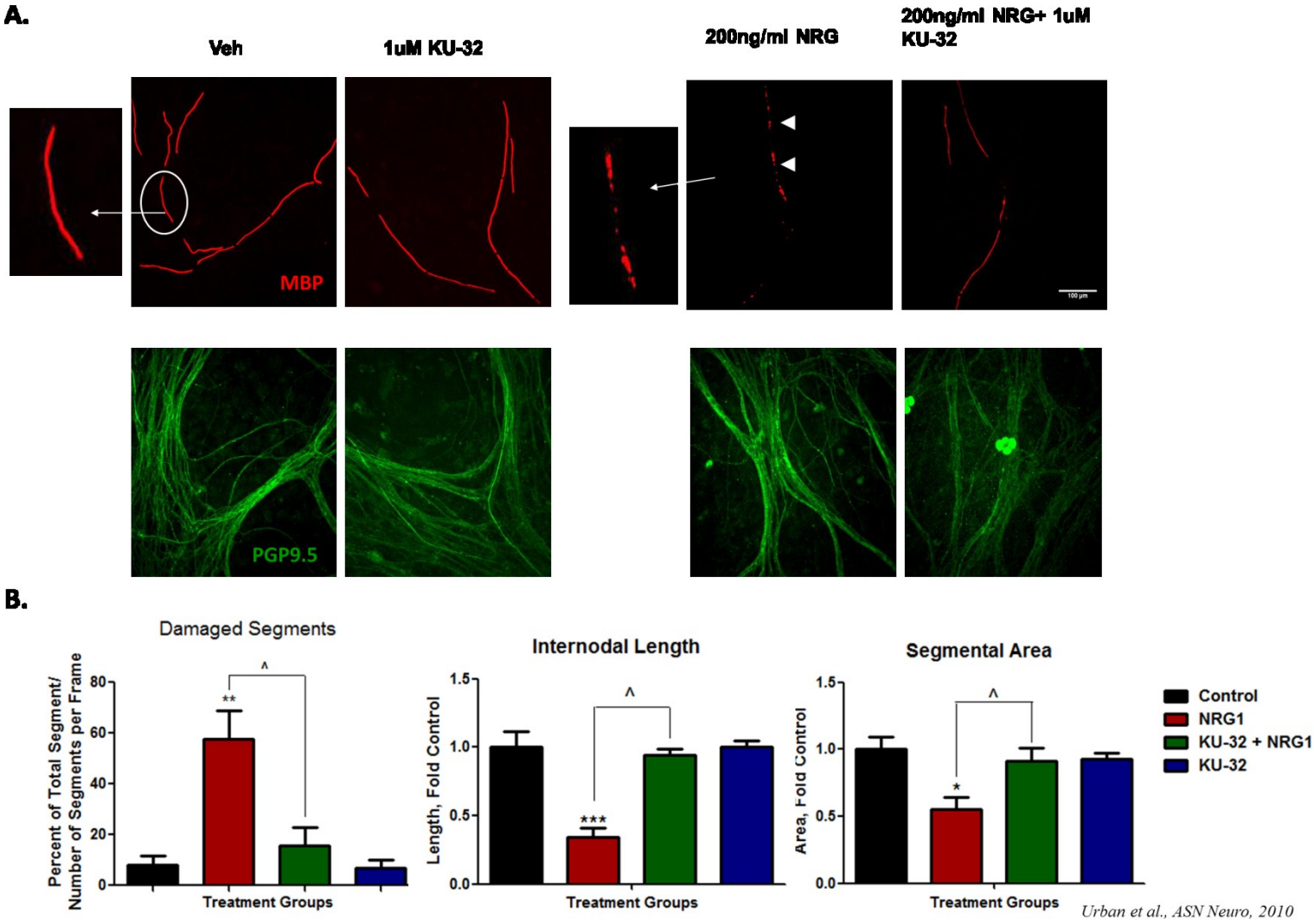

Figure 3.3.2 KU-32 prevents NRG1-induced myelin degeneration in myelinated sensory nerves. A) DRG/SC explants were established from P0 C57Bl/6 mice and myelination was permitted *in vitro* for 3 weeks. Cultures were incubated with 1μM KU-32 for 16hr prior to stimulation of demyelination by 200ng/ml NRG1 (in 0.1% BSA) for 3 days. Myelin internodes were labeled via MBP staining whereas PGP9.5 was used to indicate axonal integrity. ~5-8 images were taken for each individual cultures using confocal microscopy and number of total and degraded myelin segments were counted per picture frame. Typical intact or degenerating internodes are shown in higher magnification. **B)** Percent damaged segments were calculated for each frame. NRG1 resulted in an average of 57.5% myelin breakdown compared to 8.2% in control, KU-32 ameliorated this damage to only 15.7% without decreasing the basal degeneration (7.0%). One-way ANOVA analysis indicates significance changes in percent damaged segments [$F_{(3,12)}$=10.476; p<0.001], length [$F_{(3,12)}$=24.881, p<0.001] and area of internodes [$F_{(3,12)}$=4.489; p<0.05] among various groups. Tukey's test indicates **p<0.01, *** p<0.001, *p<0.05 for NRG1 *vs.* Control in percent damaged segments, length and area of internodes, respectively ^p<0.05 for NRG1 vs. NRG1+KU-32, df=3, n=6.

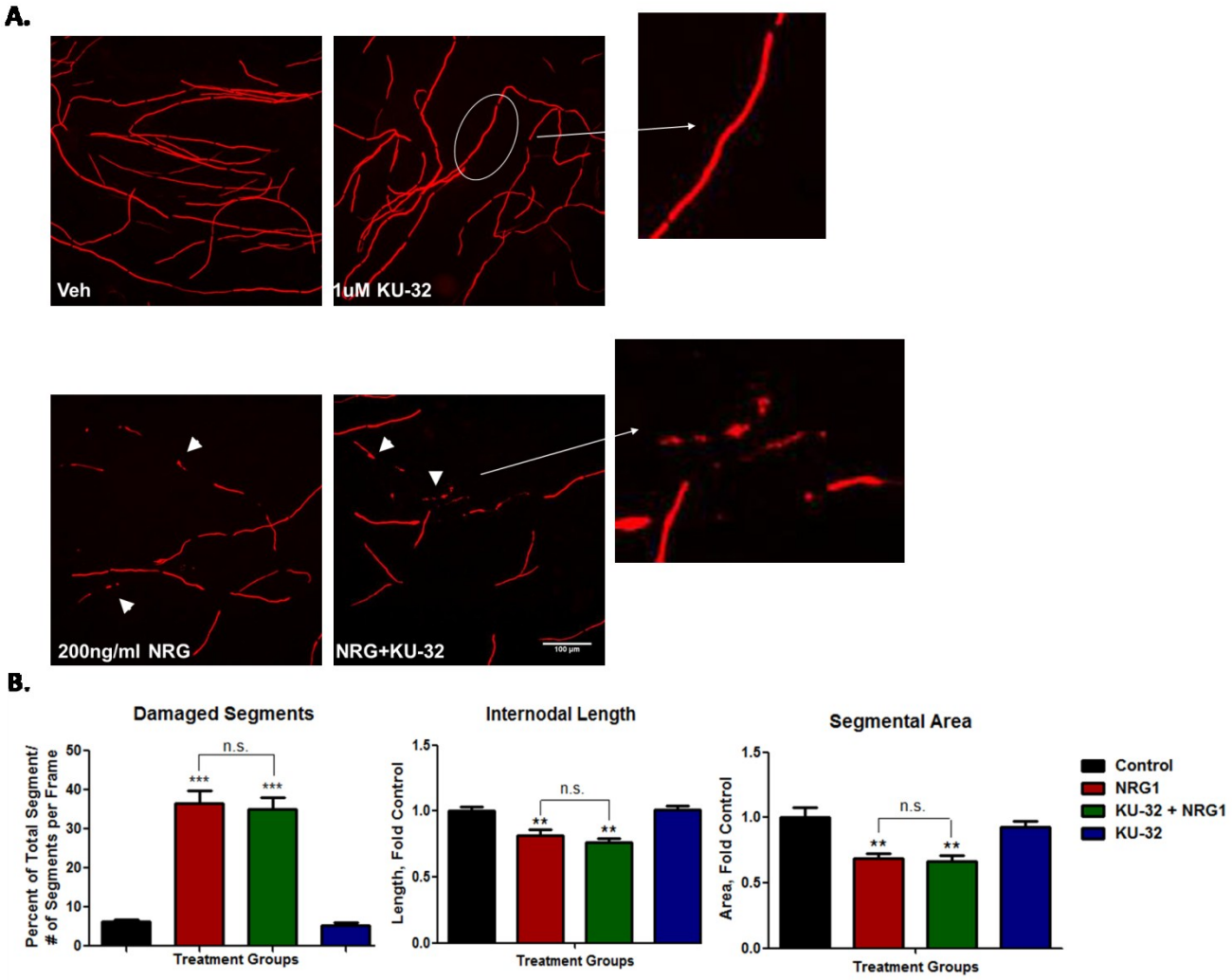

Figure 3.3.3 KU-32 is unable to prevent myelinated cultures from NRG1-induced demyelination in the absence of Hsp70. A) As described for WT, Hsp70$^{-/-}$ cultures were allowed to myelinate *in vitro* and treated with KU-32 (1μM) and NRG1 (200ng/ml) either separately or in combination. **B)** Percent degenerated segments were assessed following MBP immunostaining and compared to untreated controls. The level of demyelination observed in untreated cultures was 6.2% whereas an average of 36.5% myelin damage was obtained with NRG1. Neither basal degeneration (5.2%) nor NRG1-induced damage (35.2%) of myelin was affected by KU-32. One-way ANOVA analysis indicates significant difference among groups for percent damaged segments [$F_{(3,12)}$=28.160; p<0.001], length [$F_{(3,12)}$=13.116; p<0.01] and area of internodes [$F_{(3,12)}$=10.239; p<0.01]. Tukey's post-hoc test indicates ***p<0.05 for NRG1 vs. Control in percent damaged segments and **p<0.01 in internodal length and area. n.s indicates no significance for NRG1+KU-32 vs. NRG1. df=3, n=6

Treating wildtype (WT) myelinated nerves with 200ng/ml NRG for 72 hr led to a marked degeneration of myelin membranes as indicated by the fragmented, vesicular appearances of MBP staining (Figure 3.3.2A), which was employed to visualize myelin internodes. Importantly,

this degeneration did not seem to be a consequence of impaired axonal integrity as no decrease or irregularity in PGP9.5 staining was seen. To quantify myelin degeneration, immunofluorescent images were taken at random fields in the cultures and the number of damaged versus total myelin segments was assessed. While there was about 8% basal demyelination in control cells, the number of degenerated myelin internodes in WT cultures treated with 200ng/ml NRG1 was ~7 fold higher. Prior incubation of some of the cultures with 1μM KU-32 overnight (16hr) prevented this increase since the amount of damaged myelin segments in KU-32-pretreated NRG1 group remained close to the control level. KU-32 had no effect on the number of damaged myelin segments in the absence of NRG1 treatment (Figure 3.3.2B). Since the percent of damaged myelin segments only takes into account the gross number of "broken" segments, it does not reflect the severity of the ongoing degeneration of the myelinated internodes. To further characterize the integrity of the myelin internodes, average internodal length from each treatment group was also assessed using Cell Profiler. Briefly, individual MBP segments with a pixel-length of 20-200 microns were identified through Otsu's thresholding and segmentation. Major axis length for each segment was then automatically computed by the program to represent the internodal length (Figure 3.3.2b). Moreover, total area occupied by identified segments was measured to indicate overall internode diminishment. The result was expressed as fold of untreated control and revealed a 50-60% reduction in the average length and area of internodes by NRG1. Similar to its efficacy in decreasing amount damaged segments, KU-32 completely corrected the NRG1-induced deficits in segmental length and area of MBP. Although a similar degree of damaged segments was found in control Hsp70$^{-/-}$ cultures (~6%), NRG1 stimulated about a 6-fold increase in degenerated segments and internode loss (20-30% decrease in length and area) compared to WT. The reason for this modestly improved

resistance to NRG1 is not known, but might be due to a generally higher basal level of myelination in Hsp70$^{-/-}$ cultures. Nevertheless, pretreatment of KU-32 failed to significantly reduce the percent of damaged myelin internodes or demonstrate any significant improvement in the percentage degeneration, length or area of myelin internodes against NRG1 in these Hsp70-deficient cultures (Figure 3.3.3). This finding is consistent with our previous *in vivo* observation that Hsp70 is central to the drug efficacy in inducing neuroprotection (Urban et al., 2010).

3.4 Hsp70 is required by KU-32 to inhibit NRG1-induced c-jun expression and activation

C-jun has been established as a negative regulator of myelination and has been proposed to mediate NRG1-induced demyelination (Parkinson et al., 2008). In addition, whereas c-jun is minimally expressed in normal nerves, it is significantly upregulated in nerves affected by DPN and a number of other human demyelinating neuropathies (Hur et al., 2011; Hutton et al., 2011). We thus evaluated whether the efficacy of myelin protection by KU-32 correlated with inhibition of c-jun. Myelinated DRG/SC explants from WT or Hsp70$^{-/-}$ mice were incubated with 1μM KU-32 overnight prior to 16hr of NRG1 treatment and immunoblotting for phosphorylated c-jun (p-c-jun) and total c-jun. In agreement with previous findings (Parkinson et al., 2008), exposure of WT explants to NRG1 resulted in a marked (2-2.5 fold) increase in both c-jun and p-c-jun protein level (Figure 3.4). Without affecting c-jun activity by itself, pretreatment of KU-32 abolished NRG1-induced c-jun expression and activation in WT cultures. However, this inhibition was lost in myelinated cultures established from Hsp70 knockouts, suggesting that Hsp70 is essential in mediating c-jun inhibition by KU-32. Of note, genetic removal of Hsp70 did not alter the basal c-jun or phospho-c-jun expression but slightly augmented the upregulation of c-jun following NRG1 treatment. Therefore, Hsp70 might be selectively intersecting with c-jun induction down the NRG1 signaling axis.

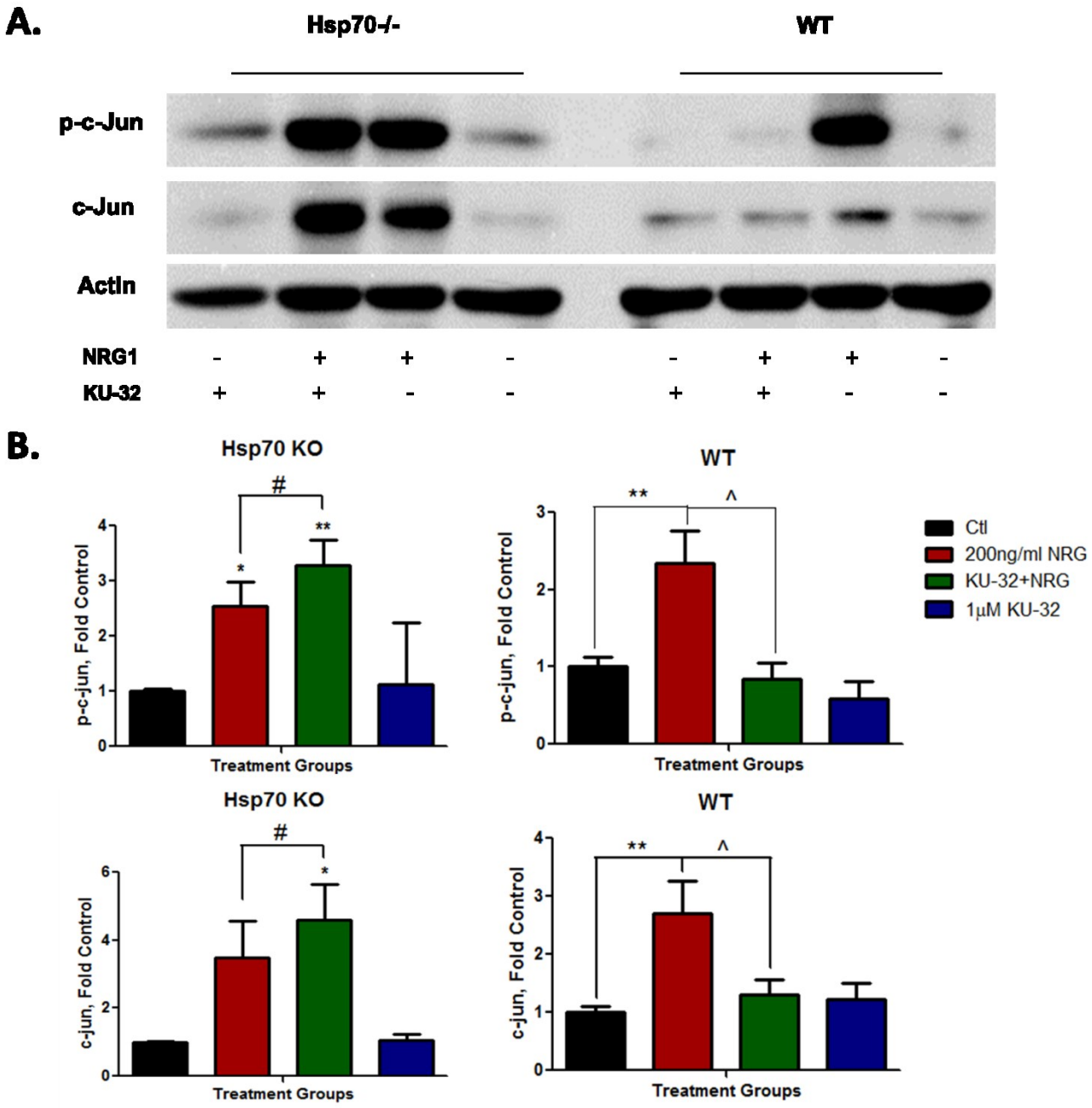

Figure 3.4 KU-32 inhibits NRG1-induced expression and activation of c-jun in WT but not Hsp70 deficient nerves. A) Fully myelinated WT or Hsp70-/- DRG explants were treated with 200ng/ml NRG for 16hr following either vehicle or 1μM KU-32 pretreatment overnight (16hr). Phospho-c-jun and c-jun content were then assessed based on the immunoreactivity of antibodies recognizing these proteins. **B)** Blots were quantified using ImageJ. Each treatment category indicated in bar graphs corresponds to individual lanes in the blots below which it is placed. Experiments were repeated 5 times in total and One-way ANOVA indicates significant difference among groups for WT p-c-jun [$F_{(3,19)}$=5.910; p<0.01], WT c-jun [$F_{(3,19)}$=3.550; p<0.05], KO p-c-jun [$F_{(3,19)}$=9.857; p<0.05], KO c-jun [$F_{(3,19)}$=5.086, p<0.05]. Tukey's testindicates *p<0.05 **p<0.01 compared to control (vehicle), ^p<0.05 for NRG1 vs. NRG1+KU-32, # denotes no statistical significance. df=3, n=5-6 for each treatment group.

3.5 Hsp70 is sufficient to prevent NRG1-induced demyelination and c-jun induction

While the above results support that Hsp70 is crucially involved in KU-32-mediated myelin protection, it is unclear whether the drug efficacy arises from a direct neuroprotective effect of Hsp70. Alternatively speaking, it remains to be determined whether induction of Hsp70 is sufficient to prevent myelin degeneration. To test this, a recombinant adenovirus carrying FLAG-tagged Hsp70 (ad-Hsp70FLAG) was generated to genetically overexpress Hsp70. Similar to KU-32 treatment, fully myelinated DRG/SC explants from WT and Hsp70

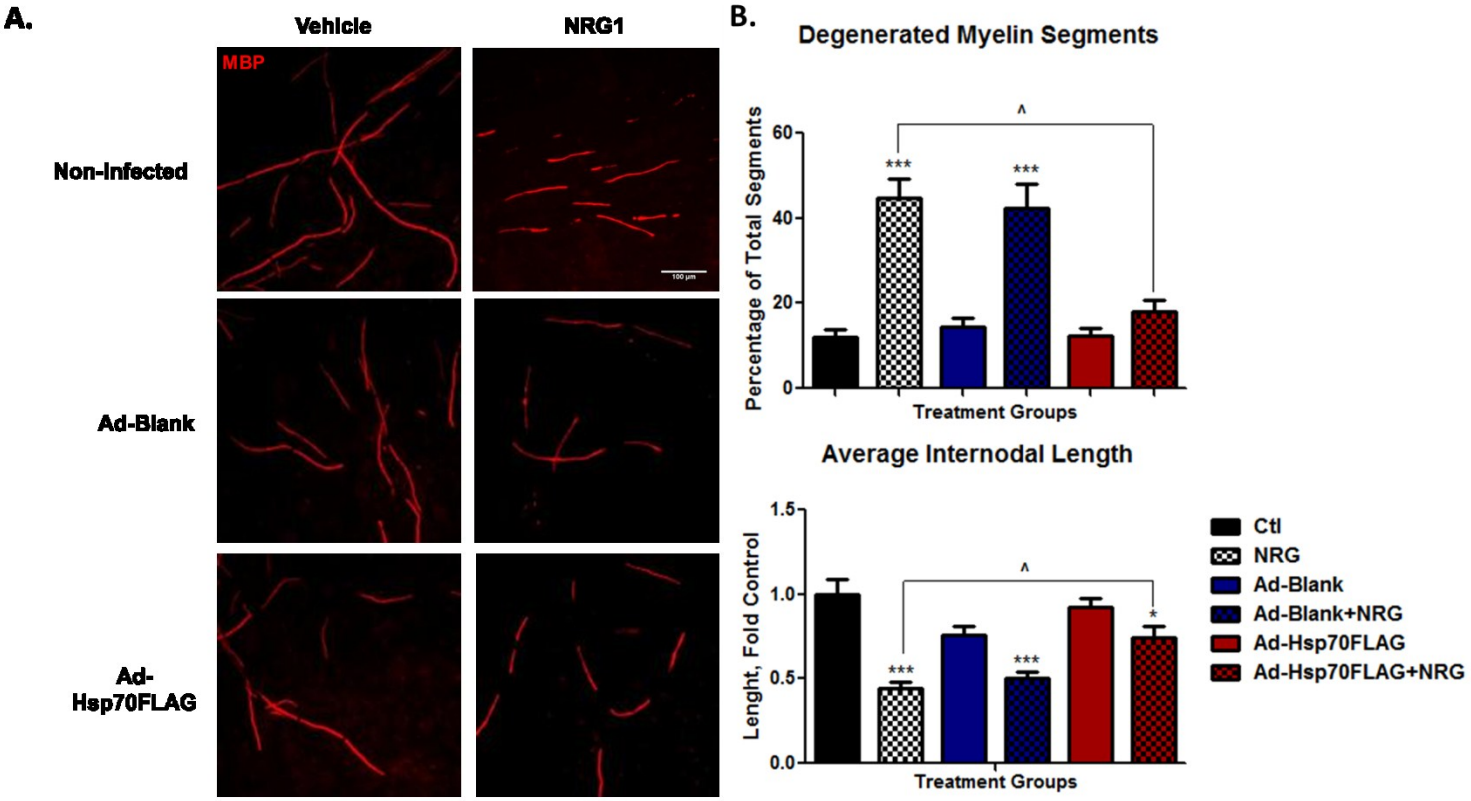

Figure 3.5.1 Adenoviral overexpression of Hsp70 ameliorates NRG1-caused internode degeneration in WT cultures. A) WT myelinated sensory nerves were uninfected or infected with either blank or Hsp70FLAG-expressing adenoviruses for 16hr prior to a 72hr myelin degeneration stimulated by NRG1. MBP and PGP9.5 (not shown) immunostaining was performed, following which **B)** degeneration and length of MBP-marked internodes were quantified manually and by CellProfiler, respectively. One-way ANOVA indicates significant difference in the percent damaged [$F_{(5,18)}$=20.928; p<0.001] and average length [$F_{(5,18)}$=14.344, p<0.001] of internodes among groups. Tukey's post-hoc test indicates *p<0.05, ***p<0.001 for treatment compared to control, ^p<0.05 for NRG1 vs. AdHsp70FLAG+NRG1, df=5, n=4

deficient mice were infected with ad-Hsp70FLAG for 16hr, the cells treated with NRG1 for 72 hr and the cultures stained for MBP. In order to maintain the myelin damage at a comparable level between WT and Hsp70 KO cultures, WT explants were treated with 150ng/ml NRG1 NRG1 while the Hsp70 KO counterparts were treated with 200ng/ml NRG1. This resulted in a similar percentage of degenerated segments in uninfected WT (~37-45%) and Hsp70$^{-/-}$ (~40%) cultures (Figure 3.5.1; 3.5.2). Prior infection with ad-Hsp70FLAG led to a substantial Hsp70

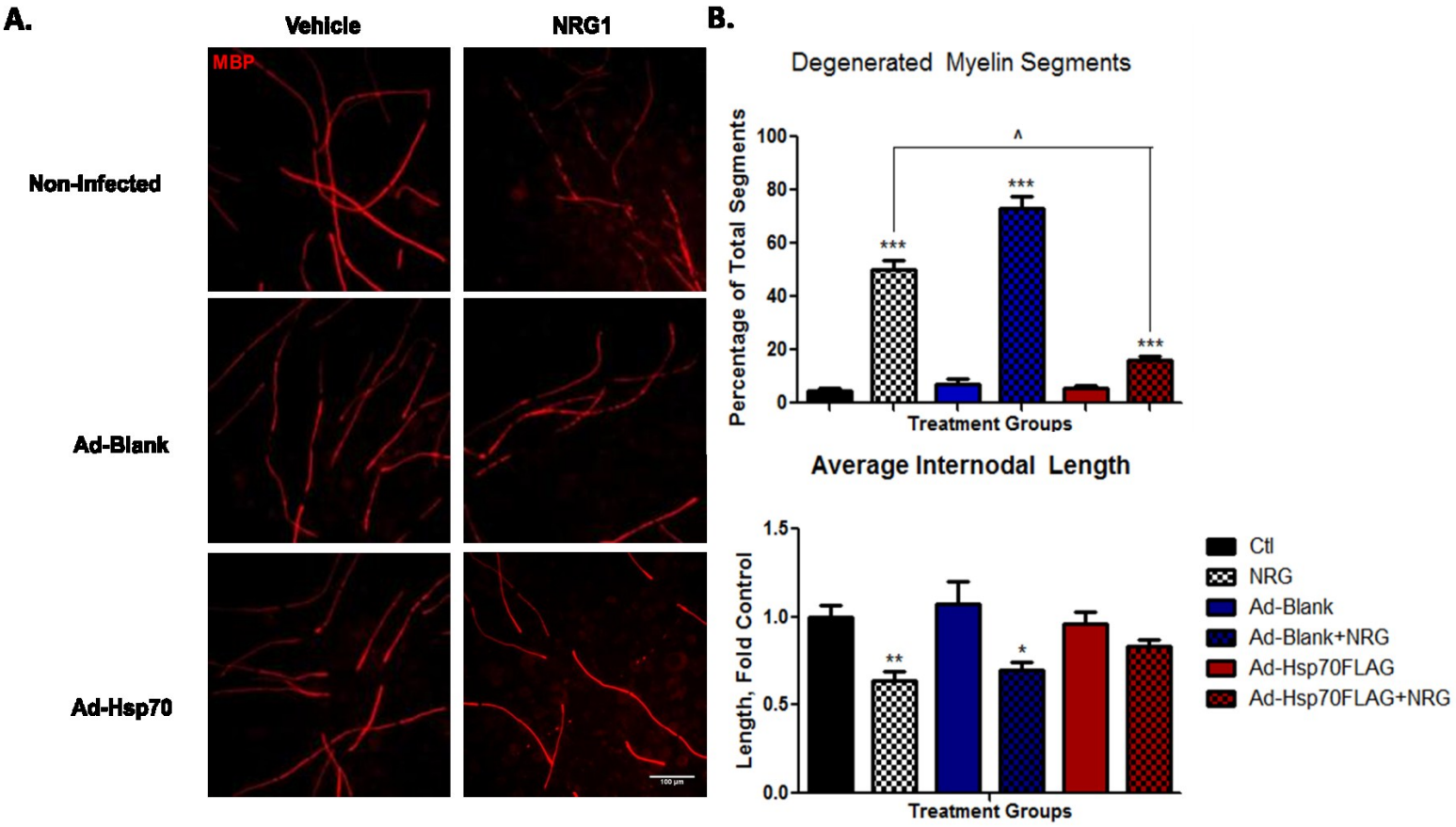

Figure 3.5.2 Adenoviral overexpression of Hsp70 ameliorates NRG1-caused internode degeneration in Hsp70-deficient cultures. A) MBP-stained internodes were examined after NRG1 treatment in uninfected, blank or ad-Hsp70FLAG adenovirus-infected Hsp70-/- sensory nerves. **B)** Percentage damaged segments and internodal length was measured as previously described. One-way ANOVA indicates significant changes in percent degenerated [$F_{(5,18)}$=5.684; p<0.001] and average length [$F_{(5,18)}$=5.960; p<0.001] of internodes. Tukey's post-hoc test indicates *p<0.05, **p<0.01, ***p<0.001 for treatment compared to control, ^p<0.05 for NRG1 *vs.* NRG1+Ad-Hsp70FLAG. df=5, n=4

Such protection is unlikely to be a result of viral infection itself since blank virus containing an expression in both WT and Hsp70$^{-/-}$ cultures as demonstrated by immunoblotting with Hsp70 and FLAG antibodies (Figure 3.5.3). This corresponded to a respective 27% and 34% reduction in the amount of damaged internodes as compared to cultures treated with NRG1 (Figure 3.5.1 & 3.5.2). empty vector did not alter the basal or NRG1-associated degeneration of myelin. Similarly, Hsp70 overexpression had no effect on endogenous demyelination. Analysis of average internodal length further revealed that NRG1 caused a 40-50% reduction in average length of internodes in WT and Hsp70$^{-/-}$ nerves. Overexpression of Hsp70 attenuated this decrease by 30% in WT cultures, which however was still significantly decreased compared to the untreated. In comparison, an average 20% increase versus NRG1 in internode length was obtained by ad-Hsp70FLAG in Hsp70 deficient nerves. The observed improvement in myelin damage correlated with the ectopic expression of the epitope-tagged Hsp70 which was similar in both WT and Hsp70 KO cultures. In addition, induction of Hsp70 was sufficient to abrogate NRG1-induced c-jun expression and phosphorylation (Figure 3.5.3). Since in the earlier study an almost complete recovery from internodal shortening was achieved using the weak Hsp70 activator KU-32, the fact that such potent overexpression of Hsp70 and c-jun inhibition substantially but not fully blocked demyelination suggest that KU-32 might act through other components than Hsp70-mediated c-jun inhibition in promoting myelin protection. Nonetheless, our results support that Hsp70 induction is sufficient to improve myelination and recapitulate the neuroprotection by KU-32.

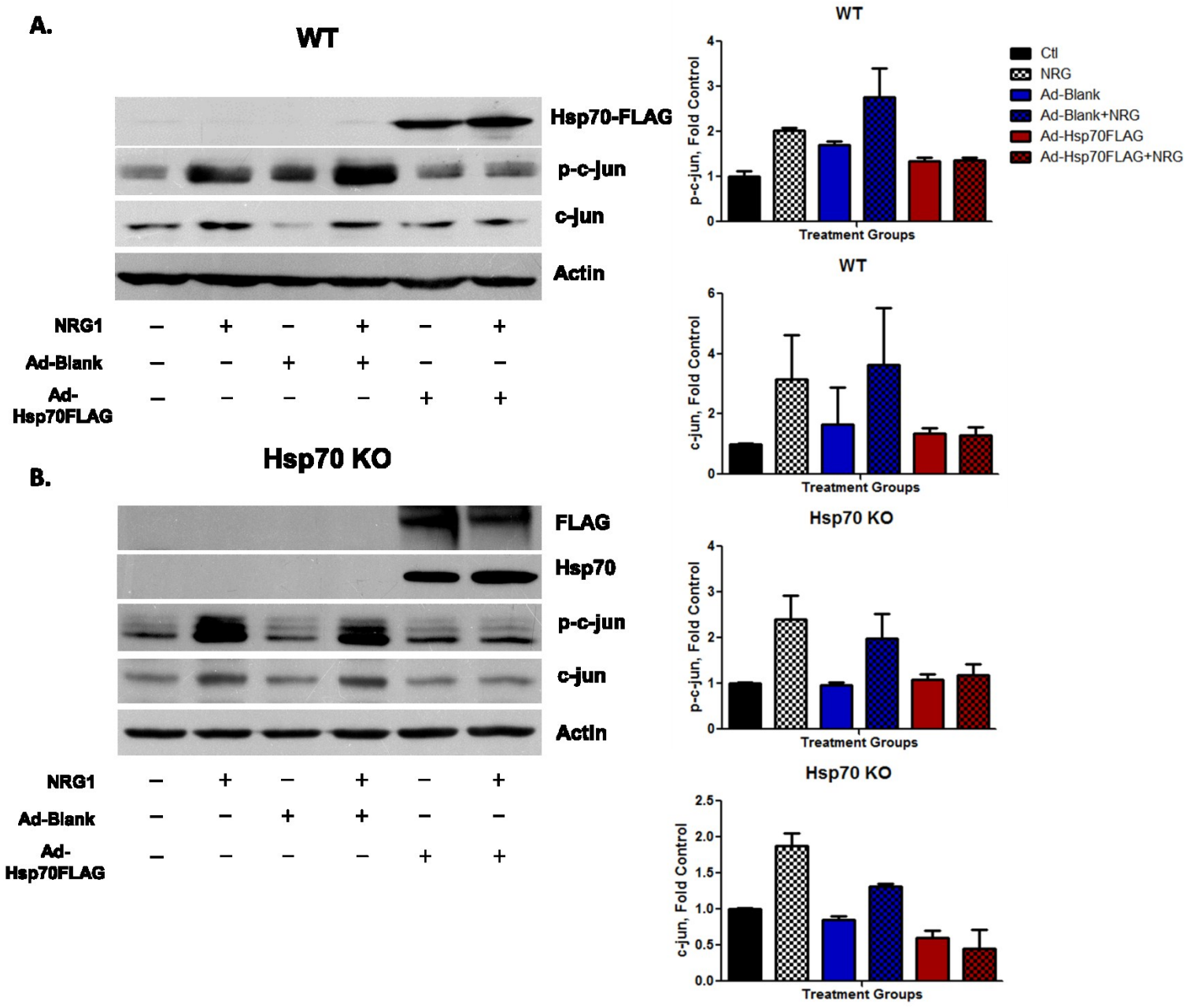

Figure 3.5.3 Hsp70 overexpression is sufficient to block c-jun expression and phosphorylation. Biochemical analysis of c-jun, phosphor-c-jun and Hsp70 protein expression in response to NRG1 were performed after adenoviral-mediated Hsp70 induction in myelinated WT **A)** or Hsp70-depleted **B)** DRG/SC cultures. Results were compared to blank infection and uninfected control. Exogenous overexpression of Hsp70 was confirmed by immunoblotting of Hsp70 and FLAG. Blots quantitation were generated from two independent experiments.

3.6 Neither JNK nor Erk was responsible for KU-32-mediated c-jun inhibition

JNK phosphorylates and activates c-jun at its N-terminus and is a well-established upstream kinase regulator of c-jun in a variety of signaling phenomena including apoptosis, inflammation and proliferation (Ham et al., 1995; Ip and Davis, 1998; Kaminska, 2009). Although overexpression of JNK can inhibit myelin gene expression, c-jun-induced demyelination does not appear to depend on JNK phosphorylation because N-terminus mutations that incapacitate JNK activation did not impair the inhibition of SC myelination by c-jun (Parkinson et al., 2008). In support of this, we failed to observe any increase in phosphorylated or total JNK level in myelinated DRG/SC explants with treatment of NRG1. Through direct or indirect interaction, Hsp70 has also been reported to negatively regulate JNK activity and subsequent apoptosis in sympathetic neurons (Bienemann et al., 2008; Salehi et al., 2006) and other contexts such as insulin resistance (Chung et al., 2008; Gupte et al., 2009). However, we observed no change in JNK activation or expression in response to KU-32 in unmyelinated or myelinated DRG/SC explants as shown in Figure 3.6A,D. In light of these results, it is highly unlikely that JNK contributes to chaperone-mediated myelin protection or NRG1-associated demyelination. The increase of c-jun activation by NRG1 observed in previous results might therefore be secondary to the upregulation of the total level of c-jun or mediated through other kinases than JNK, such as Erk.

While it is not unexpected that inhibition of NRG1-induced demyelination does not involve JNK modulation, it is surprising that KU-32 did not block induction of extracellular signal-regulated kinase (Erk) despite that this MAPK was immediately (45min) phosphorylated after addition of 200ng/ml NRG1 (Figure 3.6C). As mentioned earlier, SC dedifferentiation subsequent to high concentration of NRG1 and/or axotomy requires activation of Erk.

Mutational or pharmacological inactivation of Erk negated the reverse transition of SC phenotype driven by excessive NRG1 (Harrisingh et al., 2004). Additionally, a recent study suggests that NRG1-induced c-jun upregulation is Erk-dependent since Erk inhibitor blocked

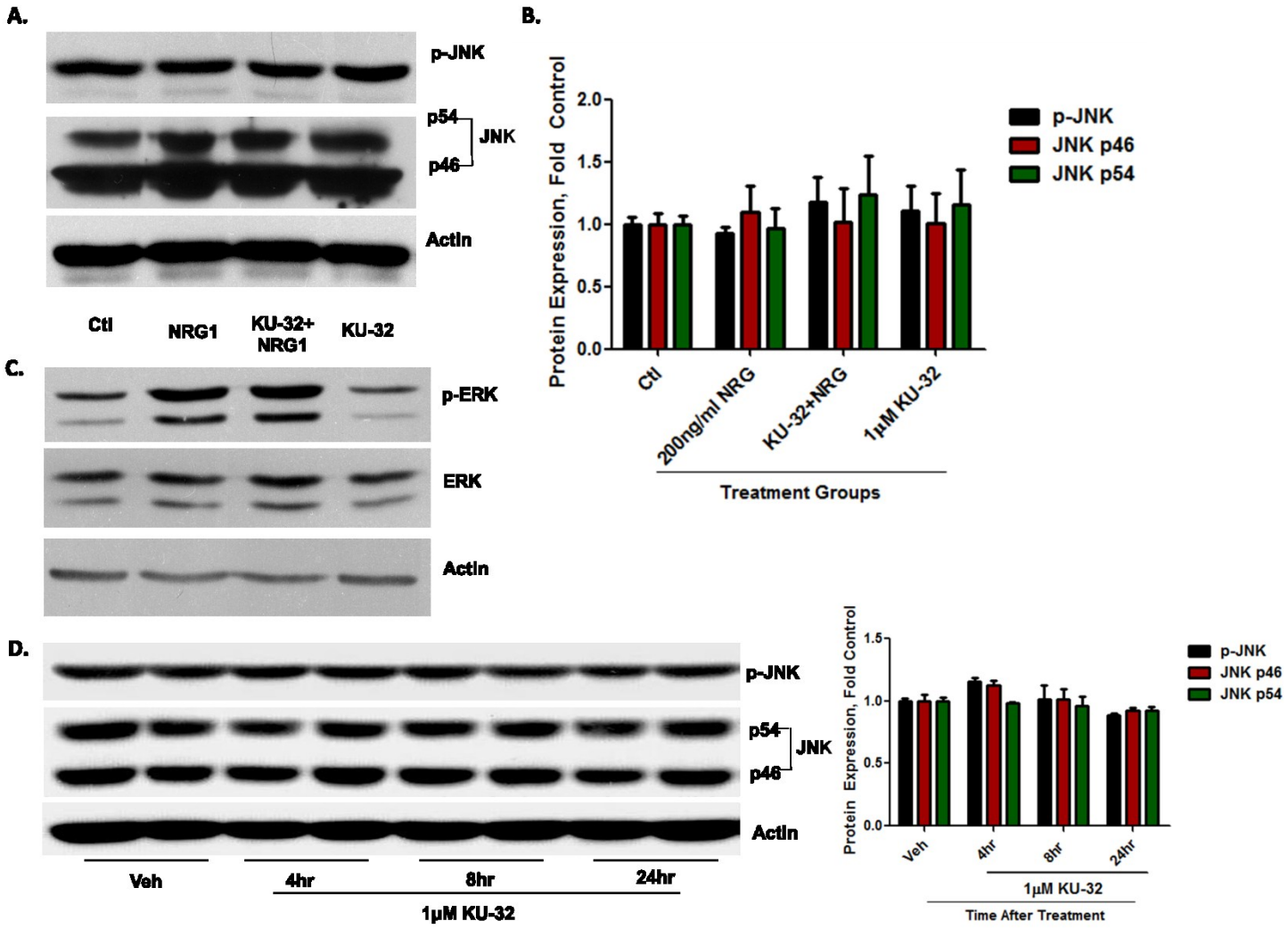

Figure 3.6 Neither JNK or Erk was altered by KU-32. Myelinated sensory explants from C57Bl/6 were treated with KU-32 for 16hr, followed by 16hr (JNK) or 45min (Erk) NRG1 at indicated concentration. **A), C)** JNK/Erk expression and activity were determined via immunoblotting of total and phosphorylated JNK. **B)** Experiments were performed for 5 independent times and no statistical significance was found irrespective of the treatments. **D)** 1-week unmyelinated DRG/SC explants were prepared from C57Bl/6 neonatal mice and treated with vehicle or 1μM KU-32 for 4, 8 or 24 hr. Cell lysates were then collected and immunoassayed for phospho-JNK and total JNK level. Graph quantitation was derived from 3 independent experiments. One-way ANOVA was performed for p-JNK [$F_{(3,19)}$=0.596; p=0.630], JNK p46 [$F_{(3,19)}$=0.048; p=0.985] and JNK p54 [$F_{(3,19)}$=0.340; p=0.797] and no statistical significance was detected among different treatment groups using Tukey's post-hoc honestly-significant test. df=3, n=5-6.

c-jun increase and demyelination (Syed et al., 2010). Although several previous results showed that Hsp70 inhibited Erk activity (Goel et al., 2010; Lee et al., 2005), our finding that increasing Hsp70 did not alter Erk phosphorylation suggests Erk blockage is not involved in c-jun downregulation. In fact, the exact role of Hsp70 in Erk regulation appears to differ in different cell types (Tsuji et al., 2000; Wang et al., 2009) and the present result may be specific to myelinating SCs. Though, it remains possible that inhibition or removal of activated Erk takes a prolonged period (>45min) to occur, the present data clearly indicates that KU-32-mediated inhibition of c-jun and demyelination is not through an early inhibition of Erk activation as reported by others (Goel et al., 2010; Lee et al., 2005).

3.7 Reduction of c-jun expression by KU-32 is proteasome-dependent

Because NRG1-induced myelin degeneration is not known to be associated with the accumulation of a particular protein misfolding or aggregation but rather disregulated gliotrophic support, chaperone-mediated assistance of protein quality control is not the likely mechanism of myelin protection by KU-32. However, chaperones may intervene with cellular signal transduction through proteasomal degradation of signaling proteins. For example, the anti-apoptotic effect of Hsp70 and its cochaperone carboxyl terminus of Hsp70-interacting protein (CHIP) have been linked to their facilitating ubiquitination and proteasomal disposal of a c-jun upstream kinase (Hwang et al., 2005). To determine whether KU-32 reduces c-jun through protein degradation, we blocked proteasomal function via addition of the proteasome inhibitor MG132 to DRG explants in conjunction with NRG1 and examined c-jun expression. As shown in western blots, NRG1 increased c-jun expression to a similar extent as in earlier experiments and 1μM KU-32 markedly blocked this induction (Figure 3.7). However, addition of 2μM MG132 abrogated the block of c-jun induction by KU-32 in these cultures. As expected,

combination of NRG1 with MG132 led to an even greater (but not statistically significant) upregulation of c-jun, which can possibly be attributed to the slight increase in c-jun accumulation due to proteasome inhibition. This observation supports that KU-32 may reduce c-jun through chaperone-targeted proteasomal clearance.

In a typical model of chaperone-targeted ubiquitin-proteasome degradation, Hsp70 and Hsp90 chaperone complex, with the assistance of co-chaperones, mediates substrate polyubiquitination and sorting to the 26S proteasome through a direct chaperone-substrate interaction. Although available data suggests that Hsp70 transiently colocalizes with c-jun in the nucleus during apoptosis (Kitamura et al., 2003), it is still unclear whether Hsp70 promotes c-jun clearance through a direct physical association. To address this, we attempted to probe the Hsp70-c-jun interaction via immunoprecipitating sciatic nerve homogenates with monoclonal Hsp70 antibody and western blotted for c-jun. Surprisingly, despite the successful pull-down of Hsp70 from cell extracts (Figure 3.8.1B), no Hsp70-bound c-jun was detected in the precipitates (Figure 3.8.1A). This is not likely a result of disruption of native protein interaction due to the mechanical or chemical stress related to experimental condition as other Hsp70 binding partner was successfully identified by this co-IP reaction (Figure 3.8.1C). However, as the basal expression of c-jun is low in nerves, any low affinity or transient interaction of c-jun with Hsp70 may have been lost during the assay. It is also possible that Hsp70 only associates with and eliminates increased c-jun in response to physiological or pathological stressors in peripheral nerves. Therefore, future immunoprecipitation assays assessing Hsp70-c-jun association may be carried out in cells treated with MG132.

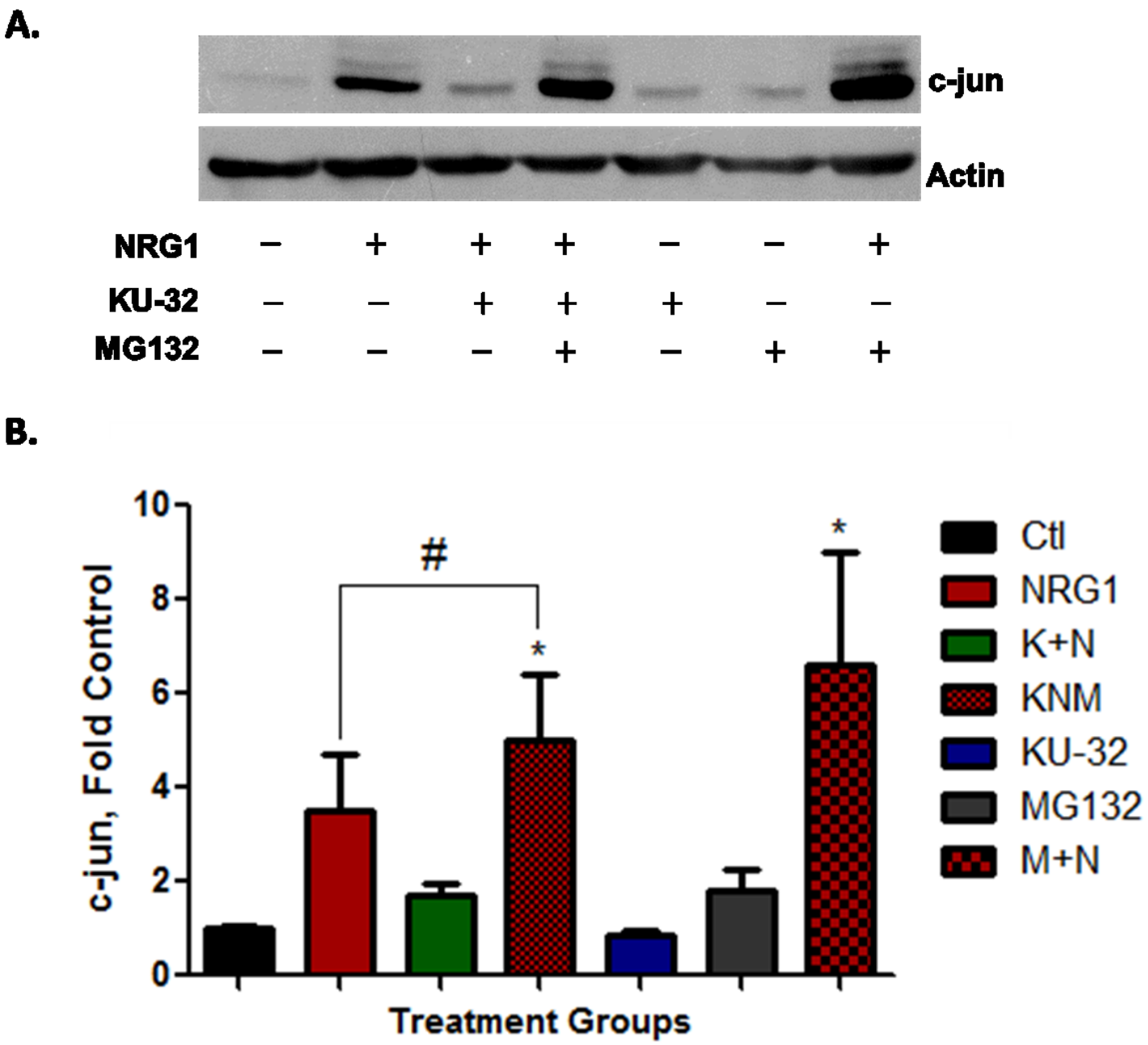

Figure 3.7 KU-32 reduces c-jun in a proteasome-dependent manner. A) 1μM KU-32 was incubated for 16hr in myelinated DRG explants from C57Bl/6 mice, which is then subjected to additional 16hr treatment of 200ng/ml NRG and/or 2μM MG132. Cells lysates were then obtained and immunoblotted for c-jun protein level. **B)** Densitometry of c-jun immunoreactivity was performed using ImageJ and statistics were generated from 5 independent experiments. KNM: KU-32+NRG1+MG132; M+N: MG132+NRG1. One-way ANOVA analysis indicates significant difference [$F_{(6,27)}$=3.582, p<0.01] in c-jun expression among various groups. Tukey's post-hoc test indicates *p<0.05 for treatment compared to control, # denotes no statistical significance was found for NRG1 *vs.* NRG1+KU-32+MG132, df=6, n=5

3.8 Hsp70 interacts with MBP in peripheral nerves

Direct binding of Hsp70 to MBP has been identified in central myelin and proposed to facilitate antigen presentation in multiple sclerosis (Cwiklinska et al., 2003). However, Hsp70 also associates with MBP in normal white matter and regulates MBP synthesis during oligodendrocyte differentiation (Aquino et al., 1998; Lund et al., 2006). In mature peripheral nerves, we further confirmed the direct Hsp70-MBP association by reciprocal co-immunoprecipitation using specific Hsp70 or MBP antibody (Figure 3.8.1C,D). Consistent with this finding, immunostaining revealed colocalization of Hsp70 with MBP in myelinating SCs of sensory explants (Figure 3.8.2). These observations suggest that Hsp70 also participates in myelin protein homeostasis. In agreement, induction of chaperones including Hsp70 aided the processing and trafficking of aggregation-prone PMP22, correlated with improved myelination in a CMT1A model (Rangaraju et al., 2008). Although it remains unclear whether metabolic changes of particular myelin proteins underlie NRG1-induced demyelination, the observed fragmentation and degradation of internode sheath in NRG1 treated cultures does indicate disrupted maintenance and stability of myelin proteins. As KU-32 increases Hsp70-MBP interaction, this may enhance myelin protein chaperoning thereby contributes to internode stabilization. Moreover, another major structural component of compact myelin P0 was not detected in Hsp70-bound proteins, suggesting that Hsp70 might selectively interact with molecules possessing a relatively fast turnover rate in myelin membrane (Lajtha et al., 1977; Quarles et al., 2006).

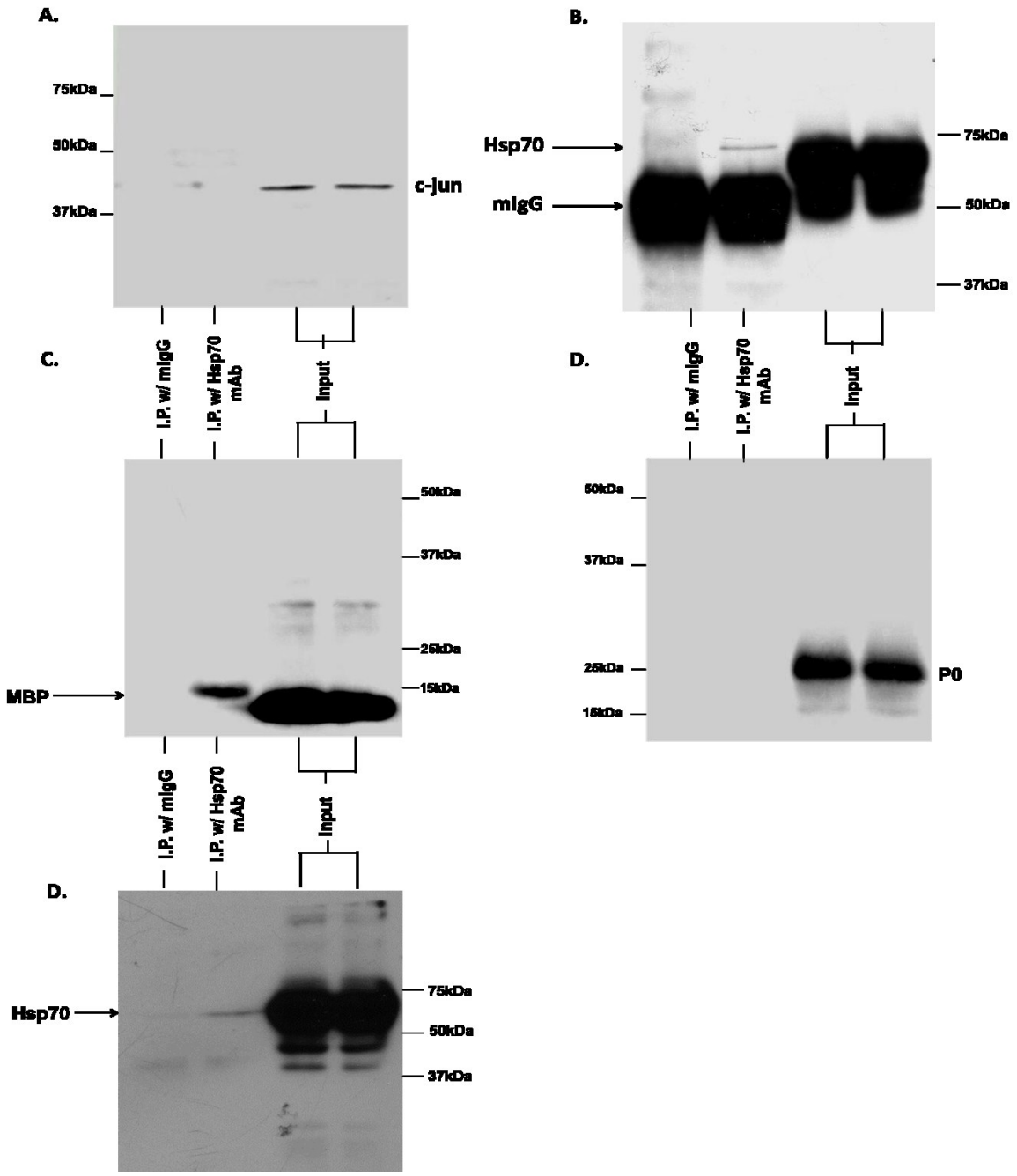

Figure 3.8.1 Hsp70 physically associates with MBP but not P0 and c-jun in normal peripheral nerves. Sciatic nerves lysates were obtained from ~1 month old C57Bl/6 mice and immunoprecipitated with Hsp70 mouse monoclonal antibody or IgG (negative control) using protein G sepharose beads. Western blotting precipitated fractions for c-jun **A)**, MBP **C)** and P0 **D)** identified MBP as direct binding partner for Hsp70. Reciprocal co-immunoprecipitation using MBP antibody further confirmed Hsp70-MBP interaction **E)**. No c-jun or P0 immunoreactivity was detected in Hsp70-bound proteins. Hsp70 pull-down was confirmed by reblotting the lysates with Hsp70 antibody **B)**. Blots are representative for two independent experiments.

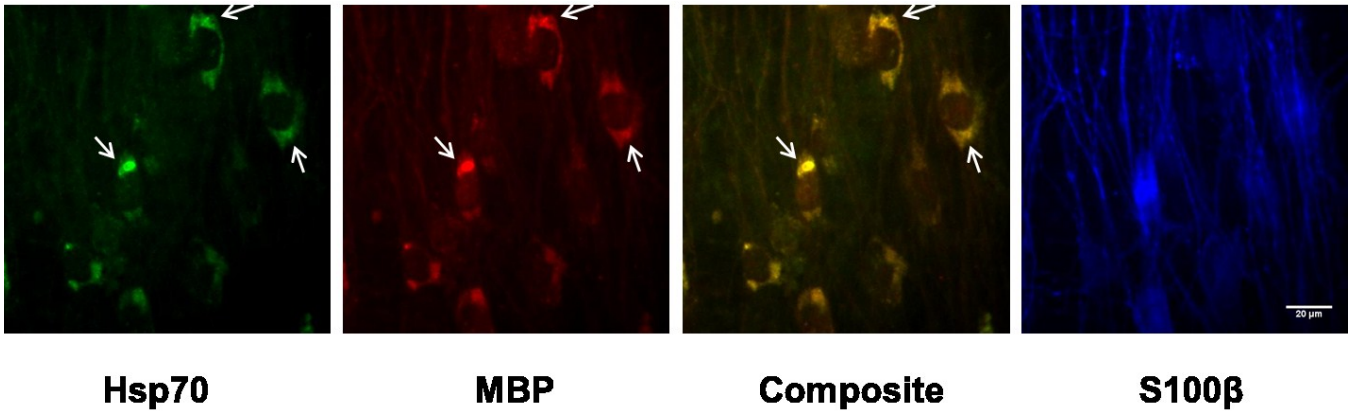

Figure 3.8.2 Hsp70 colocalizes with MBP in myelinating SCs of peripheral sensory nerves. DRG/SC explants were established from C57Bl/6 mice and induced to myelinate *in vitro* for 2 weeks by 50 µg/ml ascorbic acid. Cells were then fixed and triple-immunostained with antibodies specifically recognizing Hsp70 (green), MBP (red) and SC marker S100β (blue). Colocalization image of Hsp70 with MBP was composited using ImageJ channel merging. Immunolabeling of S100β in cultures indicates that Hsp70 largely overlaps with MBP in SCs. Experiments were performed twice and for each time triplicates were included in each experimental group.

3.9 Discussion

Altered growth factor signaling and its potential contribution to a variety of peripheral neuropathies such as DPN has drawn increasing awareness with the lack of success in nerve growth factor (NGF) therapy in eliciting the predicted protection of nerve function and amelioration of DPN symptoms (Apfel, 2002; Apfel et al., 2000). In db/db obese mice that develop features of human type 2 diabetes, upregulation of NGF and its subsequent activation of p38 MAP kinase was found to be responsible for the development of mechanical allodynia and painful diabetic neuropathy (Cheng et al., 2009; Cheng et al., 2012; Cheng et al., 2010). On the other hand, diabetes also modulates Neuregulin-1/ErbB signaling (Gui et al., 2012) that has been established to have a profound impact on the physiology of SCs (Nave and Salzer, 2006), which also undergo substantial degeneration in DPN (Eckersley, 2002). In particular, we showed that increasing ErbB2 activation deteriorated the mechanical hypoalgesia associated with myelinated

fiber response in diabetic nerve and recapitulated the deficits mentioned herein independent of diabetes (McGuire et al., 2009). Contrarily, pharmacological inhibition of ErbB2 reversed these indexes in mice that developed DPN. Clearly, altering Neuregulin-1/ErbB signaling is sufficient to affect the function of myelinated nerve. However, pathological implications of this ligand-receptor signaling axis in SC demyelination secondary to metabolic disturbances or genetic and immune insults have received scant attention. Such lack of interest is baffling given that aberrant and excessive activation of ErbB2 by Neuregulin-1 has been repeatedly demonstrated to induce SC myelin degeneration (Harrisingh et al., 2004; Yu et al., 2008; Zanazzi et al., 2001) and peripheral demyelinating neuropathy (Huijbregts et al., 2003). Nevertheless, a couple of clinical investigations have provided evidence in support of the hypothesis that over-activation of neuregulin signaling in adult nerves contributes to SC dedifferentiation and molecular phenotypes of myelin pathology. For example, a sural nerve biopsy study revealed varying degrees of ErbB2 and ErbB3 receptor overexpression in several forms of human neuropathies with demyelinating features (Massa et al., 2006). We have shown in myelinated sensory neuron/SC cocultures that high concentration of glucose sensitized myelinated internodes to neuregulin-induced degeneration (Yu et al., 2008). The enhancement of ErbB2 signaling by hyperglycemia could be attributed to a differential alteration in the expression of neuregulin isoforms as significant upregulation in NRG1 type I and downregulation in NRG1 type III in sural nerves have been noted in our streptozotocin-induced diabetic mice (unpublished observation).

Using a pharmacological Hsp90 modulator that enhances a broad cytoprotective response, we have previously reversed pre-existing neuropathic changes involving myelinated fiber function in an experimental mouse model of DPN (Urban et al., 2010). Therapeutic effectiveness

of this compound, KU-32, necessitates expression of the stress-inducible Hsp70 since Hsp70 KO diabetic mice that developed a similar neuropathy did not respond to the treatment. Hsp70 is a cytosolic chaperone that has demonstrated prominent neuroprotection in models of cerebral ischemia and a variety of neurodegenerative disorders (Kelly and Yenari, 2002; Muchowski and Wacker, 2005). In line with these findings, we showed that KU-32 prevented neuregulin-1-induced demyelination in DRG/SC explants, in correlation with its in vivo antagonism to sensory hypoalgesia. Similar to the in vivo dependency of DPN recovery on Hsp70, the drug efficacy in inhibiting demyelination was mitigated by genetic deletion of Hsp70, suggesting that the protection is likely conferred by a nerve-specific chaperone induction. Indeed, we observed no systemic metabolic correction in mice administered KU-32. In further support of this notion, we demonstrate in the present study that KU-32 promotes Hsp70 expression in sensory nerves and that adenoviral-mediated overexpression of Hsp70 was sufficient to improve myelination against neuregulin-1. This finding might be somewhat surprising considering previous documentation that high Hsp70 expression favors cellular proliferation by permitting increased protein synthesis (Mayer and Bukau, 2005; Patton et al., 1995). The relatively weak neuron-glial expression of Hsp70 versus fibroblasts and increased rate of myelin differentiation in Hsp70 KO nerves compared to WT observed in our study do seem to agree with a negative correlation between Hsp70 and cell differentiation. However, Hsp70 does slightly upregulate during postnatal neural differentiation (Herbert et al., 2007) and preferentially increase in some differentiating tissue (Dix et al., 1997; Mangurten et al., 1997) including developing peripheral myelin (Patzig et al., 2011), indicating that it might have certain utilization such as protein transport during myelin assembly. Such possibility is supported by an earlier report that Hsc70 and Hsp70 were required for MBP expression in differentiating oligodendrocytes (Aquino et al., 1998). Indirect, but

striking evidence came from the analysis of HSF1-/- mice which developed progressive myelin loss, astrogliosis, reduced white matter tracts and deficits in motor control that were exacerbated by aging (Homma et al., 2007). Since no changes in the steady-state levels of the constitutively expressed chaperones were noted, lack of the stress-responsive Hsp70 could be of potential relevance to this phenotype. Therefore, Hsp70 may regulate glia cell homeostasis and myelin stability. In agreement, a N-terminal Hsp90 inhibitor that increased Hsp70 expression in SCs corrected myelin defects in a CMT1A model, in association with enhanced turnover of PMP22 (Rangaraju et al., 2008). Through reciprocal co-immunoprecipitation, we expanded previous findings from CNS and demonstrated for the first time a direct interaction of Hsp70 with the cytoplasmic-face membrane protein MBP in myelinating SCs of peripheral nerve. In contrast, no physical interaction between Hsp70 and P0 on the extracellular surface of myelin membrane was detected. Increasing Hsp70 by treating the explants with C-terminal Hsp90 inhibitor KU-32 promoted Hsp70-MBP binding, indicating that MBP might be a frequent substrate of Hsp70 in myelinating SCs. Owing to its localization in the extrinsic surface of myelin membrane and extensive integration of protein modification, MBP tends to have a relatively dynamic metabolic turnover which would necessitate chaperone-mediated protein synthesis and trafficking (Lajtha et al., 1977; Quarles et al., 2006). Disrupting the MBP binding sequence on Hsp70 should facilitate elucidating the precise role of Hsp70 in MBP metabolism during myelin biogenesis and/or maintenance. Though the etiology of DPN-associated segmental demyelination is not linked to the accumulation of any specific misfolded or aggregated myelin protein or proteins, diabetes increases oxidative modification of amino acids and lipids (Akude et al., 2010; Obrosova et al., 2007) that can impair myelin protein folding (Muchowski and Wacker, 2005) and metabolic composition (Baynes, 2002; Brown et al., 1979; Brownlee and Cerami, 1981;

Cermenati et al., 2012; Spritz et al., 1975). It is also well-established that many hereditary neuropathies have a genetic root of myelin protein mutation which impedes correct protein expression and myelin sheath formation (Rangaraju et al., 2008; Wrabetz et al., 2004a). Hence, increasing molecular chaperones in nerves may provide an excellent endogenous protein "quality control" defense by assisting protein expression and folding/refolding, thereby enhancing myelinostasis (Figure 3.9).

Apart from protein chaperoning, we provide the evidence that Hsp70 negatively regulates neuregulin signaling in differentiated SCs and preserved SC myelination through attenuating c-jun induction. C-jun is a basic leucine zipper transcription factor of the AP-1 family and has been implicated in apoptosis (Bienemann et al., 2008; Bossy-Wetzel et al., 1997; Palmada et al., 2002). Neuregulin-1 also induces c-jun expression (Si et al., 1999) and a recent study employing Cre-Lox conditional depletion of c-jun in SCs made a strong case that it plays a central role in mediating SC dedifferentiation (Parkinson et al., 2008). Our results are in keeping with this concept and further reveal that Hsp70 suppresses c-jun in myelinated SCs. As evidence is emerging that c-jun is increased in neuropathic nerves and may contribute to myelin degeneration (Hutton et al., 2011), such an endogenous inhibitory paradigm could be utilized to treat these phenotypes. Although Hsp70 is known to inhibit c-Jun N-terminal kinase (JNK) (Gabai et al., 1998) and has been suggested to prevent neuronal apoptosis via inactivation of JNK-c-jun signaling (Bienemann et al., 2008; Salehi et al., 2006), we failed to observe any decrease in JNK expression or activity with KU-32 at the time a significant reduction in c-jun was seen. Possible explanations include that since KU-32 only weakly induces Hsp70; this might not markedly impact on basal expression of JNK. In addition, JNK activation and deactivation could occur rather rapidly and transiently, and further examination of such kinetics is needed at

an earlier time point following neuregulin treatment. Regardless, JNK phosphorylation of c-jun is not required for SC dedifferentiation (Parkinson et al., 2008). Therefore, any interaction between Hsp70 and JNK would not be of physiological significance in this context. In fact, inhibition of c-jun by KU-32 does not appear to depend on the intersection of Hsp70 with the upstream kinase of this transcription factor since KU-32 did not prevent neuregulin-stimulated Erk (extracellular signal-regulated kinase) activation. Instead, our data supports that c-jun is channeled to the proteasome wherein it is reduced. Although the proteasomal inhibitor MG132 has been shown to upregulate c-jun (Meriin et al., 1998; Nakayama et al., 2001), which may controvert our interpretation of the data as the blockage of KU-32 effect in c-jun downregulation, the concentration used in the present study is substantially lower and we observed minimal c-jun induction by MG132 alone. Our finding thus suggests a novel mechanism by which Hsp70

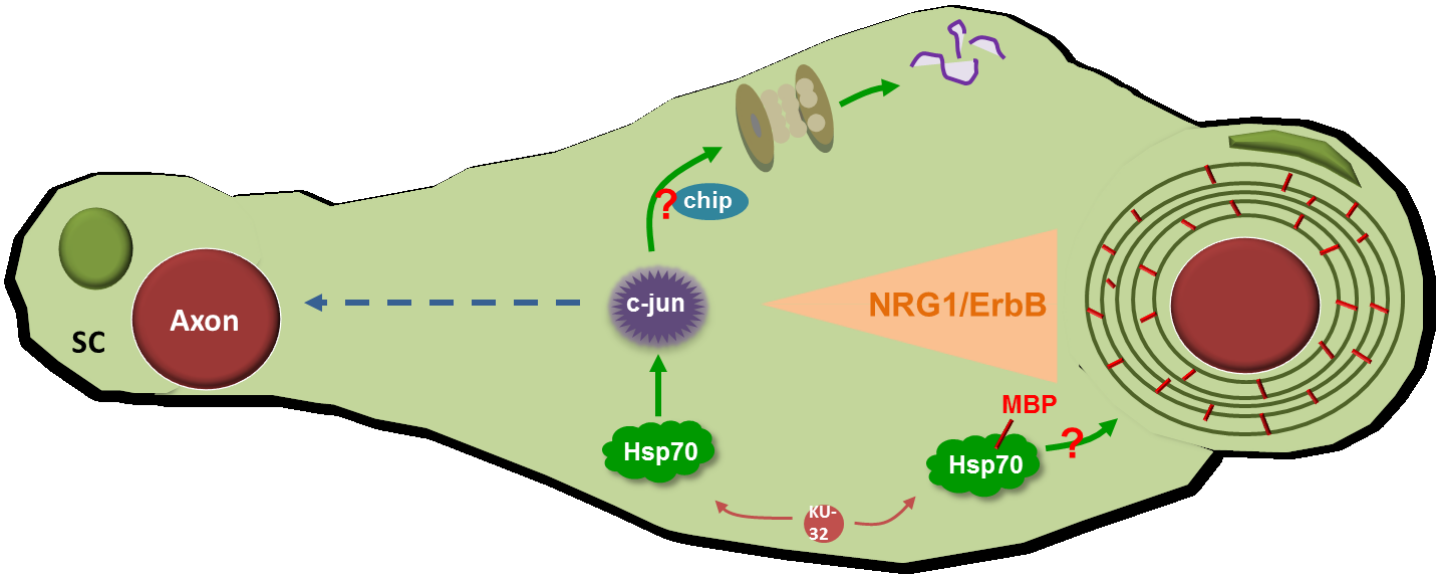

Figure 3.9 Possible mechanisms underlying KU-32/Hsp70-mediated counteraction of c-jun induction and NRG1-asscociated SC demyelination. Increasing Hsp70 by KU-32 promotes c-jun elimination via Hsp70-CHIP-mediated ubiquitin-proteosomal pathway and counteracts NRG1-induced demyelination. Increased Hsp70 may also help preserve myelin integrity through enhanced myelin protein chaperoning.

inactivates c-jun. Similar intervention of cell signaling by Hsp70 has been described in its regulation of apoptosis signal-regulating kinase 1 (Hwang et al., 2005) and transforming growth factor-beta (Yun et al., 2010). Intriguingly, c-jun is not commonly known to be directly regulated by Hsp70 and using immunoprecipitation assay we were not able to detect a physical association between these two in uninjuried nerves. This is not unexpected as it can be inferred from previous studies that interaction of Hsp70 with c-jun and other signaling proteins is rather transient and may occur only during certain cellular response (Hwang et al., 2005; Kitamura et al., 2003; Yun et al., 2010). Hence, Hsp70-c-jun interaction might only be appreciated in the presence of neuregulin or other known stimulators of c-jun in SCs. As carboxyl terminus of Hsp70-interacting protein (CHIP) has been implicated in linking chaperone substrates to ubiquitin proteolysis pathway (Petrucelli et al., 2004; Stankiewicz et al., 2010), future studies should determine whether Hsp70-CHIP-mediated ubiquitination is a prerequisite for c-jun elimination in proteasome (Figure 3.9).

Of particular interest induction of the stress chaperone Hsp70 in response to heat shock and KU-32 is greater in SCs than neuronal cell bodies. This agrees with previous findings in central and peripheral nerves (Manzerra and Brown, 1992; Pavlik and Aneja, 2007) and as suggested by a comparison between primary hippocampal neuron and glial cultures that such discrepancy in Hsp70 expression might result from the absence of a classical HSF1-driven transcriptional induction of HSP genes in neurons (Kaarniranta et al., 2002; Marcuccilli et al., 1996). Given that Parp-1 is important for fully activating Hsp70 promoter upon heat stress and KU-32 treatment (Martin et al., 2009), it is imperative to examine whether distinctive Parp-1 distribution in neuron and glia is an underlying factor. According to an assessment of primary cortical neuron and astrocytes, however, this does not seem to be the case since no significant

differences in Parp-1 content between these two types of cells were detected (Pieper et al., 2000). Rather, neuronal deficiency of heat shock response has been attributed to the lack of the principal mediator of stress response: HSF1 (Marcuccilli et al., 1996). Because Hsp90 inhibitors induce HSP transcription by utilizing the autoregulatory action of Hsp90 on HSF1, missing this key player would render the pharmacological intervention ineffective. By the same token, transfecting cells with Hsp90 siRNA that silences the presumed binding target of KU-32 abrogated the ability of the drug to elevate Hsp70. In the presence of similar SC Hsp90 and HSF1, we observed that specific deletion of Parp-1 blunted KU-32-induced Hsp70 increase (Figure A2). Whether this corresponds to abolishment of myelin protection awaits further investigation, perhaps with the aid of conditional Parp-1 knockout in myelinating SCs. If the chaperone reaction afforded through heat stress or KU-32 solely relies on cytosolic Hsp70, the above data would point to glia as the primary site of neuroprotection and neurons might benefit from absorbing exogenous Hsp70 released from adjacent glial cells in addition to gliotrophic support (Guzhova et al., 2001). However, KU-32 also protects pure sensory neurons from hyperglycemic insult (Urban et al., 2010; Urban et al., 2012), implying activation of mechanisms independent of cytosolic Hsp70. Indeed, we have identified through a quantitative proteomic screen that KU-32 translationally increased the mitochondrial paralog of Hsp70 (Grp75/mtHsp70) and improved mitochondrial bioenergetics in DRG neurons against glucose stress (Zhang et al., 2012). Since myelin impairment is increasingly associated with axonal and SC mitochondrial dysfunction in a variety of neuropathic disorders (Andrews et al., 2006; Kalman et al., 1997; Nikic et al., 2011), preserving mitochondrial homeostasis via molecular chaperones may contribute to antagonizing myelin pathology. Interestingly, chronic treatment of neuregulin enhances mitochondrial biogenesis (Canto et al., 2007; Hock and Kralli, 2009) Therefore,

determining whether deregulated neuregulin-1/ErbB signaling contributes to aberrant mitochondrial fission that occur in diabetic nerves (Edwards et al., 2010) might offer valuable insight into the pathogenesis of DPN.

3.10 Concluding Remarks

In summary, we demonstrate in the present study that a small molecule Hsp90 C-terminal modulator, KU-32, selectively upregulates Hsp70 in SCs and prevents neuregulin-induced demyelination of myelinated sensory nerves. The inducible cytosolic Hsp70 is essential to this myelin protection because genetic ablation of Hsp70 incapacitated the drug's ability to preserve myelin internodes. Hsp70 also appears to directly mediate inhibition of demyelination since adenoviral-directed Hsp70 overexpression mimicked the drug's effect in improving myelination against neuregulin. Importantly, inhibition of demyelination corresponded with reduction of neuregulin-activated c-jun, a well-characterized stimulator of SC dedifferentiation. In line with the dependency on Hsp70 for myelin protection, Hsp70 is both necessary and sufficient to suppress c-jun induction. This inhibition is not achieved through blocking signaling effectors upstream of c-jun, including JNK and Erk, but rather facilitating proteasomal degradation of c-jun. Such an action is reminiscent of other growth factor and signaling protein regulation by Hsp70 and may represent a typical mechanism of cell signal transduction intervention by the chaperone machinery. In addition, increasing Hsp70 promoted its association with the metabolically active myelin protein MBP, suggesting a potential involvement of Hsp70 in myelin protein chaperoning. Reducing Hsp90 diminished Hsp70 induction by KU-32, corroborating the specific targeting of Hsp90-HSF1 in modulating heat shock response by C-terminal inhibitors. The mechanism by which KU-32 upregulates Hsp70 may also involve Parp-1 modification, as KU-32 failed to elicit Hsp70 expression in Parp-1-deficient neuroglial explants

(Appendix). Further characterization of the affect of Parp-1 knockout on the drug efficacy may resort to conditional Parp-1-null SCs. Together, our data provide evidence that Hsp70 protects peripheral nerve myelin from degenerating through regulation of neuregulin signaling and possibly maintenance of myelin proteins. Since alterations in neuregulin-1/ErbB signaling and myelin components contribute to pathological changes in myelinated fibers in DPN, and may lead to demyelination in diabetic nerves and other demyelinating disorders, increasing Hsp70 may counteract aberrant gliotrophic signaling and protein denaturation thereby ameliorating myelin degeneration in these neuropathologies. With particular regard to DPN, it is important to note that while our model emphasizes the impact of chaperones on demyelination that arises from pathological activation of neuregulin-1/ErbB, our hypothesis does not necessitate altered gliotrophic support as the primary pathogenesis or site of chaperone protection in diabetes. There is no doubt that both neurons and their supporting cells are subject to diabetic insult and very limited success can be obtained by targeting one of the many biochemical events that contribute to the progression in DPN in a temporally non-uniform nature. Targeting molecular chaperones may circumvent this obstacle by upregulating a broad cytoprotective response and reparative potential in both neurons and glia that may allow nerves to tolerate otherwise pathogenic consequences of hyperglycemia. As degenerative changes in myelinating SCs either primary or secondary to axonal pathology is a substantial feature in DPN, understanding how molecular chaperones modulate signaling events underlying peripheral myelination and demyelination may open new translational avenues for clinical management of DPN and/or other human neuropathies.

Chapter 4: Estrogen, GPR30 and Peripheral Myelination

Abstract

As efficient remyelination primarily depends on the cellular and molecular signals that recapitulate developmental myelination, elucidating their molecular targets and signaling mechanisms will provide mechanistic insight and may help develop therapeutic approaches for demyelinating or demyelination-related diseases. Recent studies suggest that estrogen is neuroprotective and is involved in regulating myelination. Using SC/DRG neuron co-cultures, a well-established *in vitro* system that recapitulates the myelinating peripheral nerve, we hereby identify estrogen as a positive regulator of peripheral myelination since treatment of estradiol was sufficient to elicit SC myelination. Particularly, genetic knockdown supports that GPR30, a novel G-protein coupled estrogen receptor, is critically involved in mediating estrogen effects in myelination. However, a GPR30-specific agonist G-1, was not able to recapitulate estrogenic effect in inducing myelination at the concentrations tested. Whether or not this suggests other estrogen receptors are necessary to execute estrogen-stimulated myelination awaits further investigation. Moreover, we provided the first evidence for a molecular dependency between GPR30 and the membrane scaffolding protein Caveolin-1 (Cav-1) by showing that myelination-incompetent Cav-1 KO nerves have diminished GPR30 and increasing Cav-1 expression rescued GPR30 expression. Based on these data, we propose the hypothesis that Cav-1 promotes estrogen-stimulated myelination through regulating GPR30 expression. Further elucidation of the molecular and cellular events underlying above observations may facilitate developing and refining hormone-based therapy for treating myelin pathology.

4.1 Estrogen as A Neurohormone and Myelinotrophic Factor

Despite the ongoing effort of combating the myelin loss in human neuropathies, current treatment strategies are limited to preventive therapies. Little progress has been made towards pharmacologically enhancing damage repair and restoring myelin structure, which oftentimes fails even in the absence of active disease (Franklin and Ffrench-Constant, 2008). Owing to its importance in regulating myelin thickness, neuregulin-1 has received increasing attention to its potential utilization in treating demyelinating diseases. However, experimental analysis of this growth factor has yielded equivocal results in different models of demyelination (Cannella et al., 1998; Marchionni et al., 1999; Penderis et al., 2003). Such limited success reflects the later discovery that neuregulin-1 is not sufficient to initiate myelination (Taveggia et al., 2005) and may even provoke demyelination if the ligand concentration is too high. This duality of action draws strict limits to the therapeutic window by which neuregulins may be used to promote myelination. Meanwhile, elucidating additional cellular and molecular signals that work in concert to drive myelination is of high scientific impact on preventing demyelination as well as developing approaches by which remyelination might be enhanced therapeutically. Recent studies suggest that estrogen is neuroprotective and is involved in regulating myelination.

Although estrogen has long been confined to the category of "female sex hormones", its involvement in glial cell myelination is now revealed by accumulating evidence. Estrogen belongs to a superfamily of nuclear steroid hormones that signal via nuclear estrogen receptors (ERs) and regulate target gene transcription. In addition to this canonical genomic mechanism, cytoplasmic nuclear receptors ER-α and ER-β can be targeted to the membrane surface and mediate rapid non-genomic actions that support important functions such as cell proliferation, survival and differentiation (Segars and Driggers, 2002). Apart from these ligand-activated

transcription receptors, it has also been uncovered that estrogen can bind directly to and activate a seven-transmembrane G-protein coupled receptor (GPCR) termed GPR30. GPR30 was identified through its ability to mediate rapid physiological response of this hormone in ER-α/ER-β negative cells (Prossnitz et al., 2008). Due to evidence that estrogen may delay the onset or ameliorate the severity of several neurological disorders such as Alzheimer's and Parkinson's disease (Brann et al., 2007; Henderson, 2006), its role has been extensively studied in the brain.

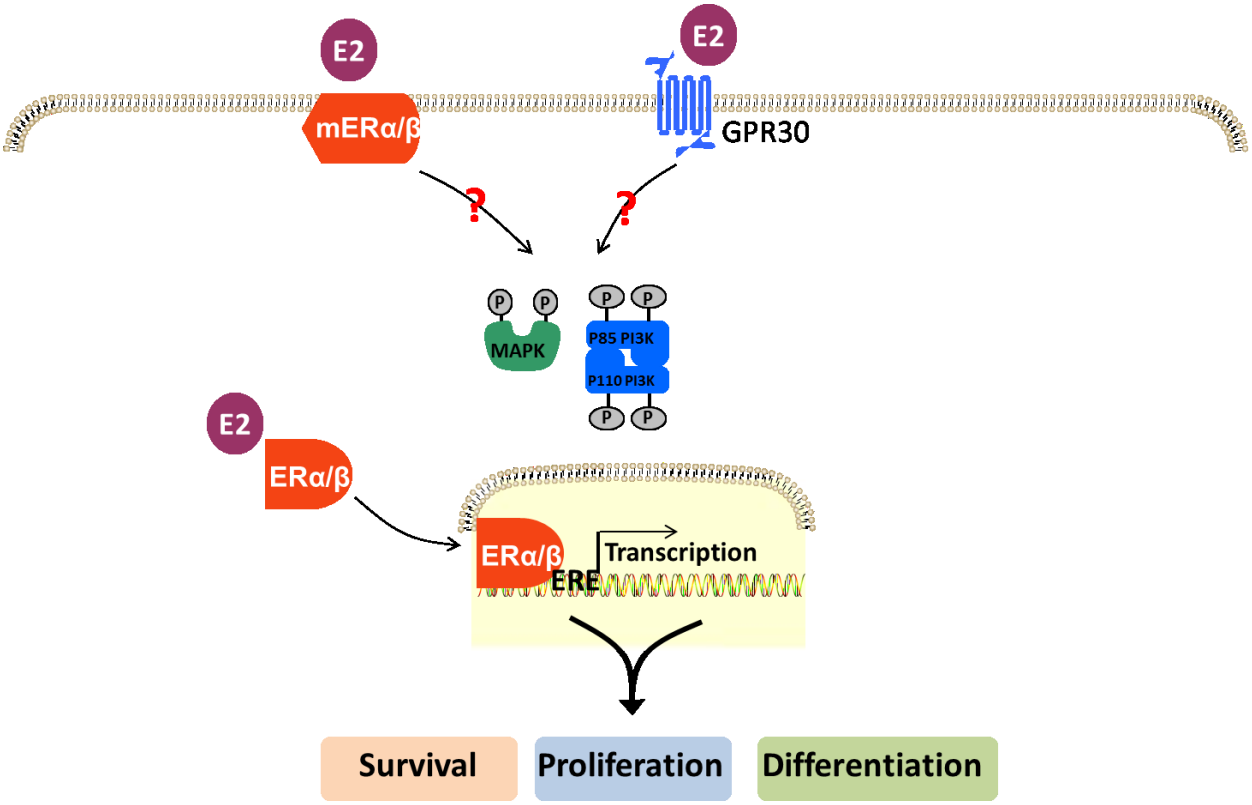

Figure 4.1 Estrogen stimulates both genomic and nongenomic signaling transduction in regulating cell survival, proliferation and differentiation. E2: estradiol. mERα/β: membrane-bound ERα/β. MAPK: mitogen-activated protein kinase. PI3K: phosphatidylinositol 3-kinase. ERE: estrogen response element. Question mark indicates through unknown mechanisms.

It is now becoming evident that estrogen also exerts neuroprotective and cognition-enhancing effects, such as reduction of stress and improvement of learning and memory (Kelly et al., 2005). Whereas the effect of estrogen in promoting neuronal homeostasis and synaptic plasticity has been well recognized, scant attention has been given to its role in the development of glial cells,

a major site of estrogen synthesis in neuronal tissue. The demyelinating disease multiple sclerosis (MS) is two times more prevalent in females than in males after puberty, but pregnancy has a protective effect, which implicates a role for estrogen in MS (Whitacre et al., 1999). Indeed, estrogen therapy ameliorated MS in humans. Animals pretreated with estradiol (E2) before immunization to induce experimental allergic encephalomyelitis were protected from clinical signs of the disease (Bebo et al., 2001; Soldan et al., 2003). Although the therapeutic efficacy of estrogens has long been considered as an immunomodulatory effect, direct effects of estrogen in neuronal tissue were recently shown and should not be dismissed. Evidence for direct actions of estrogen in glial cell physiology come from studies showing the stimulation of proliferation and expression of myelin genes following estradiol treatment in cultured oligodendrocytes (OLGs) which demonstrated abundant expression of ER-α and ER-β (Jung-Testas et al., 1992). This is consistent with a previous classical study showing estrogen administration increased brain myelination of neonatal rat (Curry and Heim, 1966). Of note, the presence of a membrane-associated ER was identified in the OLG plasma membrane and myelin sheath by using Triton X-100 extraction, suggesting an intimate relationship between the membrane ER and CNS myelin (Arvanitis et al., 2004). In comparison, very limited interest has been devoted to estrogenic effects in the peripheral nervous system despite the fact that ER-α and ER-β transcripts have both been amplified from dorsal root ganglia (DRGs) (Taleghany et al., 1999). Similar to ER-α and ER-β, GPR30 is expressed in DRGs and has been implicated in their nociceptive and mechanical response to estradiol (Kuhn et al., 2008). Estrogen also induced a substantial increase in SC proliferation in sciatic nerve segments dissociated from rats (Fex Svenningsen and Kanje, 1999), but elicited mitogenic effects in primary SCs only in the presence of elevated intracellular cAMP level (Jung-Testas and Baulieu, 1998). However, estrogen does

not seem to be only a mitogenic factor to glial cells. Another group showed that addition of estradiol not only inhibited SC dedifferentiation, but also augmented remyelination following mitogen withdrawal in previously-myelinated DRG/SC co-cultures (Zhu and Glaser, 2008). Therefore, estrogen may exert a direct effect on peripheral myelination. To directly test this hypothesis, we examined the sufficiency of estrogen in inducing SC myelination and identified the corresponding receptor necessary for this myelinogenic effect. The overall scientific goal is to elucidate the molecular and cellular events underlying estrogen-regulated peripheral myelination, thereby providing a mechanistic basis for the development of new therapeutic approaches for treating demyelinating neuropathy.

4.2 Caveolin-1, Estrogen Receptor and Myelination

As it is evident from the amino acid sequence, Caveolin-1 (Cav-1) is best known as an integral membrane protein that forms the specialized vesicular lipid rafts, caveolae, at the plasma membrane in various cell types including the myelinated SCs (Meier et al., 2004; Mikol et al., 1999). The significance of this function is clearly demonstrated in Cav-1-null mice which are deficient in plasmalemmal caveolae (Razani et al., 2001). By oligomerizing as a scaffold in caveolae, Cav-1 assembles and concentrates a variety of signaling complexes into distinct regions at the cell surface and regulates membrane-associated signaling events (Okamoto et al., 1998). One such event has been proposed to be cell cycle control, inasmuch as the expression of Cav-1 is tightly linked to cellular differentiation (Mikol et al., 2002). Consistent with this hypothesis, Cav-1 expression in SCs was upregulated during myelination and downregulated following SC dedifferentiation during axotomy (Mikol et al., 2002). Although this could be explained through the increasing need for cholesterol shuttling by the cytosolic pool of Cav-1 in myelinating SCs (Dobrowsky et al., 2005), we further provided evidence that downregulation of

Cav-1 increased ErbB2 activation in SCs (Tan et al., 2003) and sensitized myelinated SC/DRG co-cultures to NRG-1-initiated demyelination (Yu et al., 2008). Therefore, Cav-1 may function to stabilize the myelinating phenotype of SCs by negatively modulating ErbB2 signaling. Cav-1 also co-localizes with ER in CNS myelin (Arvanitis et al., 2004) and is essentially involved in rapid non-genomic estrogen signaling at neuronal membrane (Luoma et al., 2008). However, whether and how Cav-1 regulates ER signaling in peripheral glia and myelination remains unexplored. In the present study, we show that Cav-1 may play an important role in estrogen-induced SC myelination by supporting GPR30 expression.

4.3 Estrogen is sufficient to induce moderate SC myelination

To test our hypothesis, mouse embryonic DRG/SC explants were established as an *in vitro* model of myelinating peripheral nerve and incubated with 0.05% DMSO (negative control), 50nM or 100nM β-estradiol (E2), or 50μg/ml ascorbic acid (positive control) for 2 weeks. Immunostainning with MBP antibody was then performed to visualize myelinated axons in these cultures. Imaging was undertaken by confocal microscopy and the number of myelinated segments and average internodal length were quantified from a montage area consisting of 36 microscopic fields ($24x10^6 micron^2$). Whereas 50nM E2 was not able to significantly increase internode formation compared to vehicle-treated control, 100nM E2 increased the number of MBP-segments from ~12 to ~33 per montage area, albeit still ~50% lower than that from ascorbic acid-treated cultures. E2 promoted formation of long internodes (~70-100microns) at both concentrations though their average internodal length appeared shorter than the positive control.

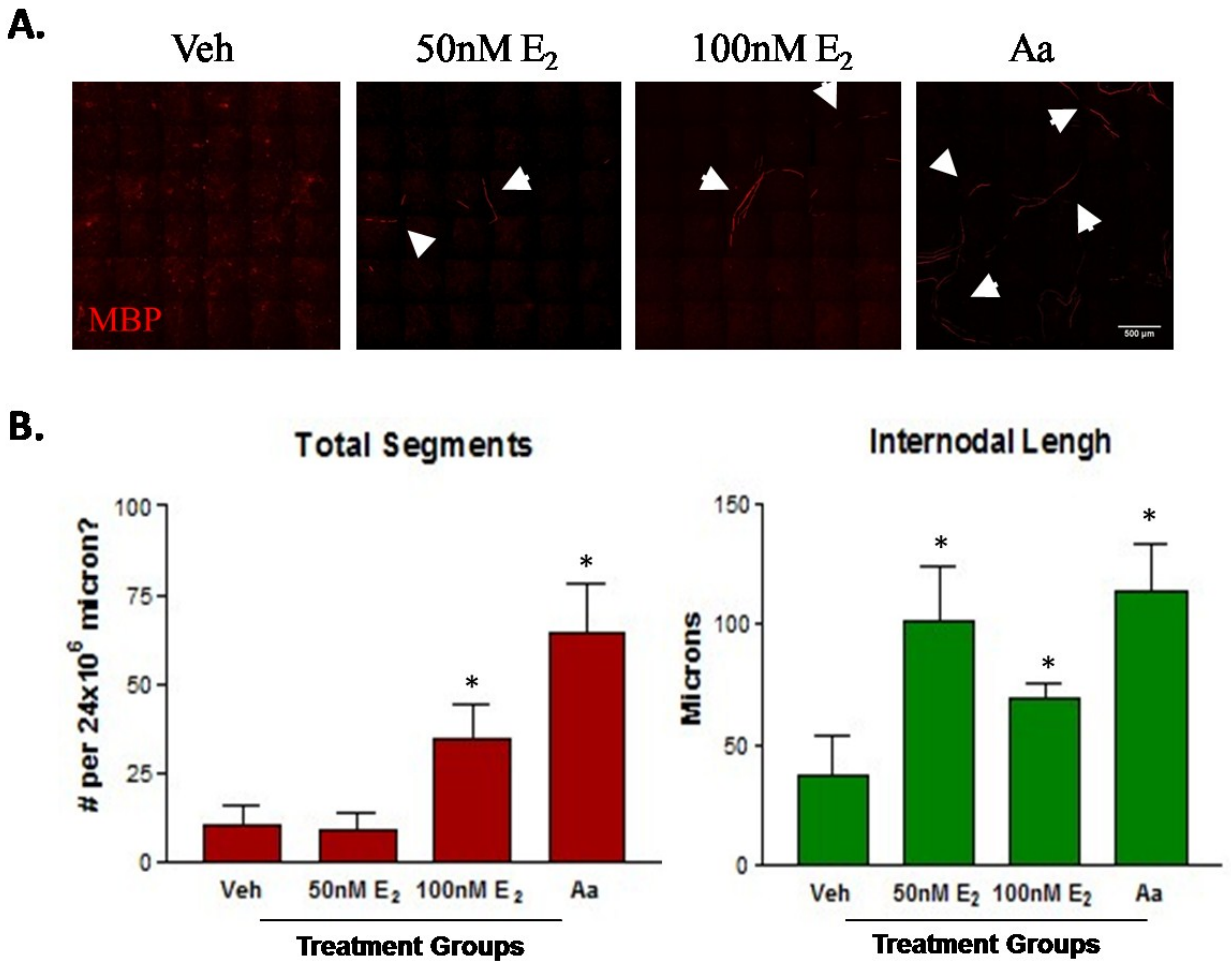

Fig.4.2 Estrogen induces moderate myelination in DRG-SC explants. A, Embryonic DRG-SC explants from C57Bl/6 mice were treated with vehicle, 50nME2, 100nM E2 and 50µg/ml ascorbic acid for 2 weeks and myelin segments were visualized by immunostaining for myelin basic protein (MBP) (red) (SMI-94R antibody, Covance). **B,** Total number of MBP-stained segments and average internodal length from each culture (coverslip) were quantified from 36 montage images using SlideBook 4.0. One-way ANOVA indicates a significant difference in total segments [$F_{(3,12)}$=4.10; p<0.05] and intermodal length [$F_{(3,12)}$=3.396; p<0.05] among groups. Tukey's test indicates *p<0.05 for treatment compared to control. df=3, n=4.

4.4 Estrogen induces myelination in DRG-SC explants in the presence but not absence of GPR30- As shown in Fig.4.3, estradiol induced significant myelination in WT explants to a level that is comparable to that induced by ascorbic acid, whereas no response was observed in co-cultures from mice with genetic deletion of Caveolin-1 (Cav-1) regardless of the treatment. This result was also evident in biochemical data since the expression of compact myelin protein

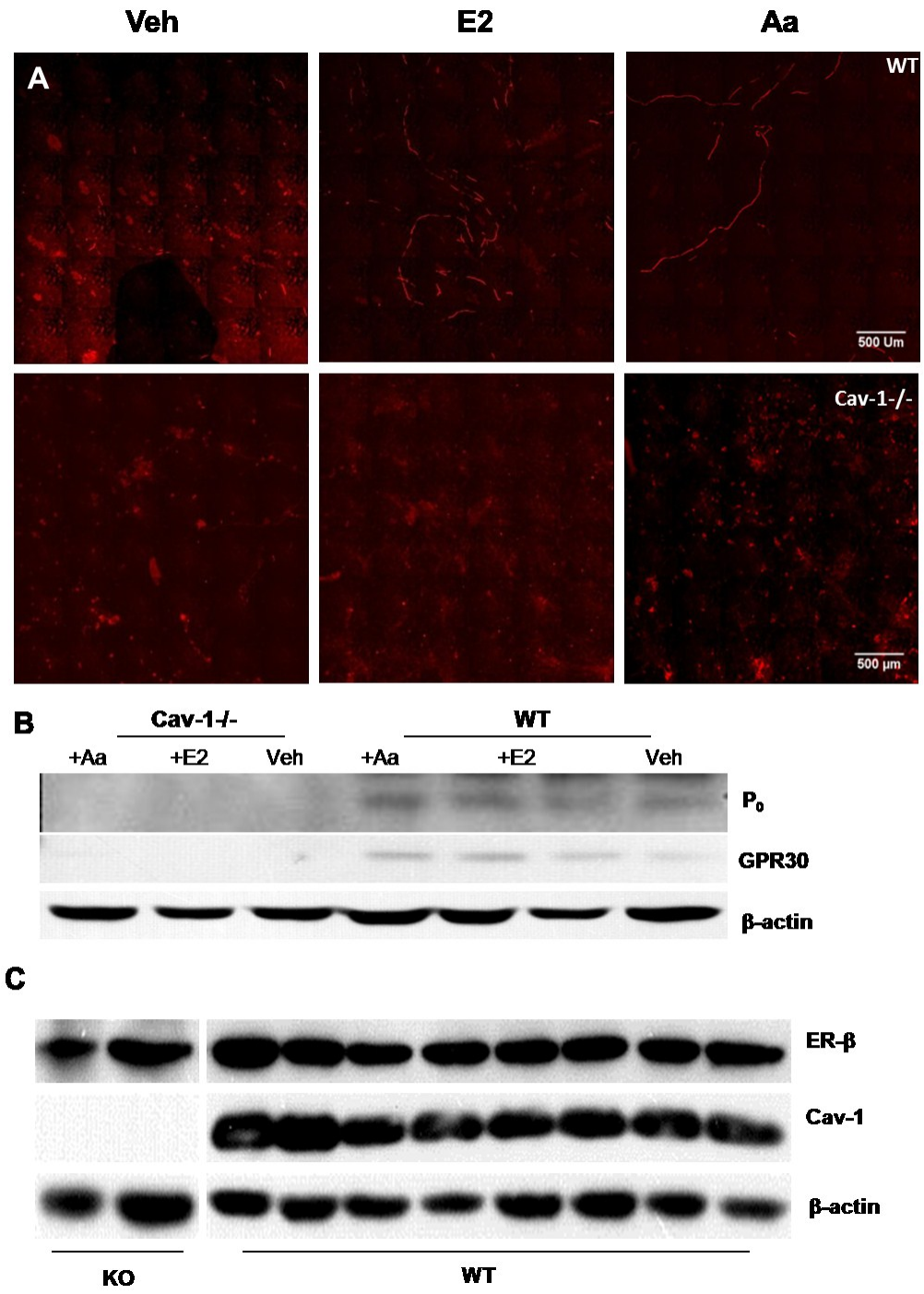

Fig.4.3. Estrogen selectively increases myelination in DRG-SC explants with GPR30 expression. A, Embryonic DRG-SC explants from wt and Cav-1-/- were treated with vehicle, 100nM E2 and 50µg/ml ascorbic acid for 2 weeks and myelin segments were visualized by immunostaining for myelin basic protein (MBP) (red) (SMI-94R antibody, Covance). B,C, Whole cell lysates from each sample were prepared and immunoblotted for P0, GPR30, ER-β, Cav-1 and β-actin. For immunofluorescence analysis 3 replicates were contained in each group. Data shown are representative of two independent experiments.

P_0 was only detectable in myelinated WT cultures. Cav-1 is a membrane scaffolding protein that may function in the trafficking and docking nuclear ERs into plasma membrane, where ERs initiate rapid non-genomic signaling cascades. Interestingly, Cav-1 ablation diminished GPR30 expression, but did not alter the expression of ER-β (Fig.4.3), suggesting an intimate relationship between Cav-1 and GPR30 expression in sensory neurons. Of note, WT co-cultures treated with E2 and ascorbic acid demonstrated an increased GPR30 expression compared to those treated with vehicle only, indicating an upregulation of GPR30 during myelinogenesis. In summary, the data support that estrogen stimulates peripheral nerve myelination *in vitro* and this correlates with an increased GPR30 expression.

4.5 GPR30 is necessary for estrogen-induced myelination-

We propose that GPR30 is necessary for estrogen-induced myelination. In support of this hypothesis, we assessed the effect of siRNA-directed GPR30 downregulation on the ability of estradiol to induce myelination. Results in Fig.4.4 show that compared to non-infected control and scrambled siRNA, GPR30-targeted siRNA caused a marked decrease in the number of MBP-stained (green) myelin segments in WT cultures treated with estradiol but not ascorbic acid. This indicates that ascorbic acid and estradiol may regulate myelination through heterogenous mechanisms. Of note, although GPR30 knock-down significantly reduced the number of myelinated fibers, no change in average internodal length was observed. This suggests that the regulation of the length of internodes formed is independent of GPR30 signaling. Importantly, the immunofluorescence data correlated with parallel studies using immunoblot which showed a significant decrease in P_0 expression, concomitant with the reduced level of GPR30. Although sufficient data is yet to be obtained to address the statistical significance, the observed

differences were rather robust. Overall, these data support our hypothesis that estrogen stimulates peripheral myelination via a GPR30 dependent mechanism.

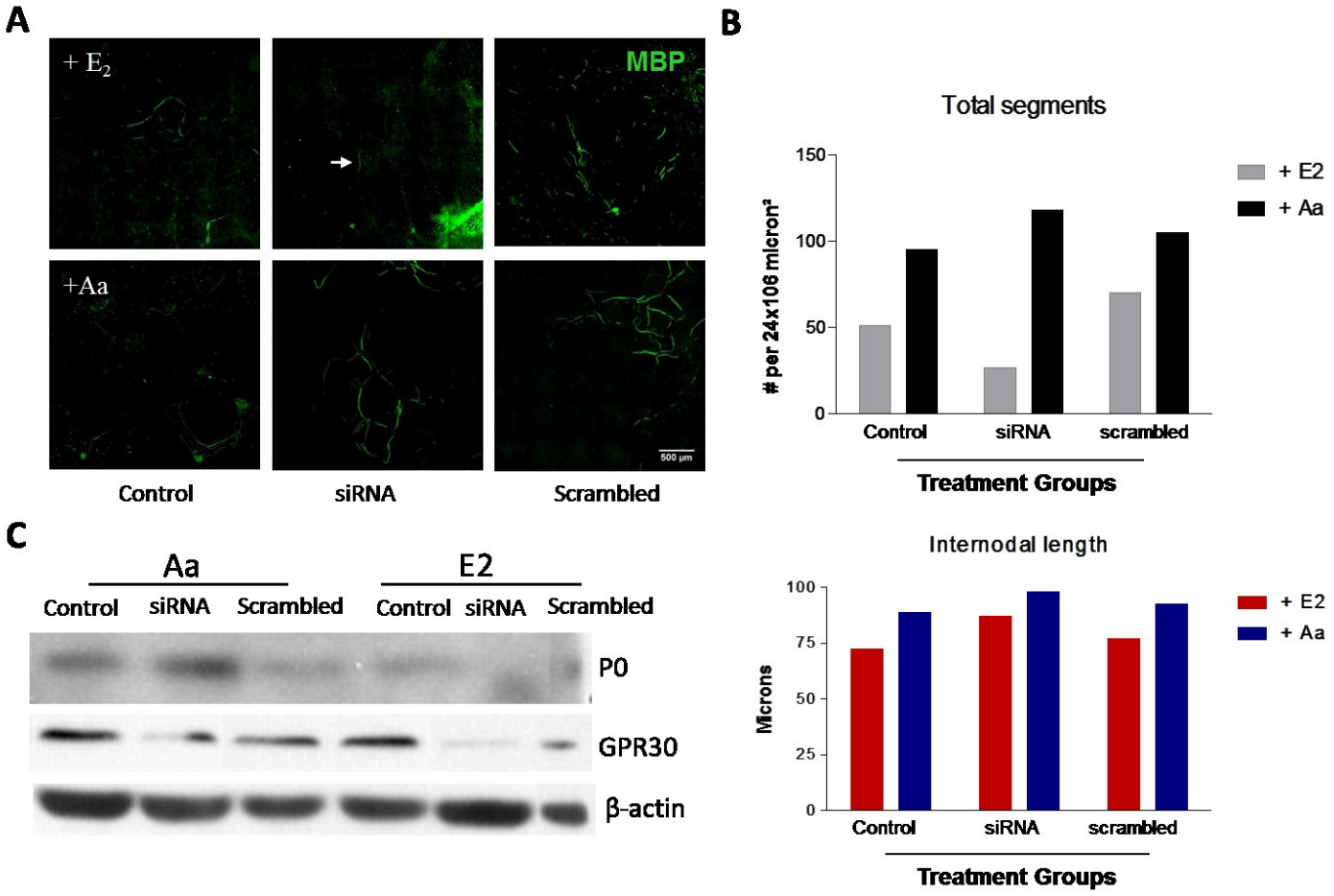

Fig.4.4 GPR30 downregulation inhibited estrogen-induced myelination in DRG-SC explants. A, DRG-SC explants from wt were either non-infected, infected with scrambled siRNA or GPR30 specific siRNA-expressing adenovirus upon treatment of 100nM E2 or 50μg/ml ascorbic acid for 2 weeks. Myelinated axons were stained with MBP (green). **B,** Total number of myelin segments and average length of internodes were quantified from 3 independent samples per treatment. **C,** Immunoblot analysis was performed on lysates of co-culture from each group and expression of P0 and GPR30 were assessed.

4.6 Adenoviral-mediated Cav-1 expression rescues GPR30 expression but not myelination in Cav-1$^{-/-}$ explants One interesting observation is that depletion of Cav-1 expression in the present model also diminished GPR30 protein level, suggesting that stable expression of this

receptor in peripheral nerves requires Cav-1. Cav-1 is a principal integral component of caveolae, specialized plasma membrane microdomains in which Cav-1 participates in the scaffolding and

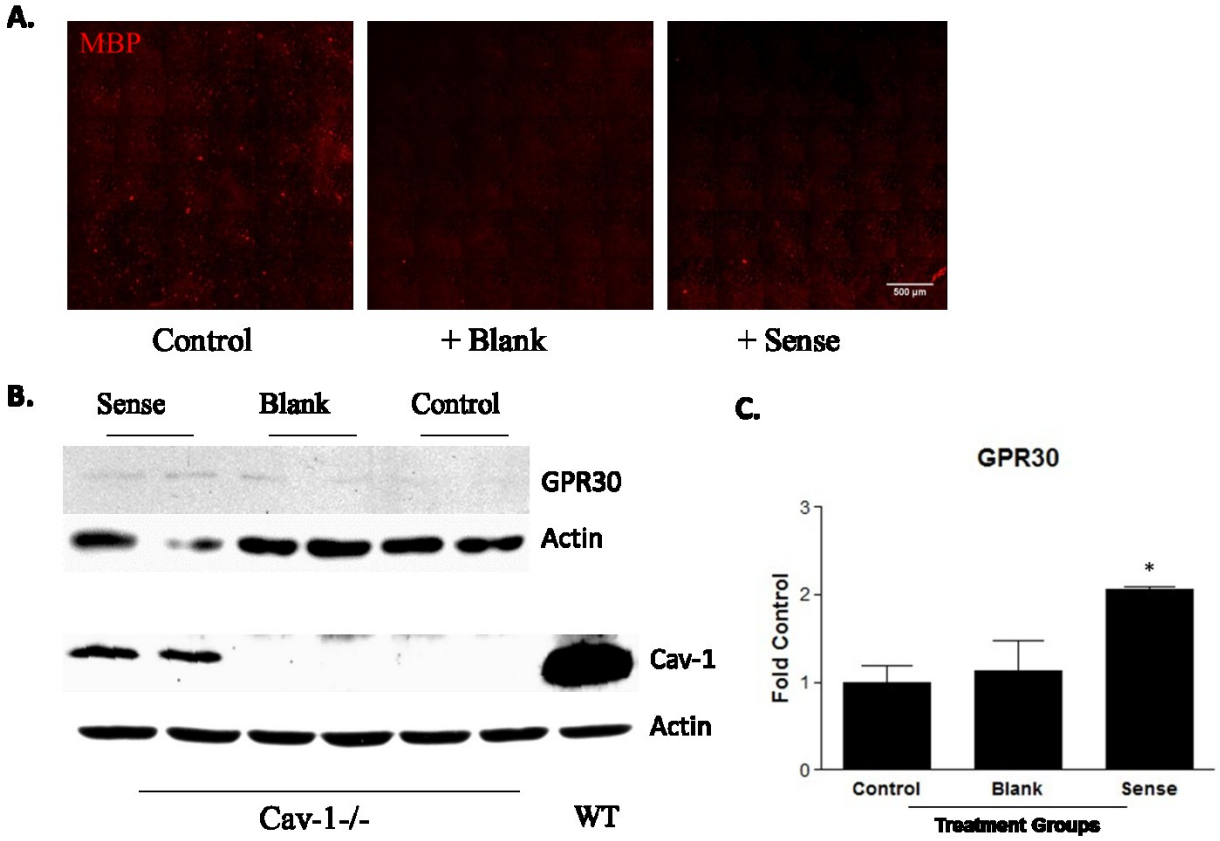

Figure 4.5 Adenoviral expression of Cav-1 in Cav-1-/- explants restored GPR30 expression but not myelination. A, Cav-1-/- DRG explants were established and infected with blank or sense Cav-1 adenovirus, or left uninfected for two weeks while receiving 100nM E2. Myelination was inspected via MBP staining. **B,** Protein expression of Cav-1 and GPR30 was measured with the aid of antibodies against Cav-1 and GPR30, respectively. **C,** Quantitation of GPR30 expression was derived from average of two independent experiments. One-way ANOVA indicates significant difference in GPR30 expression among groups [$F_{(2,9)}$=3.16; p<0.05]. Tukey's test indicates *p<0.05 compared to control. df=2, n=4.

compartmentalization of various signaling molecules thereby regulating membrane-associated signal transduction (Liu et al., 2002; Okamoto et al., 1998). A small pool of soluble Cav-1 has also been found in multiple cellular compartments such as cytosol where it has been implicated in protein and lipid transport (Liu et al., 2002). Recent evidence suggests that Cav-1 associates

with and targets membrane localization of ER-α (Kim et al., 1999; Razandi et al., 2002), and is essential for activation and functional isolation of discrete estradiol-triggered signaling cascades from the membrane (Boulware et al., 2007). Based on these findings, we hypothesized that neuronl/glial GPR30 expression and estrogen-stimulated myelination is mediated through Cav-1. If this is the case, re-expression of Cav-1 in the cells should concomitantly restore GPR30 levels. Indeed, adenovirus-mediated expression of Cav-1 enabled GPR30 detection by immunoblotting (Figure 4.5). However, the amount of GPR30 induced was apparently not sufficient to rescue myelination in Cav-1 KO nerves as no MBP-stained compact myelin was seen. This might due to the low exogenous incorporation of Cav-1 into the cultures which may not support the minimal amount of GPR30 necessary for the initiation of internode formation. Higher expression of Cav-1 might be needed in order to confer physiologically significant expression of GPR30.

4.7 GPR30 activation was not sufficient to induce myelination

While above data clearly supports that the magnitude of myelination correlates with the extent of GPR30 expression, an unresolved issue is whether GPR30 is sufficient for estrogen effect or are there additional ERs involved? To address this, we evaluated whether selective

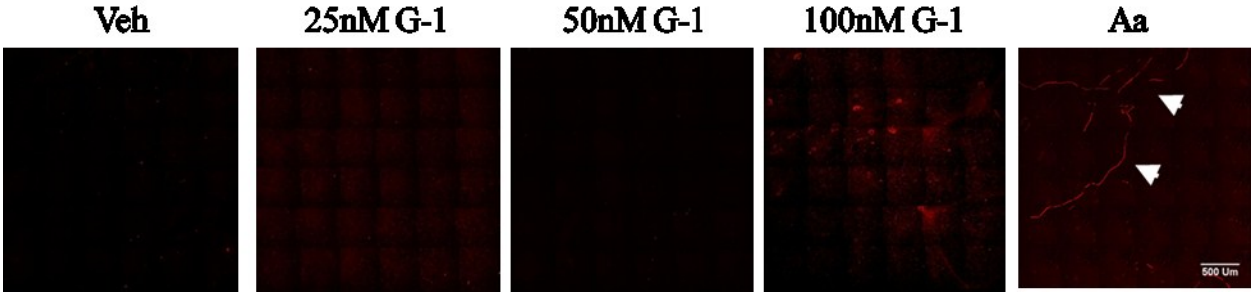

Figure 4.6 GPR30-specific agonist did not induce myelination. WT DRG explants were established *in vitro* and treated with 25, 50,100nM G1 or 50ng/ml ascorbic acid for 2 weeks. Immunostainning for MBP was performed for visual inspection of myelination. Data shown are representative of 2 independent experiments, no myelin internode formation was observed in G-1-treated cultures regardless of the concentration tested.

activation of GPR30 is able to recapitulate the myelination induced by estrogen. For this purpose, GPR30-specific agonist G1 substituted estradiol as the myelin-inducing agent and cultures were immunostained for myelinated internodes after the same amount of incubation time as in previous experiments. Unfortunately, regardless of the concentration tested (25nM, 50nM, 100nM), none of the cultures showed assembly of compact myelin sheath, whereas internode formation was readily observed in ascorbic acid-treated explants. Such an outcome yields two interpretations: higher concentrations of G1 are needed or GPR30 is not sufficient for myelination. Future study using increased concentration of G1 is justified to support and/or refute above possibilities.

4.8 Summary and Discussion

Using SC/DRG neuron co-cultures, a well-established *in vitro* system that recapitulates myelinating peripheral nerve, we hereby identify estrogen as a positive regulator of peripheral myelination. Particularly, genetic knockdown supports that GPR30 is critically involved in mediating estrogen effects in myelination. GPR30 is a GPCR that is activated by estrogen and induces second messenger signaling including mitogen-activated protein kinases (MAPK), phosphatidylinositol 3-kinase (PI3K), and Src/Shc (Revankar et al., 2005; Thomas et al., 2005). Treatment with estradiol elicited a significant amount of myelination in WT cultures, whereas no myelin segment was observed in cultures expressing little or no GPR30. In purified sensory neurons, the expression and activity of ERs have been described in several studies. For example, GPR30 was found to be expressed in DRG neurons and elicited mechanical hyperalgesia via PKCε activation upon stimulation by either estrogen or specific agonist G-1 (Kuhn et al., 2008). The above hormonal effects on myelination could therefore be regarded as a phenomenon secondary to neuronal influence and warrant further investigation on GPR30 action in the

activity of neurons, such as dependence on myelin-promoting factor-NRG1typeIII (Taveggia et al., 2005) (Figure 4.7.1). However, SCs also demonstrate abundant ER distribution and increased mitogenesis in response to estrogen treatment, suggesting that estrogen might directly modulate SCs as well. Indeed, ER expression in SCs has been confirmed by studies from immunoblot and immunofluorescence (Thi et al., 1998). Nevertheless, the precise localization and subtypes of ER(s) in the co-cultures are yet to be clarified, since both neuronal and glial, long-term nuclear ER and short-term membrane ER actions may contribute to the pro-myelinating effects of estrogen. Moreover, although the myelin-enhancing function of estrogen has been supported by

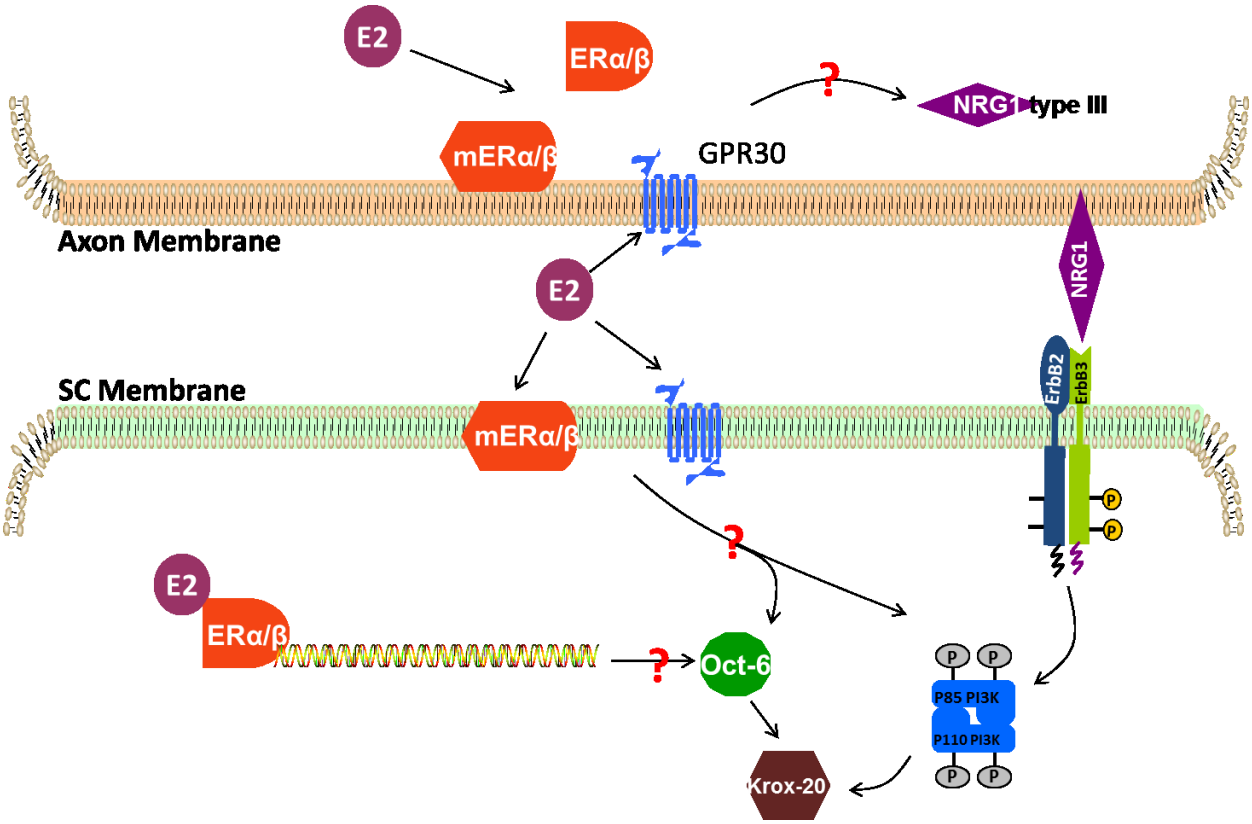

Figure 4.7.1 Potential mechanisms underlying estrogen-stimulated SC myelination. Stimulation of ERs in neurons by estradiol (E2) may enhance axonal production of cellular/molecular signals, for instance NRG1 type III, which in turn activate ErbB2/3 receptors on SCs and drive SC myelination. Estrogen could also directly activate GPR30 and/or ERα/β in SCs, which directly or indirectly leads to upregulation of myelin-promoting signaling and/or transcription factors including PI3-Akt and Oct6-Krox-20. Characterizing the content and distribution of different ER subtypes in neurons and glia will facilitate understanding the molecular mechanisms underlying estrogen-regulated peripheral myelination.

increasing evidence, the underlying molecular mechanism is largely unexplored. Pursuing this gap promises to aid our development of targeted treatment regimens in clinical settings. PI3K is an essential signaling event that determines SC myelinating fate (Maurel and Salzer, 2000a). Of note, this signaling kinase has also been coupled to various cellular effects elicited by estrogen (Segars and Driggers, 2002). Whether or not PI3K is involved in estrogen-induced myelination awaits further characterization (Figure 4.7.1). In addition, expression of transcription factors such as Krox-20 and Oct-6 are critical components in myelin protein expression and crucial step in the transition from promyelinating to the myelinating stage of SCs (Kamholz et al., 1999; Svaren and Meijer, 2008). Given that Krox-20 and Oct-6 expression are downstream to the activation of fast signaling cascades, direct influences on their expression might as well explain the effect of estrogen on SC myelination.

Our finding that Cav-1 deficient nerves also displayed impaired expression of GPR30 suggests an intimate relationship between this membrane ER and Cav-1. To our knowledge, this is the first evidence provided for a molecular link of these two and is consistent with previous reports that Cav-1 associates with and regulates membrane-bound ER-α and/or ER-β signaling (Boulware et al., 2007; Kim et al., 1999; Razandi et al., 2002). Unlike ER-α and ER-β, GPCRs contain innate seven transmembrane domain and may not rely on other proteins for membrane anchoring. However, GPCRs and their interacting molecules are also enriched in lipid rafts and caveolae and may require Cav-1 in such localization and trafficking (Chini and Parenti, 2004; Kong et al., 2007). Therefore, lack of Cav-1-mediated membrane targeting and trafficking may detain GPR30 in the cytosol and subject it to degradation. Given the critical association between Cav-1 expression with SC GPR30 expression and degree of myelination, it is tempting to speculate that Cav-1 controls estrogen-stimulated myelination through targeted membrane

transport and scaffolding of GPR30 (Figure 4.7.2). Whether this is achieved through direct or indirect interaction of Cav-1 with GPR30 is yet to be determined.

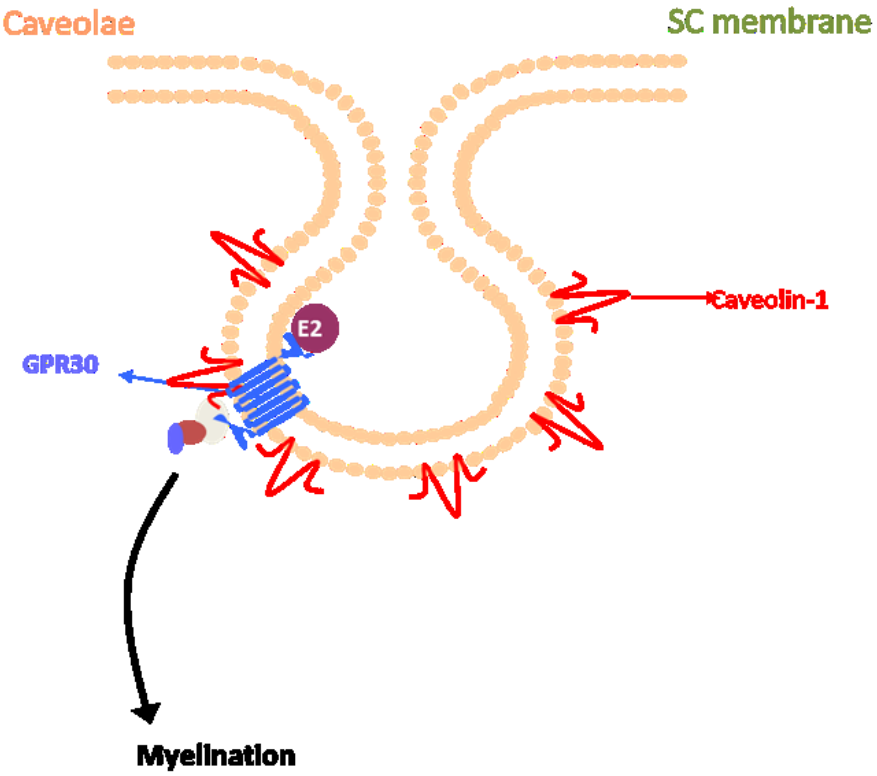

Figure 4.7.2 Cav-1 regulates estrogen-mediated peripheral myelination through membrane targeting of GPR30. Caveolin-1 may anchor and/or associate with GPR30 in caveolae at SC membrane, thereby regulate its activation or coupling with the downstream signaling involved in myelination upon ligand (estradiol) binding. E2:estradiol.

Overall, elucidating these events will lend insight into our understanding of the cellular and molecular components necessary for proper remyelination and facilitate the design of targeted hormone therapy in demyelinating neuropathies. Along this line, estradiol and other steroids have proven promising efficacy in reducing demyelination and enhancing remyelination in numerous *in vitro* and *in vivo* models (Acs et al., 2009; Li et al., 2006; Tiwari-Woodruff et al., 2007; Zhu and Glaser, 2008). Of particular note, administration of another neuroactive female hormone progesterone and its metabolite to STZ-rats ameliorated diabetes-induced myelin abnormalities (Veiga et al., 2006) and MBP deficiency (Pesaresi et al., 2010). It can be

anticipated that further definition of the biochemical mechanism underlying this protective effect would assist the rational identification of novel treatment towards counteracting myelin complications in diabetes.

Chapter 5: Outlook

Myelin and myelinated fiber functions are frequently affected in DPN and other human neuropathies, which display a trend of climbing global prevalence. To date, little success has been achieved in disease arrestment and prevention, and even scarce therapeutic strategies are available for addressing the substantial myelin loss and nerve damage. As irreversible consequences often occur as a result of prolonged disease progression and unattended neurodegenerative change, novel approaches are needed for upregulating neuroprotective response and harnessing the reparative potential of demyelinating nerves. In this regard, molecular chaperones and neurosteroids offer promising therapeutic alternatives and may provide a powerful tool in improving myelin genesis and maintenance. Clearly, identifying these "druggable" molecular targets and endogenous mechanisms is of paramount impact on the long-term medical management of these diseases. However, caution must be taken while developing pharmacological regimens to modulate these molecules as they carry multiple physiological functions and non-specific intervention with other pathways can undermine the therapeutic effectiveness. For instance, since Hsp70 facilitates the antigen presentation and autoimmune response directed against myelin proteins (Mycko et al., 2004), induction of Hsp70 may stimulate the immunogenic aspect of this chaperone and increase the risk of MS-associated demyelination. Although above data clearly demonstrates that Hsp70 enhances the integrity of mature myelin, Hsp70 may impose an inhibitory regulation on the rate and/or extent of developmental myelination since depletion of this chaperone in Hsp70 knockout sensory nerves increased the level of basal myelin formation compared to same-aged WT nerves (Figure 3.3.3). In line with this, Hsp70 gene transcription is significantly upregulated during early phase of myelination (postnatal day 5) (Patzig et al., 2011), when active transition of promyelinating SCs

into myelinating SCs occurs (Svaren and Meijer, 2008). Future studies should determine whether such postnatal, temporal elevation of Hsp70 serves to diverge the umyelinating SCs from the myelinating fate and/or to regulate appropriate timing and rate of myelination, as elucidating these events may yield insightful application of Hsp70 intervention in treating developmental deficits associated with peripheral myelin. Outside the nervous system, evidence is also accumulating that increasing Hsp70 enhances cell growth and tumorigenesis (Patton et al., 1995). Overstimulation of the pro-survival HSR could promote development of malignant phenotypes and interfere with the chemotherapeutic treatment. On the contrary, although Hsp90 inhibitors upregulate HSR, their utility as neuroprotective agents is antagonized by induction of Hsp90 client protein degradation and necessitates efficient dissociation of neuroprotection from cytotoxicity. Owing to the above-mentioned versatility of Hsp70 funciton, the extent and specificity of chaperone modulation in treating demyelinating neuropathies require careful consideration before its translational potential can be realized.

While the present study supports that increasing Hsp70 inhibits altered neuregulinism-induced peripheral demyelination and improves myelinated fiber function in diabetes, it does not negate nor exclude the intersection of Hsp70 with other neuropathic changes and biochemical insults underlying the development of DPN. In fact, we have published the findings that KU-32 protected unmyelinated, embryonic sensory neurons from glucose-induced death, reversed the loss and improved the innervation of unmyelinated, plantar, intra-epidermal nerve fibers in diabetic mice (Urban et al., 2010; Urban et al., 2012). The decrease in neurodegenerative aspects of DPN by KU-32 is paralleled by increased cytosolic and mitochondrial Hsp70 paralogs, attenuated oxidative stress and improved mitochondrial energetics; the last two have been established as central pathogenetic components in DPN. Thus, chaperone induction is

pharmacologically beneficial in upregulating a broad neuroprotective response and protecting both myelinated and unmyelinated fiber function and understanding how “stress proteins” may antagonize these diabetes-induced biochemical and organellar stress will not only facilitate developing a novel mono- or conjunctional therapy for the neurodegenerative complication of diabetes but also reveal some of the pathogenetic aspects of DPN.

Appendix

PARP-1 and Hsp70 induction

As the master regulator of HSR, HSF-1 activates HSP gene expression by recruiting transcriptional coactivator complex such as P-TEFb (positive transcription elongation factor b) to the Hsp70 promoter (Lis et al., 2000; Park et al., 2001). Additionally, HSF-1 is necessary to activate poly(ADP-ribose) polymerase-1(PARP-1) enzymatic activity whereby it promotes its release from the promoter region and redistribution through Hsp70 loci upon HS (Petesch and Lis, 2012). The clearance of PARP-1 from the promoter appears to be indispensable for full activation of the inducible Hsp70.1 since genetic deletion of PARP-1 significantly impaired the ability of HS to activate Hsp70 gene expression (Martin et al., 2009). Given that Hsp90 inhibitors are proposed to recapitulate heat stress by inducing the dissociation of HSF-1 from Hsp90 sequestration, we therefore investigated the involvement of PARP-1 in the neuroprotective effect of KU-32. Since it has been previously demonstrated that HS-induced removal of PARP-1 from Hsp70 promoter is mediated through PARP-1 sumoylation and subsequent clearance (Martin et al., 2009), we first validated that KU-32 reduced nuclear content of full length PARP-1 in HEK-293 cells (Figure A1B). Further, KU-32 failed to enhance Hsp70 expression in DRG explants established from PARP-1-deficient mice at the same concentration to which WT cultures responded with about 4 fold induction (Figure A2). It is also worth mentioning that PARP-1 depletion increased the basal expression of Hsp70 and Hsp60 as compared to WT. This is in accordance with the notion that PARP-1 represses HSP

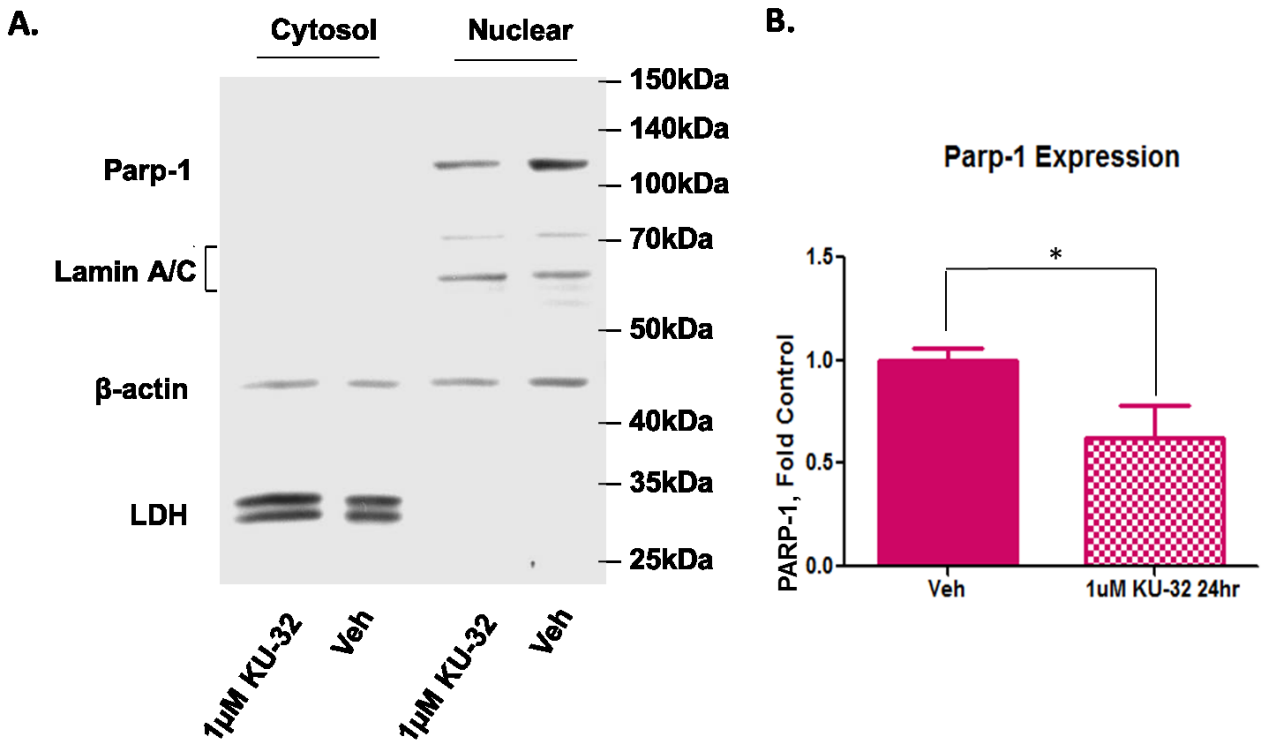

Figure Al: KU-32 promotes PARP-1 degradation in HEK-293 cells. A) HEK-293 cells were treated with either 0.05% DMSO or 1μM KU-32 for 24 hr. Cells were then collected and lysates were subfractionated to separate and obtain the nuclear and cytosolic fractions. Fractions were then analyzed through electrophoresis and PARP-1 protein contents were assessed by immunoblotting using monoclonal antibody against PARP-1. **B)** Data were repeated 4 times. One-way ANOVA indicates a significant difference in Parp-1 expression between veh and 1μM KU-32-treated groups [$F_{(1,6)}$=4.207; p<0.05]. Tukey's post-hoc test indicates *p<0.05 for 24hr KU-32 *vs.* Veh, df=1, n=4.

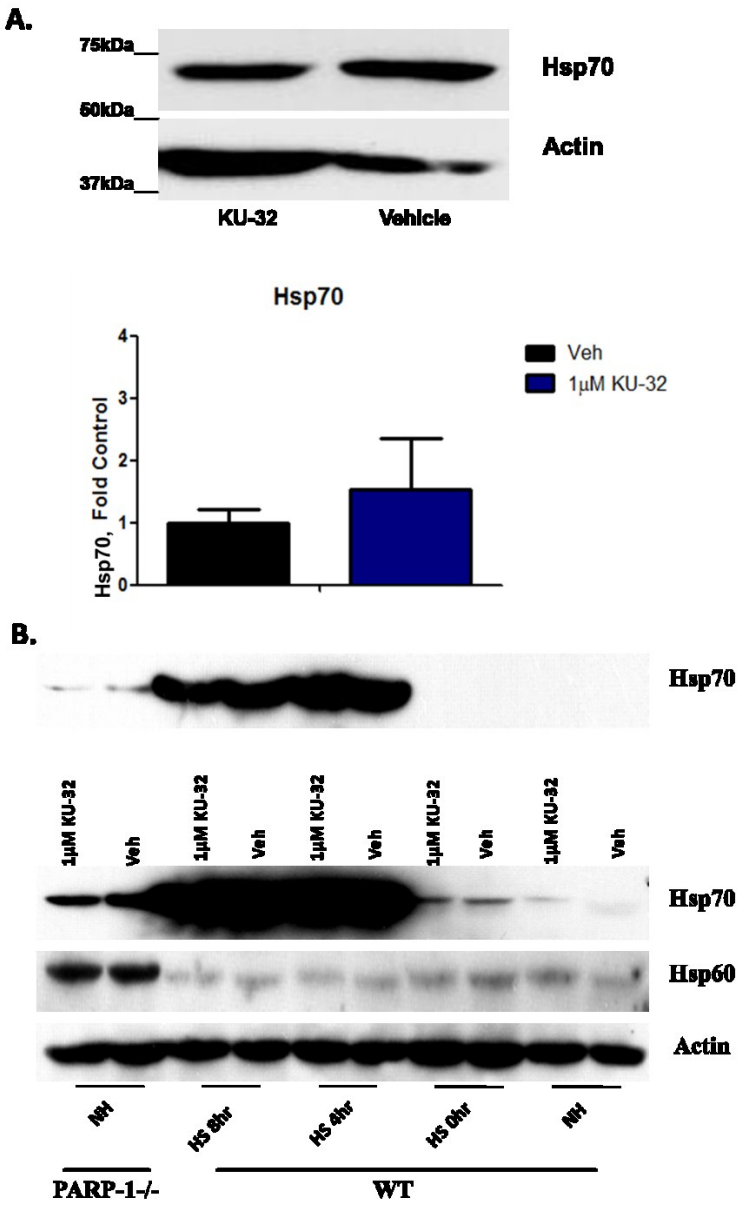

Figure A2 PARP-1 deficiency abolishes Hsp70 induction by KU-32. DRG/SC explants from PARP-1$^{-/-}$ mice were treated with vehicle or KU-32 for 24hr, or HS for 30 min plus appropriate recovery time as indicated above. Hsp70 and Hsp60 expression was examined by immunoblotting. No statistical difference in Hsp70 expression was found between vehicle and KU-32-treated PARP-1$^{-/-}$ cells. Bar graph quantification was generated from 3 independent experiments. One-way ANOVA detected no significant change in Hsp70 expression between veh and KU-32-treated groups [$F_{(1,6)}$=0.901; p=0.892]. df=1, n=4 **A)**. Basal expression of Hsp70 and Hsp60 in PARP-1$^{-/-}$ DRGs were significantly higher compared to WT vehicle-treated cultures in the absence of HS. Top blot demonstrates shorter exposure of X-ray film to chemiluminescence activity conjugated to Hsp70 antibody **B)**. β-actin was blotted as loading control. NH: no heatshock.

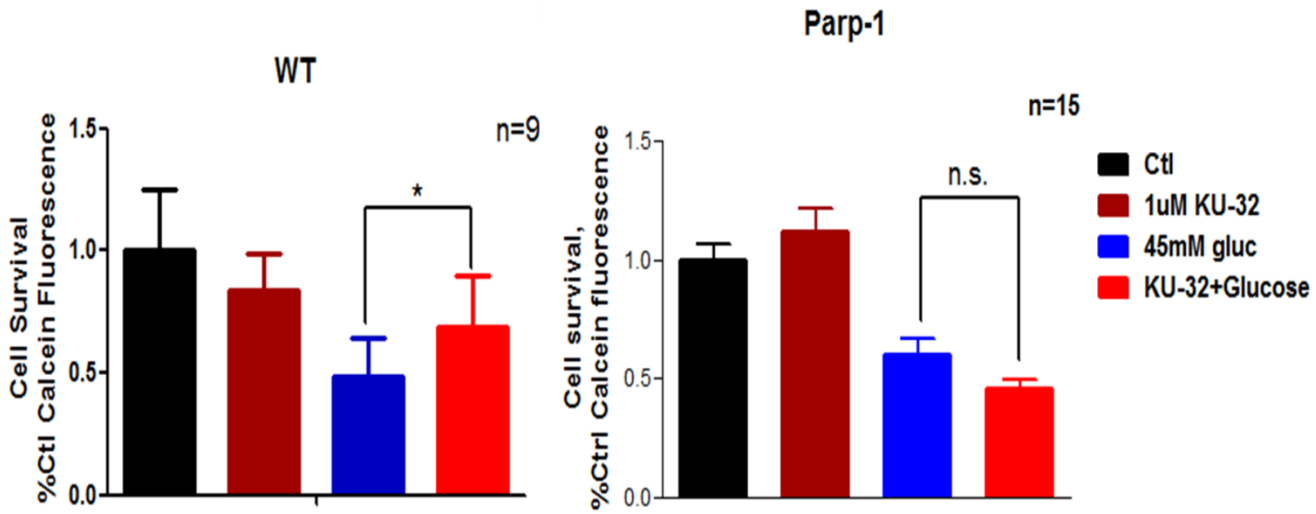

Figure A3 PARP-1 is required by KU-32 to protect unmyelinated sensory nerves against glucose neurotoxicity. DRG explants isolated from neonatal WT or PARP-1-/- mice were plated onto tissue culture plates at equal density and immediately treated with antimitotics to remove proliferating fibroblasts for 1 day. Cultures were pretreated with vehicle or KU-32 overnight (16hr) and maintained in medium containing 25mM glucose prior to 4hr high glucose stress (45mM). calcein AM (The acetomethoxy derivate of calcein) were then incubated with cells for 30 min to label live cells. The number of viable cells is proportional to the fluorescence intensity reading of calcein and normalized to total protein concentration in each well. Results were presented in arithmetic mean±SD and expressed as fold of untreated control. 45mM glucose caused ~50% cell death in both WT and PARP-1 KO DRGs. KU-32 improved cell survival in WT cultures by ~25% whereas elicited no significant change in the rate of cell survival in PARP-1-/- DRGs. One-way ANOVA analysis indicates a significant difference in cell survival in both WT [$F_{(3,32)}$=3.960; p<0.05] and Parp-1-/- [$F_{(3,56)}$=1.012; p<0.01]. Tukey's post-hoc test indicates *p<0.05 for Glucose *vs.* KU-32+Glucose. n.s. denotes no statistical difference. df=3.

promoter activation at quiescent state. Further, pretreatment of 1μM KU-32 overnight alleviated hyperglycemia-induced cell death in WT DRG explants (Figure A3). However, no improvement in neural survival was observed in PARP-1-/- DRGs treated with KU-32. Therefore, above results support a critical role of PARP-1 in mediating the effect of KU-32 in protecting unmyelinated nerves against hyperglycemic insult in diabetes. To test directly the hypothesis that Parp-1 is indispensable for the drug efficacy, we sought to determine whether Parp-1 gene

deletion affects myelin protection. Unfortunately, this is hindered by the inate defect in myelin formation of DRG explants extracted from PARP-1-/- mice (Figure A4) (Plane et al., 2012).

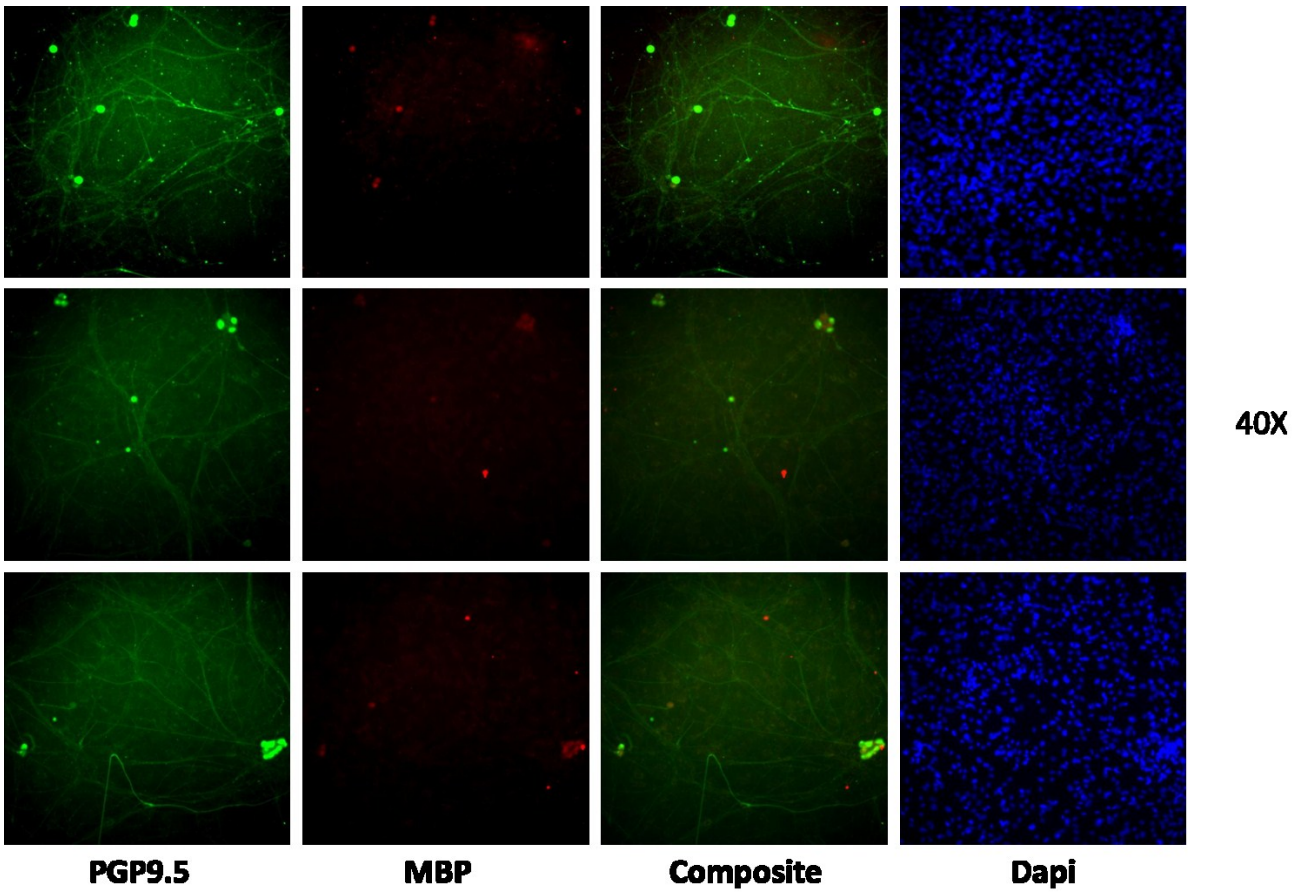

Figure A4 Genetic deletion of PARP-1 abolishes sensory nerve myelination *in vitro*. As with WT, neonatal DRG/SC explants were isolated from PARP-1-/- mice pups and induced to myelinate by addition of ascorbic acid after removal of fibroblasts. After 3-4 weeks, cells were immunostained with PGP9.5 and MBP for examination of myelin internodes. Despite the abundance of neurons and SCs in the culture, no compact myelin was formed. Experiments were performed 3 times and no myelination was observed.

Reference

Acs P, Kipp M, Norkute A, Johann S, Clarner T, Braun A, Berente Z, Komoly S and Beyer C (2009) 17beta-estradiol and progesterone prevent cuprizone provoked demyelination of corpus callosum in male mice. *Glia* **57**:807-814.

Adlkofer K, Martini R, Aguzzi A, Zielasek J, Toyka KV and Suter U (1995) Hypermyelination and demyelinating peripheral neuropathy in Pmp22-deficient mice. *Nat Genet* **11**:274-280.

Akude E, Zherebitskaya E, Roy Chowdhury SK, Girling K and Fernyhough P (2010) 4-Hydroxy-2-nonenal induces mitochondrial dysfunction and aberrant axonal outgrowth in adult sensory neurons that mimics features of diabetic neuropathy. *Neurotox Res* **17**:28-38.

Anand P, Terenghi G, Warner G, Kopelman P, Williams-Chestnut RE and Sinicropi DV (1996) The role of endogenous nerve growth factor in human diabetic neuropathy. *Nat Med* **2**:703-707.

Andrews H, White K, Thomson C, Edgar J, Bates D, Griffiths I, Turnbull D and Nichols P (2006) Increased axonal mitochondrial activity as an adaptation to myelin deficiency in the Shiverer mouse. *J Neurosci Res* **83**:1533-1539.

Ansar S, Burlison JA, Hadden MK, Yu XM, Desino KE, Bean J, Neckers L, Audus KL, Michaelis ML and Blagg BS (2007) A non-toxic Hsp90 inhibitor protects neurons from Abeta-induced toxicity. *Bioorg Med Chem Lett* **17**:1984-1990.

Apfel SC (2002) Nerve growth factor for the treatment of diabetic neuropathy: what went wrong, what went right, and what does the future hold? *Int Rev Neurobiol* **50**:393-413.

Apfel SC, Schwartz S, Adornato BT, Freeman R, Biton V, Rendell M, Vinik A, Giuliani M, Stevens JC, Barbano R and Dyck PJ (2000) Efficacy and safety of recombinant human nerve growth factor in patients with diabetic polyneuropathy: A randomized controlled trial. rhNGF Clinical Investigator Group. *Jama* **284**:2215-2221.

Aquino DA, Peng D, Lopez C and Farooq M (1998) The constitutive heat shock protein-70 is required for optimal expression of myelin basic protein during differentiation of oligodendrocytes. *Neurochem Res* **23**:413-420.

Arbuthnott ER, Boyd IA and Kalu KU (1980) Ultrastructural dimensions of myelinated peripheral nerve fibres in the cat and their relation to conduction velocity. *J Physiol* **308**:125-157.

Arvanitis DN, Wang H, Bagshaw RD, Callahan JW and Boggs JM (2004) Membrane-associated estrogen receptor and caveolin-1 are present in central nervous system myelin and oligodendrocyte plasma membranes. *J Neurosci Res* **75**:603-613.

Asbury AK, Arnason BG and Adams RD (1969) The inflammatory lesion in idiopathic polyneuritis. Its role in pathogenesis. *Medicine (Baltimore)* **48**:173-215.

Atanasoski S, Scherer SS, Sirkowski E, Leone D, Garratt AN, Birchmeier C and Suter U (2006) ErbB2 signaling in Schwann cells is mostly dispensable for maintenance of myelinated peripheral nerves and proliferation of adult Schwann cells after injury. *J Neurosci* **26**:2124-2131.

Balice-Gordon RJ, Bone LJ and Scherer SS (1998) Functional gap junctions in the schwann cell myelin sheath. *J Cell Biol* **142**:1095-1104.

Baynes JW (2002) Glycation and Advanced Glycation Reactions, in *Textbook of Diabetic Neuropathy* (F.Arnold Gries, Cameron NE, Low PA and Ziegler D eds) pp 105-112, Thieme, Stuttgart
New York.

Bebo BF, Jr., Fyfe-Johnson A, Adlard K, Beam AG, Vandenbark AA and Offner H (2001) Low-dose estrogen therapy ameliorates experimental autoimmune encephalomyelitis in two different inbred mouse strains. *J Immunol* **166**:2080-2089.

Behse F, Buchthal F and Carlsen F (1977) Nerve biopsy and conduction studies in diabetic neuropathy. *J Neurol Neurosurg Psychiatry* **40**:1072-1082.

Bergoffen J, Scherer SS, Wang S, Scott MO, Bone LJ, Paul DL, Chen K, Lensch MW, Chance PF and Fischbeck KH (1993) Connexin mutations in X-linked Charcot-Marie-Tooth disease. *Science* **262**:2039-2042.

Berthold CH (1968) Ultrastructure of postnatally developing feline peripheral nodes of Ranvier. *Acta Soc Med Ups* **73**:145-168.

Bhat MA, Rios JC, Lu Y, Garcia-Fresco GP, Ching W, St Martin M, Li J, Einheber S, Chesler M, Rosenbluth J, Salzer JL and Bellen HJ (2001) Axon-glia interactions and the domain organization of myelinated axons requires neurexin IV/Caspr/Paranodin. *Neuron* **30**:369-383.

Bhatheja K and Field J (2006) Schwann cells: origins and role in axonal maintenance and regeneration. *Int J Biochem Cell Biol* **38**:1995-1999.

Bienemann AS, Lee YB, Howarth J and Uney JB (2008) Hsp70 suppresses apoptosis in sympathetic neurones by preventing the activation of c-Jun. *J Neurochem* **104**:271-278.

Boiko T, Rasband MN, Levinson SR, Caldwell JH, Mandel G, Trimmer JS and Matthews G (2001) Compact myelin dictates the differential targeting of two sodium channel isoforms in the same axon. *Neuron* **30**:91-104.

Bossy-Wetzel E, Bakiri L and Yaniv M (1997) Induction of apoptosis by the transcription factor c-Jun. *Embo J* **16**:1695-1709.

Boulton AJ and Malik RA (1998) Diabetic neuropathy. *The Medical clinics of North America* **82**:909-929.

Boulware MI, Kordasiewicz H and Mermelstein PG (2007) Caveolin proteins are essential for distinct effects of membrane estrogen receptors in neurons. *J Neurosci* **27**:9941-9950.

Boyden KM (2000) The pathophysiology of demyelination and the ionic basis of nerve conduction in multiple sclerosis: an overview. *J Neurosci Nurs* **32**:49-53, 60.

Boyle ME, Berglund EO, Murai KK, Weber L, Peles E and Ranscht B (2001) Contactin orchestrates assembly of the septate-like junctions at the paranode in myelinated peripheral nerve. *Neuron* **30**:385-397.

Brann DW, Dhandapani K, Wakade C, Mahesh VB and Khan MM (2007) Neurotrophic and neuroprotective actions of estrogen: basic mechanisms and clinical implications. *Steroids* **72**:381-405.

Britsch S, Li L, Kirchhoff S, Theuring F, Brinkmann V, Birchmeier C and Riethmacher D (1998) The ErbB2 and ErbB3 receptors and their ligand, neuregulin-1, are essential for development of the sympathetic nervous system. *Genes Dev* **12**:1825-1836.

Brodal P (2010) *The Central Nervous System: Structure and Function*, Oxford University Press, New York.

Brown MJ, Iwamori M, Kishimoto Y, Rapoport B, Moser HW and Asbury AK (1979) Nerve lipid abnormalities in human diabetic neuropathy: a correlative study. *Annals of neurology* **5**:245-252.

Brownlee M and Cerami A (1981) The biochemistry of the complications of diabetes mellitus. *Annu Rev Biochem* **50**:385-432.

Bruzzone R, White TW and Paul DL (1996) Connections with connexins: the molecular basis of direct intercellular signaling. *Eur J Biochem* **238**:1-27.

Bunge MB, Bunge RP and Pappas GD (1962) Electron microscopic demonstration of connections between glia and myelin sheaths in the developing mammalian central nervous system. *J Cell Biol* **12**:448-453.

Buonanno A and Fischbach GD (2001) Neuregulin and ErbB receptor signaling pathways in the nervous system. *Curr Opin Neurobiol* **11**:287-296.

Burlison JA, Neckers L, Smith AB, Maxwell A and Blagg BS (2006) Novobiocin: redesigning a DNA gyrase inhibitor for selective inhibition of hsp90. *J Am Chem Soc* **128**:15529-15536.

Cannella B, Hoban CJ, Gao YL, Garcia-Arenas R, Lawson D, Marchionni M, Gwynne D and Raine CS (1998) The neuregulin, glial growth factor 2, diminishes autoimmune demyelination and enhances

remyelination in a chronic relapsing model for multiple sclerosis. *Proc Natl Acad Sci U S A* **95**:10100-10105.

Canto C, Pich S, Paz JC, Sanches R, Martinez V, Orpinell M, Palacin M, Zorzano A and Guma A (2007) Neuregulins increase mitochondrial oxidative capacity and insulin sensitivity in skeletal muscle cells. *Diabetes* **56**:2185-2193.

Carroll SL, Miller ML, Frohnert PW, Kim SS and Corbett JA (1997) Expression of neuregulins and their putative receptors, ErbB2 and ErbB3, is induced during Wallerian degeneration. *J Neurosci* **17**:1642-1659.

Cermenati G, Abbiati F, Cermenati S, Brioschi E, Volonterio A, Cavaletti G, Saez E, De Fabiani E, Crestani M, Garcia-Segura LM, Melcangi RC, Caruso D and Mitro N (2012) Diabetes-induced myelin abnormalities are associated with an altered lipid pattern: protective effects of LXR activation. *J Lipid Res* **53**:300-310.

Chan JR, Cosgaya JM, Wu YJ and Shooter EM (2001) Neurotrophins are key mediators of the myelination program in the peripheral nervous system. *Proc Natl Acad Sci U S A* **98**:14661-14668.

Charles P, Tait S, Faivre-Sarrailh C, Barbin G, Gunn-Moore F, Denisenko-Nehrbass N, Guennoc AM, Girault JA, Brophy PJ and Lubetzki C (2002) Neurofascin is a glial receptor for the paranodin/Caspr-contactin axonal complex at the axoglial junction. *Curr Biol* **12**:217-220.

Chen S, Rio C, Ji RR, Dikkes P, Coggeshall RE, Woolf CJ and Corfas G (2003) Disruption of ErbB receptor signaling in adult non-myelinating Schwann cells causes progressive sensory loss. *Nat Neurosci* **6**:1186-1193.

Chen S, Velardez MO, Warot X, Yu ZX, Miller SJ, Cros D and Corfas G (2006) Neuregulin 1-erbB signaling is necessary for normal myelination and sensory function. *J Neurosci* **26**:3079-3086.

Cheng HL, Russell JW and Feldman EL (1999) IGF-I promotes peripheral nervous system myelination. *Ann N Y Acad Sci* **883**:124-130.

Cheng HT, Dauch JR, Hayes JM, Hong Y and Feldman EL (2009) Nerve growth factor mediates mechanical allodynia in a mouse model of type 2 diabetes. *J Neuropathol Exp Neurol* **68**:1229-1243.

Cheng HT, Dauch JR, Hayes JM, Yanik BM and Feldman EL (2012) Nerve growth factor/p38 signaling increases intraepidermal nerve fiber densities in painful neuropathy of type 2 diabetes. *Neurobiol Dis* **45**:280-287.

Cheng HT, Dauch JR, Oh SS, Hayes JM, Hong Y and Feldman EL (2010) p38 mediates mechanical allodynia in a mouse model of type 2 diabetes. *Mol Pain* **6**:28.

Chini B and Parenti M (2004) G-protein coupled receptors in lipid rafts and caveolae: how, when and why do they go there? *J Mol Endocrinol* **32**:325-338.

Chiosis G, Huezo H, Rosen N, Mimnaugh E, Whitesell L and Neckers L (2003) 17AAG: low target binding affinity and potent cell activity--finding an explanation. *Mol Cancer Ther* **2**:123-129.

Chopra JS, Hurwitz LJ and Montgomery DA (1969) The pathogenesis of sural nerve changes in diabetes mellitus. *Brain* **92**:391-418.

Chopra JS, Sawhney BB and Chakravorty RN (1977) Pathology and time relationship of peripheral nerve changes in experimental diabetes. *J Neurol Sci* **32**:53-67.

Chung J, Nguyen AK, Henstridge DC, Holmes AG, Chan MH, Mesa JL, Lancaster GI, Southgate RJ, Bruce CR, Duffy SJ, Horvath I, Mestril R, Watt MJ, Hooper PL, Kingwell BA, Vigh L, Hevener A and Febbraio MA (2008) HSP72 protects against obesity-induced insulin resistance. *Proc Natl Acad Sci U S A* **105**:1739-1744.

Clarke EC and O'Malley CD (1968) The Human Brain and Spinal Cord. *Berkely: University of Califormia Press*.

Coetzee T, Fujita N, Dupree J, Shi R, Blight A, Suzuki K and Popko B (1996) Myelination in the absence of galactocerebroside and sulfatide: normal structure with abnormal function and regional instability. *Cell* **86**:209-219.

Cooper EC and Jan LY (2003) M-channels: neurological diseases, neuromodulation, and drug development. *Arch Neurol* **60**:496-500.

Couers C and Hildebrand J (1965) Latent Neuropathy in Diabetes and Alcoholism: Electromyographic and Histological Study. *Neurology* **15**:19-38.

Crosby E, Humphrey T and Lauer E (1962) Correlative Anatomy of the Nervous System, in *Textbook of human and nonhuman primate neuroanatomy*, New York.

Cuervo AM, Stefanis L, Fredenburg R, Lansbury PT and Sulzer D (2004) Impaired degradation of mutant alpha-synuclein by chaperone-mediated autophagy. *Science* **305**:1292-1295.

Curry JJ, 3rd and Heim LM (1966) Brain myelination after neonatal administration of oestradiol. *Nature* **209**:915-916.

Cwiklinska H, Mycko MP, Luvsannorov O, Walkowiak B, Brosnan CF, Raine CS and Selmaj KW (2003) Heat shock protein 70 associations with myelin basic protein and proteolipid protein in multiple sclerosis brains. *Int Immunol* **15**:241-249.

D'Urso D, Brophy PJ, Staugaitis SM, Gillespie CS, Frey AB, Stempak JG and Colman DR (1990) Protein zero of peripheral nerve myelin: biosynthesis, membrane insertion, and evidence for homotypic interaction. *Neuron* **4**:449-460.

Danaei G, Finucane MM, Lu Y, Singh GM, Cowan MJ, Paciorek CJ, Lin JK, Farzadfar F, Khang YH, Stevens GA, Rao M, Ali MK, Riley LM, Robinson CA and Ezzati M (2011) National, regional, and global trends in fasting plasma glucose and diabetes prevalence since 1980: systematic analysis of health examination surveys and epidemiological studies with 370 country-years and 2.7 million participants. *Lancet*.

Debanne D, Campanac E, Bialowas A, Carlier E and Alcaraz G (2011) Axon physiology. *Physiol Rev* **91**:555-602.

Dickey CA, Kamal A, Lundgren K, Klosak N, Bailey RM, Dunmore J, Ash P, Shoraka S, Zlatkovic J, Eckman CB, Patterson C, Dickson DW, Nahman NS, Jr., Hutton M, Burrows F and Petrucelli L (2007) The high-affinity HSP90-CHIP complex recognizes and selectively degrades phosphorylated tau client proteins. *J Clin Invest* **117**:648-658.

Dix DJ, Allen JW, Collins BW, Poorman-Allen P, Mori C, Blizard DR, Brown PR, Goulding EH, Strong BD and Eddy EM (1997) HSP70-2 is required for desynapsis of synaptonemal complexes during meiotic prophase in juvenile and adult mouse spermatocytes. *Development* **124**:4595-4603.

Dobrowsky RT, Rouen S and Yu C (2005) Altered neurotrophism in diabetic neuropathy: spelunking the caves of peripheral nerve. *J Pharmacol Exp Ther* **313**:485-491.

Donnelly AC, Mays JR, Burlison JA, Nelson JT, Vielhauer G, Holzbeierlein J and Blagg BS (2008) The design, synthesis, and evaluation of coumarin ring derivatives of the novobiocin scaffold that exhibit antiproliferative activity. *J Org Chem* **73**:8901-8920.

Dupree JL, Coetzee T, Blight A, Suzuki K and Popko B (1998) Myelin galactolipids are essential for proper node of Ranvier formation in the CNS. *J Neurosci* **18**:1642-1649.

Dyck PJ, Lais A, Karnes JL, O'Brien P and Rizza R (1986) Fiber loss is primary and multifocal in sural nerves in diabetic polyneuropathy. *Ann Neurol* **19**:425-439.

Dzhashiashvili Y, Zhang Y, Galinska J, Lam I, Grumet M and Salzer JL (2007) Nodes of Ranvier and axon initial segments are ankyrin G-dependent domains that assemble by distinct mechanisms. *J Cell Biol* **177**:857-870.

Eckersley L (2002) Role of the Schwann cell in diabetic neuropathy. *Int Rev Neurobiol* **50**:293-321.

Edwards JL, Quattrini A, Lentz SI, Figueroa-Romero C, Cerri F, Backus C, Hong Y and Feldman EL (2010) Diabetes regulates mitochondrial biogenesis and fission in mouse neurons. *Diabetologia* **53**:160-169.

Ehrenberg CG (1837) Observations on the structure hitherto unknown of the nervous system in man and animals. *Edinburgh Medical and Surgical Journal* **48**:257-305.

Einheber S, Bhat MA and Salzer JL (2006) Disrupted Axo-Glial Junctions Result in Accumulation of Abnormal Mitochondria at Nodes of Ranvier. *Neuron Glia Biol* **2**:165-174.

Einheber S, Zanazzi G, Ching W, Scherer S, Milner TA, Peles E and Salzer JL (1997) The axonal membrane protein Caspr, a homologue of neurexin IV, is a component of the septate-like paranodal junctions that assemble during myelination. *J Cell Biol* **139**:1495-1506.

Ellis J (1987) Proteins as molecular chaperones. *Nature* **328**:378-379.

Eshed Y, Feinberg K, Poliak S, Sabanay H, Sarig-Nadir O, Spiegel I, Bermingham JR, Jr. and Peles E (2005) Gliomedin mediates Schwann cell-axon interaction and the molecular assembly of the nodes of Ranvier. *Neuron* **47**:215-229.

Esper RM, Pankonin MS and Loeb JA (2006) Neuregulins: versatile growth and differentiation factors in nervous system development and human disease. *Brain Res Rev* **51**:161-175.

Falls DL (2003) Neuregulins and the neuromuscular system: 10 years of answers and questions. *J Neurocytol* **32**:619-647.

Feinberg K, Eshed-Eisenbach Y, Frechter S, Amor V, Salomon D, Sabanay H, Dupree JL, Grumet M, Brophy PJ, Shrager P and Peles E (2010) A glial signal consisting of gliomedin and NrCAM clusters axonal Na+ channels during the formation of nodes of Ranvier. *Neuron* **65**:490-502.

Fex Svenningsen A and Kanje M (1999) Estrogen and progesterone stimulate Schwann cell proliferation in a sex- and age-dependent manner. *J Neurosci Res* **57**:124-130.

Filbin MT, Walsh FS, Trapp BD, Pizzey JA and Tennekoon GI (1990) Role of myelin P0 protein as a homophilic adhesion molecule. *Nature* **344**:871-872.

Franklin RJ and Ffrench-Constant C (2008) Remyelination in the CNS: from biology to therapy. *Nat Rev Neurosci* **9**:839-855.

Frei R, Motzing S, Kinkelin I, Schachner M, Koltzenburg M and Martini R (1999) Loss of distal axons and sensory Merkel cells and features indicative of muscle denervation in hindlimbs of P0-deficient mice. *J Neurosci* **19**:6058-6067.

Friede RL and Samorajski T (1967) Relation between the number of myelin lamellae and axon circumference in fibers of vagus and sciatic nerves of mice. *J Comp Neurol* **130**:223-231.

Gabai VL, Meriin AB, Yaglom JA, Volloch VZ and Sherman MY (1998) Role of Hsp70 in regulation of stress-kinase JNK: implications in apoptosis and aging. *FEBS Lett* **438**:1-4.

Garcia-Fresco GP (2006) The Molecular Organization and Function of Paranodal Septate Junctions, in *Neurobiology* p 178, University of North Carolina at Chapel Hill, Chapel Hill.

Garratt AN, Britsch S and Birchmeier C (2000a) Neuregulin, a factor with many functions in the life of a schwann cell. *Bioessays* **22**:987-996.

Garratt AN, Voiculescu O, Topilko P, Charnay P and Birchmeier C (2000b) A dual role of erbB2 in myelination and in expansion of the schwann cell precursor pool. *J Cell Biol* **148**:1035-1046.

Geren BB (1954) The formation fromthe Schwann cell suface of myelin in the peripheral nerves of chick embryos. *Exp Cell Res* **7**:558-562.

Geuna S, Raimondo S, Ronchi G, Scipio FD, Tos P, Czaja K and Fornaro M (2009) Histology of the Peripheral Nerve and Changes Occurring During Nerve Regeneration, in *Essays on Peripheral Nerve Repair and Regeneration* (Geuna S, Tos P and Battiston B eds) pp 28-41.

Giese KP, Martini R, Lemke G, Soriano P and Schachner M (1992) Mouse P0 gene disruption leads to hypomyelination, abnormal expression of recognition molecules, and degeneration of myelin and axons. *Cell* **71**:565-576.

Goel G, Guo M, Ding J, Dornbos D, 3rd, Ali A, Shenaq M, Guthikonda M and Ding Y (2010) Combined effect of tumor necrosis factor (TNF)-alpha and heat shock protein (HSP)-70 in reducing apoptotic injury in hypoxia: a cell culture study. *Neurosci Lett* **483**:162-166.

Gollan L, Salomon D, Salzer JL and Peles E (2003) Caspr regulates the processing of contactin and inhibits its binding to neurofascin. *J Cell Biol* **163**:1213-1218.

Greenbaum D, Richardson PC, Salmon MV and Urich H (1964) Pathological Observations on Six Cases of Diabetic Neuropathy. *Brain* **87**:201-214.

Griffin JW and Hoffman PN (1993) Degeneration and regeneration in the peripheral nervous system., in *Peripheral Neuropathy* (Dyck PJ, Thomas PK, Low PA and Poduslo JF eds) pp 361-276, W.B. Saunders, Philadelphia.

Griffin JW and Sheikh K (2004) Guillain-Barre Syndrome, in *Myelin Biology and Disorders* (Lazzarini RA ed) pp 887-904, Elsevier Academic Press.

Guertin AD, Zhang DP, Mak KS, Alberta JA and Kim HA (2005) Microanatomy of axon/glial signaling during Wallerian degeneration. *J Neurosci* **25**:3478-3487.

Gui C, Zhu L, Hu M, Lei L and Long Q (2012) Neuregulin-1/ErbB signaling is impaired in the rat model of diabetic cardiomyopathy. *Cardiovasc Pathol*.

Gupte AA, Bomhoff GL, Swerdlow RH and Geiger PC (2009) Heat treatment improves glucose tolerance and prevents skeletal muscle insulin resistance in rats fed a high-fat diet. *Diabetes* **58**:567-578.

Guzhova I, Kislyakova K, Moskaliova O, Fridlanskaya I, Tytell M, Cheetham M and Margulis B (2001) In vitro studies show that Hsp70 can be released by glia and that exogenous Hsp70 can enhance neuronal stress tolerance. *Brain Res* **914**:66-73.

Habib AA and Brannagan TH, 3rd (2010) Therapeutic strategies for diabetic neuropathy. *Current neurology and neuroscience reports* **10**:92-100.

Hahn AF, Ainsworth PJ, Bolton CF, Bilbao JM and Vallat JM (2001) Pathological findings in the x-linked form of Charcot-Marie-Tooth disease: a morphometric and ultrastructural analysis. *Acta Neuropathol* **101**:129-139.

Halliday AM and McDonald WI (1977) Pathophysiology of demyelinating disease. *Br Med Bull* **33**:21-27.

Ham J, Babij C, Whitfield J, Pfarr CM, Lallemand D, Yaniv M and Rubin LL (1995) A c-Jun dominant negative mutant protects sympathetic neurons against programmed cell death. *Neuron* **14**:927-939.

Harati Y (2010) Diabetic peripheral neuropathies. *Methodist DeBakey cardiovascular journal* **6**:15-19.

Harrisingh MC, Perez-Nadales E, Parkinson DB, Malcolm DS, Mudge AW and Lloyd AC (2004) The Ras/Raf/ERK signalling pathway drives Schwann cell dedifferentiation. *Embo J* **23**:3061-3071.

Hellweg R and Hartung HD (1990) Endogenous levels of nerve growth factor (NGF) are altered in experimental diabetes mellitus: a possible role for NGF in the pathogenesis of diabetic neuropathy. *J Neurosci Res* **26**:258-267.

Hellweg R, Raivich G, Hartung HD, Hock C and Kreutzberg GW (1994) Axonal transport of endogenous nerve growth factor (NGF) and NGF receptor in experimental diabetic neuropathy. *Exp Neurol* **130**:24-30.

Henderson VW (2006) Estrogen-containing hormone therapy and Alzheimer's disease risk: understanding discrepant inferences from observational and experimental research. *Neuroscience* **138**:1031-1039.

Herbert KR, Samali A and Gorman A (2007) The Role of Hsps in Neuronal Differentiation and Development., in *Heat Shock Proteins in Neural Cells* (Richter-Landsberg C ed) pp 25-37, Landes Bioscience and Springer Science+Business Media.

Herzog RI, Cummins TR, Ghassemi F, Dib-Hajj SD and Waxman SG (2003) Distinct repriming and closed-state inactivation kinetics of Nav1.6 and Nav1.7 sodium channels in mouse spinal sensory neurons. *J Physiol* **551**:741-750.

Hock MB and Kralli A (2009) Transcriptional control of mitochondrial biogenesis and function. *Annu Rev Physiol* **71**:177-203.

Homma S, Jin X, Wang G, Tu N, Min J, Yanasak N and Mivechi NF (2007) Demyelination, astrogliosis, and accumulation of ubiquitinated proteins, hallmarks of CNS disease in hsf1-deficient mice. *J Neurosci* **27**:7974-7986.

Honke K, Hirahara Y, Dupree J, Suzuki K, Popko B, Fukushima K, Fukushima J, Nagasawa T, Yoshida N, Wada Y and Taniguchi N (2002) Paranodal junction formation and spermatogenesis require sulfoglycolipids. *Proc Natl Acad Sci U S A* **99**:4227-4232.

Hooper PL (1999) Hot-tub therapy for type 2 diabetes mellitus. *N Engl J Med* **341**:924-925.

Hooper PL (2003) Diabetes, nitric oxide, and heat shock proteins. *Diabetes Care* **26**:951-952.

Horresh I, Bar V, Kissil JL and Peles E (2010) Organization of myelinated axons by Caspr and Caspr2 requires the cytoskeletal adapter protein 4.1B. *J Neurosci* **30**:2480-2489.

Huijbregts RP, Roth KA, Schmidt RE and Carroll SL (2003) Hypertrophic neuropathies and malignant peripheral nerve sheath tumors in transgenic mice overexpressing glial growth factor beta3 in myelinating Schwann cells. *J Neurosci* **23**:7269-7280.

Hunt C and Morimoto RI (1985) Conserved features of eukaryotic hsp70 genes revealed by comparison with the nucleotide sequence of human hsp70. *Proc Natl Acad Sci U S A* **82**:6455-6459.

Hunt CR, Dix DJ, Sharma GG, Pandita RK, Gupta A, Funk M and Pandita TK (2004) Genomic instability and enhanced radiosensitivity in Hsp70.1- and Hsp70.3-deficient mice. *Mol Cell Biol* **24**:899-911.

Hur J, Sullivan KA, Pande M, Hong Y, Sima AA, Jagadish HV, Kretzler M and Feldman EL (2011) The identification of gene expression profiles associated with progression of human diabetic neuropathy. *Brain* **134**:3222-3235.

Hutton EJ, Carty L, Laura M, Houlden H, Lunn MP, Brandner S, Mirsky R, Jessen K and Reilly MM (2011) c-Jun expression in human neuropathies: a pilot study. *J Peripher Nerv Syst* **16**:295-303.

Hwang JR, Zhang C and Patterson C (2005) C-terminus of heat shock protein 70-interacting protein facilitates degradation of apoptosis signal-regulating kinase 1 and inhibits apoptosis signal-regulating kinase 1-dependent apoptosis. *Cell Stress Chaperones* **10**:147-156.

Ip YT and Davis RJ (1998) Signal transduction by the c-Jun N-terminal kinase (JNK)--from inflammation to development. *Curr Opin Cell Biol* **10**:205-219.

Isom LL (2002) The role of sodium channels in cell adhesion. *Front Biosci* **7**:12-23.

Jaattela M and Wissing D (1992) Emerging role of heat shock proteins in biology and medicine. *Annals of medicine* **24**:249-258.

Jakobsen J, Brimijoin S, Skau K, Sidenius P and Wells D (1981) Retrograde axonal transport of transmitter enzymes, fucose-labeled protein, and nerve growth factor in streptozotocin-diabetic rats. *Diabetes* **30**:797-803.

Jung-Testas I and Baulieu EE (1998) Steroid hormone receptors and steroid action in rat glial cells of the central and peripheral nervous system. *J Steroid Biochem Mol Biol* **65**:243-251.

Jung-Testas I, Renoir M, Bugnard H, Greene GL and Baulieu EE (1992) Demonstration of steroid hormone receptors and steroid action in primary cultures of rat glial cells. *J Steroid Biochem Mol Biol* **41**:621-631.

Kaarniranta K, Oksala N, Karjalainen HM, Suuronen T, Sistonen L, Helminen HJ, Salminen A and Lammi MJ (2002) Neuronal cells show regulatory differences in the hsp70 gene response. *Brain Res Mol Brain Res* **101**:136-140.

Kalman B, Lublin FD and Alder H (1997) Impairment of central and peripheral myelin in mitochondrial diseases. *Mult Scler* **2**:267-278.

Kamal A, Thao L, Sensintaffar J, Zhang L, Boehm MF, Fritz LC and Burrows FJ (2003) A high-affinity conformation of Hsp90 confers tumour selectivity on Hsp90 inhibitors. *Nature* **425**:407-410.

Kamholz J, Awatramani R, Menichella D, Jiang H, Xu W and Shy M (1999) Regulation of myelin-specific gene expression. Relevance to CMT1. *Ann N Y Acad Sci* **883**:91-108.

Kaminska B (2009) Molecular characterization of inflammation-induced JNK/c-Jun signaling pathway in connection with tumorigenesis. *Methods Mol Biol* **512**:249-264.

Kamiya H, Zhang W and Sima AA (2006) Degeneration of the Golgi and neuronal loss in dorsal root ganglia in diabetic BioBreeding/Worcester rats. *Diabetologia* **49**:2763-2774.

Kearney JA, Buchner DA, De Haan G, Adamska M, Levin SI, Furay AR, Albin RL, Jones JM, Montal M, Stevens MJ, Sprunger LK and Meisler MH (2002) Molecular and pathological effects of a modifier gene on deficiency of the sodium channel Scn8a (Na(v)1.6). *Hum Mol Genet* **11**:2765-2775.

Kelly MJ, Qiu J and Ronnekleiv OK (2005) Estrogen signaling in the hypothalamus. *Vitam Horm* **71**:123-145.

Kelly S and Yenari MA (2002) Neuroprotection: heat shock proteins. *Current medical research and opinion* **18 Suppl 2**:s55-60.

Kim HP, Lee JY, Jeong JK, Bae SW, Lee HK and Jo I (1999) Nongenomic stimulation of nitric oxide release by estrogen is mediated by estrogen receptor alpha localized in caveolae. *Biochem Biophys Res Commun* **263**:257-262.

Kitamura C, Ogawa Y, Nishihara T, Morotomi T and Terashita M (2003) Transient co-localization of c-Jun N-terminal kinase and c-Jun with heat shock protein 70 in pulp cells during apoptosis. *J Dent Res* **82**:91-95.

Klucken J, Shin Y, Masliah E, Hyman BT and McLean PJ (2004) Hsp70 Reduces alpha-Synuclein Aggregation and Toxicity. *J Biol Chem* **279**:25497-25502.

Kong MM, Hasbi A, Mattocks M, Fan T, O'Dowd BF and George SR (2007) Regulation of D1 dopamine receptor trafficking and signaling by caveolin-1. *Mol Pharmacol* **72**:1157-1170.

Kramer R, Bucay N, Kane DJ, Martin LE, Tarpley JE and Theill LE (1996) Neuregulins with an Ig-like domain are essential for mouse myocardial and neuronal development. *Proc Natl Acad Sci U S A* **93**:4833-4838.

Kuhn J, Dina OA, Goswami C, Suckow V, Levine JD and Hucho T (2008) GPR30 estrogen receptor agonists induce mechanical hyperalgesia in the rat. *Eur J Neurosci* **27**:1700-1709.

Kurthy M, Mogyorosi T, Nagy K, Kukorelli T, Jednakovits A, Talosi L and Biro K (2002) Effect of BRX-220 against peripheral neuropathy and insulin resistance in diabetic rat models. *Ann N Y Acad Sci* **967**:482-489.

Kusunoki S, Hitoshi S, Kaida K, Arita M and Kanazawa I (1999) Monospecific anti-GD1b IgG is required to induce rabbit ataxic neuropathy. *Ann Neurol* **45**:400-403.

Lajtha A, Toth J, Fujimoto K and Agrawal HC (1977) Turnover of myelin proteins in mouse brain in vivo. *Biochem J* **164**:323-329.

Landon DN and Williams PL (1963) Ultrastructure of the Node of Ranvier. *Nature* **199**:575-577.

Lascelles RG and Thomas PK (1966) Changes due to age in internodal length in the sural nerve in man. *J Neurol Neurosurg Psychiatry* **29**:40-44.

Law AJ, Lipska BK, Weickert CS, Hyde TM, Straub RE, Hashimoto R, Harrison PJ, Kleinman JE and Weinberger DR (2006) Neuregulin 1 transcripts are differentially expressed in schizophrenia and regulated by 5' SNPs associated with the disease. *Proc Natl Acad Sci U S A* **103**:6747-6752.

Lee JS, Lee JJ and Seo JS (2005) HSP70 deficiency results in activation of c-Jun N-terminal Kinase, extracellular signal-regulated kinase, and caspase-3 in hyperosmolarity-induced apoptosis. *J Biol Chem* **280**:6634-6641.

Leimeroth R, Lobsiger C, Lussi A, Taylor V, Suter U and Sommer L (2002) Membrane-bound neuregulin1 type III actively promotes Schwann cell differentiation of multipotent Progenitor cells. *Dev Biol* **246**:245-258.

Lemaillet G, Walker B and Lambert S (2003) Identification of a conserved ankyrin-binding motif in the family of sodium channel alpha subunits. *J Biol Chem* **278**:27333-27339.

Li C and Dobrowsky RT (2012) Targeting Molecular Chaperones in Diabetic Peripheral Neuropathy., in *Peripheral Neuropathy - Advances in Diagnostic and Therapeutic Approaches* (Hayat G ed) pp 39-62, InTech.

Li GC and Werb Z (1982) Correlation between synthesis of heat shock proteins and development of thermotolerance in Chinese hamster fibroblasts. *Proc Natl Acad Sci U S A* **79**:3218-3222.

Li WW, Penderis J, Zhao C, Schumacher M and Franklin RJ (2006) Females remyelinate more efficiently than males following demyelination in the aged but not young adult CNS. *Exp Neurol* **202**:250-254.

Li X, Lynn BD, Olson C, Meier C, Davidson KG, Yasumura T, Rash JE and Nagy JI (2002) Connexin29 expression, immunocytochemistry and freeze-fracture replica immunogold labelling (FRIL) in sciatic nerve. *Eur J Neurosci* **16**:795-806.

Lindquist S (1986) The heat-shock response. *Annu Rev Biochem* **55**:1151-1191.

Lis JT, Mason P, Peng J, Price DH and Werner J (2000) P-TEFb kinase recruitment and function at heat shock loci. *Genes Dev* **14**:792-803.

Liu P, Rudick M and Anderson RG (2002) Multiple functions of caveolin-1. *J Biol Chem* **277**:41295-41298.

Lund BT, Chakryan Y, Ashikian N, Mnatsakanyan L, Bevan CJ, Aguilera R, Gallaher T and Jakowec MW (2006) Association of MBP peptides with Hsp70 in normal appearing human white matter. *J Neurol Sci* **249**:122-134.

Luo W, Dou F, Rodina A, Chip S, Kim J, Zhao Q, Moulick K, Aguirre J, Wu N, Greengard P and Chiosis G (2007) Roles of heat-shock protein 90 in maintaining and facilitating the neurodegenerative phenotype in tauopathies. *Proc Natl Acad Sci U S A* **104**:9511-9516.

Luo W, Rodina A and Chiosis G (2008) Heat shock protein 90: translation from cancer to Alzheimer's disease treatment? *BMC Neurosci* **9 Suppl 2**:S7.

Luoma JI, Boulware MI and Mermelstein PG (2008) Caveolin proteins and estrogen signaling in the brain. *Mol Cell Endocrinol* **290**:8-13.

Mahmood D, Singh BK and Akhtar M (2009) Diabetic neuropathy: therapies on the horizon. *The Journal of pharmacy and pharmacology* **61**:1137-1145.

Mangurten AB, Brader KR, Loos BM, Lee E, Quiroga AI, Bathori J, Lurain JR, Laszlo A and Phillips B (1997) Hsp70 and Hsc70 are preferentially expressed in differentiated epithelial cells in normal human endometrium and ectocervix. *Cell Stress Chaperones* **2**:168-174.

Manzerra P and Brown IR (1992) Expression of heat shock genes (hsp70) in the rabbit spinal cord: localization of constitutive and hyperthermia-inducible mRNA species. *J Neurosci Res* **31**:606-615.

Manzerra P, Rush SJ and Brown IR (1993) Temporal and spatial distribution of heat shock mRNA and protein (hsp70) in the rabbit cerebellum in response to hyperthermia. *J Neurosci Res* **36**:480-490.

Marchionni MA, Cannella B, Hoban C, Gao YL, Garcia-Arenas R, Lawson D, Happel E, Noel F, Tofilon P, Gwynne D and Raine CS (1999) Neuregulin in neuron/glial interactions in the central nervous system. GGF2 diminishes autoimmune demyelination, promotes oligodendrocyte progenitor expansion, and enhances remyelination. *Adv Exp Med Biol* **468**:283-295.

Marcuccilli CJ, Mathur SK, Morimoto RI and Miller RJ (1996) Regulatory differences in the stress response of hippocampal neurons and glial cells after heat shock. *J Neurosci* **16**:478-485.

Marcus J and Popko B (2002) Galactolipids are molecular determinants of myelin development and axo-glial organization. *Biochim Biophys Acta* **1573**:406-413.

Martin N, Schwamborn K, Schreiber V, Werner A, Guillier C, Zhang XD, Bischof O, Seeler JS and Dejean A (2009) PARP-1 transcriptional activity is regulated by sumoylation upon heat shock. *Embo J* **28**:3534-3548.

Massa R, Palumbo C, Cavallaro T, Panico MB, Bei R, Terracciano C, Rizzuto N, Bernardi G and Modesti A (2006) Overexpression of ErbB2 and ErbB3 receptors in Schwann cells of patients with Charcot-Marie-tooth disease type 1A. *Muscle Nerve* **33**:342-349.

Maturana HR (1960) The fine anatomy of the optic nerve of anurans--an electron microscope study. *J Biophys Biochem Cytol* **7**:107-120.

Maurel P and Salzer JL (2000a) Axonal regulation of Schwann cell proliferation and survival and the initial events of myelination requires PI 3-kinase activity. *J Neurosci* **20**:4635-4645.

Maurel P and Salzer JL (2000b) Axonal regulation of Schwann cell proliferation and survival and the initial events of myelination requires PI 3-kinase activity. *J Neurosci* **20**:4635-4645.

Mayer MP and Bukau B (2005) Hsp70 chaperones: cellular functions and molecular mechanism. *Cell Mol Life Sci* **62**:670-684.

McAllister CE, Creech RD, Kimball PA, Muma NA and Li Q (2012) GPR30 is necessary for estradiol-induced desensitization of 5-HT(1A) receptor signaling in the paraventricular nucleus of the rat hypothalamus. *Psychoneuroendocrinology*.

McGuire JF, Rouen S, Siegfreid E, Wright DE and Dobrowsky RT (2009) Caveolin-1 and altered neuregulin signaling contribute to the pathophysiological progression of diabetic peripheral neuropathy. *Diabetes* **58**:2677-2686.

Meier C, Dermietzel R, Davidson KG, Yasumura T and Rash JE (2004) Connexin32-containing gap junctions in Schwann cells at the internodal zone of partial myelin compaction and in Schmidt-Lanterman incisures. *J Neurosci* **24**:3186-3198.

Melcangi RC, Azcoitia I, Ballabio M, Cavarretta I, Gonzalez LC, Leonelli E, Magnaghi V, Veiga S and Garcia-Segura LM (2003) Neuroactive steroids influence peripheral myelination: a promising opportunity for preventing or treating age-dependent dysfunctions of peripheral nerves. *Prog Neurobiol* **71**:57-66.

Menegoz M, Gaspar P, Le Bert M, Galvez T, Burgaya F, Palfrey C, Ezan P, Arnos F and Girault JA (1997) Paranodin, a glycoprotein of neuronal paranodal membranes. *Neuron* **19**:319-331.

Meriin AB, Gabai VL, Yaglom J, Shifrin VI and Sherman MY (1998) Proteasome inhibitors activate stress kinases and induce Hsp72. Diverse effects on apoptosis. *J Biol Chem* **273**:6373-6379.

Meyer D and Birchmeier C (1995) Multiple essential functions of neuregulin in development. *Nature* **378**:386-390.

Meyer D, Yamaai T, Garratt A, Riethmacher-Sonnenberg E, Kane D, Theill LE and Birchmeier C (1997) Isoform-specific expression and function of neuregulin. *Development* **124**:3575-3586.

Michailov GV, Sereda MW, Brinkmann BG, Fischer TM, Haug B, Birchmeier C, Role L, Lai C, Schwab MH and Nave KA (2004) Axonal neuregulin-1 regulates myelin sheath thickness. *Science* **304**:700-703.

Michels AA, Kanon B, Konings AW, Ohtsuka K, Bensaude O and Kampinga HH (1997) Hsp70 and Hsp40 chaperone activities in the cytoplasm and the nucleus of mammalian cells. *J Biol Chem* **272**:33283-33289.

Mikol DD, Hong HL, Cheng HL and Feldman EL (1999) Caveolin-1 expression in Schwann cells. *Glia* **27**:39-52.

Mikol DD, Scherer SS, Duckett SJ, Hong HL and Feldman EL (2002) Schwann cell caveolin-1 expression increases during myelination and decreases after axotomy. *Glia* **38**:191-199.

Minami Y, Hohfeld J, Ohtsuka K and Hartl FU (1996) Regulation of the heat-shock protein 70 reaction cycle by the mammalian DnaJ homolog, Hsp40. *J Biol Chem* **271**:19617-19624.

Mir KA, Pugazhendhi S, Paul MJ, Nair A and Ramakrishna BS (2009) Heat-shock protein 70 gene polymorphism is associated with the severity of diabetic foot ulcer and the outcome of surgical treatment. *The British journal of surgery* **96**:1205-1209.

Mitchell LS, Griffiths IR, Morrison S, Barrie JA, Kirkham D and McPhilemy K (1990) Expression of myelin protein gene transcripts by Schwann cells of regenerating nerve. *J Neurosci Res* **27**:125-135.

Mitterauer B (2007) The incoherence hypothesis of schizophrenia: based on decomposed oligodendrocyte-axonic relations. *Med Hypotheses* **69**:1299-1304.

Mizisin AP, Nelson RW, Sturges BK, Vernau KM, Lecouteur RA, Williams DC, Burgers ML and Shelton GD (2007) Comparable myelinated nerve pathology in feline and human diabetes mellitus. *Acta Neuropathol* **113**:431-442.

Mizisin AP and Powell HC (2003) Pathogenesis and Pathology of Diabetic Neuropathy, in *Textbook of Diabetic Neuropathy* (Gries FA, Low PA, Cameron NE and Ziegler D eds) pp 83-169, Thieme, New York.

Muchowski PJ and Wacker JL (2005) Modulation of neurodegeneration by molecular chaperones. *Nat Rev Neurosci* **6**:11-22.

Mycko MP, Cwiklinska H, Szymanski J, Szymanska B, Kudla G, Kilianek L, Odyniec A, Brosnan CF and Selmaj KW (2004) Inducible heat shock protein 70 promotes myelin autoantigen presentation by the HLA class II. *J Immunol* **172**:202-213.

Nakayama K, Furusu A, Xu Q, Konta T and Kitamura M (2001) Unexpected transcriptional induction of monocyte chemoattractant protein 1 by proteasome inhibition: involvement of the c-Jun N-terminal kinase-activator protein 1 pathway. *J Immunol* **167**:1145-1150.

Narhi M (2010) Dentinal and Pulpal Pain, in *Textbook of Endodontology* (Bergenholtz G ed) p 33, Wiley-Blackwell.

Nave KA (2010a) Myelination and support of axonal integrity by glia. *Nature* **468**:244-252.

Nave KA (2010b) Myelination and the trophic support of long axons. *Nat Rev Neurosci* **11**:275-283.

Nave KA and Salzer JL (2006) Axonal regulation of myelination by neuregulin 1. *Curr Opin Neurobiol* **16**:492-500.

Neurology E-RSGoCaEPi (1998) Guillain-Barre syndrome variants in Emilia-Romagna, Italy, 1992-3: incidence, clinical features, and prognosis. Emilia-Romagna Study Group on Clinical and Epidemiological Problems in Neurology. *J Neurol Neurosurg Psychiatry* **65**:218-224.

NIDDK (2009) What are diabetic neuropathies?, in *Diabetic Neuropathies: The Nerve Damage of Diabetes*, National Institutes of Diabetes and Digestive and Kidney Diseases.

Nikic I, Merkler D, Sorbara C, Brinkoetter M, Kreutzfeldt M, Bareyre FM, Bruck W, Bishop D, Misgeld T and Kerschensteiner M (2011) A reversible form of axon damage in experimental autoimmune encephalomyelitis and multiple sclerosis. *Nat Med* **17**:495-499.

Obrosova IG (2009) Diabetes and the peripheral nerve. *Biochim Biophys Acta* **1792**:931-940.

Obrosova IG, Drel VR, Oltman CL, Mashtalir N, Tibrewala J, Groves JT and Yorek MA (2007) Role of nitrosative stress in early neuropathy and vascular dysfunction in streptozotocin-diabetic rats. *Am J Physiol Endocrinol Metab* **293**:E1645-1655.

Ogata T, Iijima S, Hoshikawa S, Miura T, Yamamoto S, Oda H, Nakamura K and Tanaka S (2004) Opposing extracellular signal-regulated kinase and Akt pathways control Schwann cell myelination. *J Neurosci* **24**:6724-6732.

Ogawa-Goto K, Funamoto N, Ohta Y, Abe T and Nagashima K (1992) Myelin gangliosides of human peripheral nervous system: an enrichment of GM1 in the motor nerve myelin isolated from cauda equina. *J Neurochem* **59**:1844-1849.

Okamoto T, Schlegel A, Scherer PE and Lisanti MP (1998) Caveolins, a family of scaffolding proteins for organizing "preassembled signaling complexes" at the plasma membrane. *J Biol Chem* **273**:5419-5422.

Olsson Y, Save-Soderbergh J, Sourander P and Angervall L (1968) A patho-anatomical study of the central and peripheral nervous system in diabetes of early onset and long duration. *Pathol Eur* **3**:62-79.

Oomes PG, Jacobs BC, Hazenberg MP, Banffer JR and van der Meche FG (1995) Anti-GM1 IgG antibodies and Campylobacter bacteria in Guillain-Barre syndrome: evidence of molecular mimicry. *Ann Neurol* **38**:170-175.

Otsu N (1979) A threshold selection method from gray-level histograms. *IEEE Trans Sys Man Cyber*:62-66.

Ozaki K, Miura K, Tsuchitani M and Narama I (1996) Peripheral neuropathy in the spontaneously diabetic WBN/Kob rat. *Acta Neuropathol* **92**:603-607.

Palmada M, Kanwal S, Rutkoski NJ, Gustafson-Brown C, Johnson RS, Wisdom R and Carter BD (2002) c-jun is essential for sympathetic neuronal death induced by NGF withdrawal but not by p75 activation. *J Cell Biol* **158**:453-461.

Pan Z, Kao T, Horvath Z, Lemos J, Sul JY, Cranstoun SD, Bennett V, Scherer SS and Cooper EC (2006) A common ankyrin-G-based mechanism retains KCNQ and NaV channels at electrically active domains of the axon. *J Neurosci* **26**:2599-2613.

Park JM, Werner J, Kim JM, Lis JT and Kim YJ (2001) Mediator, not holoenzyme, is directly recruited to the heat shock promoter by HSF upon heat shock. *Mol Cell* **8**:9-19.

Parkinson DB, Bhaskaran A, Arthur-Farraj P, Noon LA, Woodhoo A, Lloyd AC, Feltri ML, Wrabetz L, Behrens A, Mirsky R and Jessen KR (2008) c-Jun is a negative regulator of myelination. *J Cell Biol* **181**:625-637.

Pasik P and Pasik T (2004) Cajal, Achucarro, Rio Hortega, and the Early Exploration of Neuroglia, in *Myelin Biology and Disorders* (Lazzarini R., Griffin J., Lassman H., Nave K., Miller R. and B. T eds) p xxiii, Elsevier Academic Press.

Patton WF, Erdjument-Bromage H, Marks AR, Tempst P and Taubman MB (1995) Components of the protein synthesis and folding machinery are induced in vascular smooth muscle cells by hypertrophic and hyperplastic agents. Identification by comparative protein phenotyping and microsequencing. *J Biol Chem* **270**:21404-21410.

Patzig J, Jahn O, Tenzer S, Wichert SP, de Monasterio-Schrader P, Rosfa S, Kuharev J, Yan K, Bormuth I, Bremer J, Aguzzi A, Orfaniotou F, Hesse D, Schwab MH, Mobius W, Nave KA and Werner HB (2011) Quantitative and integrative proteome analysis of peripheral nerve myelin identifies novel myelin proteins and candidate neuropathy loci. *J Neurosci* **31**:16369-16386.

Pavlik A and Aneja IS (2007) Cerebral neurons and glial cell types inducing heat shock protein Hsp70 following heat stress in the rat. *Prog Brain Res* **162**:417-431.

Pavlik A, Aneja IS, Lexa J and Al-Zoabi BA (2003) Identification of cerebral neurons and glial cell types inducing heat shock protein Hsp70 following heat stress in the rat. *Brain Res* **973**:179-189.

Pearson RJ, Jr. and Carroll SL (2004) ErbB transmembrane tyrosine kinase receptors are expressed by sensory and motor neurons projecting into sciatic nerve. *J Histochem Cytochem* **52**:1299-1311.

Penderis J, Woodruff RH, Lakatos A, Li WW, Dunning MD, Zhao C, Marchionni M and Franklin RJ (2003) Increasing local levels of neuregulin (glial growth factor-2) by direct infusion into areas of demyelination does not alter remyelination in the rat CNS. *Eur J Neurosci* **18**:2253-2264.

Pesaresi M, Giatti S, Calabrese D, Maschi O, Caruso D and Melcangi RC (2010) Dihydroprogesterone increases the gene expression of myelin basic protein in spinal cord of diabetic rats. *J Mol Neurosci* **42**:135-139.

Peters A (1960) The structure of myelin sheaths in the central nervous system of Xenopus laevis (Daudin). *J Biophys Biochem Cytol* **7**:121-126.

Peters A, Palay SL and HD W (1991) The fine structure of the nervous system., in *Oxford University Press* p 494, New York.

Peterson LB and Blagg BS (2009) To fold or not to fold: modulation and consequences of Hsp90 inhibition. *Future medicinal chemistry* **1**:267-283.

Petesch SJ and Lis JT (2012) Activator-induced spread of poly(ADP-ribose) polymerase promotes nucleosome loss at Hsp70. *Mol Cell* **45**:64-74.

Petrucelli L, Dickson D, Kehoe K, Taylor J, Snyder H, Grover A, De Lucia M, McGowan E, Lewis J, Prihar G, Kim J, Dillmann WH, Browne SE, Hall A, Voellmy R, Tsuboi Y, Dawson TM, Wolozin B, Hardy J and Hutton M (2004) CHIP and Hsp70 regulate tau ubiquitination, degradation and aggregation. *Hum Mol Genet* **13**:703-714.

Pieper AA, Blackshaw S, Clements EE, Brat DJ, Krug DK, White AJ, Pinto-Garcia P, Favit A, Conover JR, Snyder SH and Verma A (2000) Poly(ADP-ribosyl)ation basally activated by DNA strand breaks reflects glutamate-nitric oxide neurotransmission. *Proc Natl Acad Sci U S A* **97**:1845-1850.

Pillai AM, Thaxton C, Pribisko AL, Cheng JG, Dupree JL and Bhat MA (2009) Spatiotemporal ablation of myelinating glia-specific neurofascin (Nfasc NF155) in mice reveals gradual loss of paranodal axoglial junctions and concomitant disorganization of axonal domains. *J Neurosci Res* **87**:1773-1793.

Plane JM, Grossenbacher SK and Deng W (2012) PARP-1 deletion promotes subventricular zone neural stem cells toward a glial fate. *J Neurosci Res*.

Poliak S, Gollan L, Martinez R, Custer A, Einheber S, Salzer JL, Trimmer JS, Shrager P and Peles E (1999) Caspr2, a new member of the neurexin superfamily, is localized at the juxtaparanodes of myelinated axons and associates with K+ channels. *Neuron* **24**:1037-1047.

Poliak S, Salomon D, Elhanany H, Sabanay H, Kiernan B, Pevny L, Stewart CL, Xu X, Chiu SY, Shrager P, Furley AJ and Peles E (2003) Juxtaparanodal clustering of Shaker-like K+ channels in myelinated axons depends on Caspr2 and TAG-1. *J Cell Biol* **162**:1149-1160.

Privat A, Jacque C, Bourre JM, Dupouey P and Baumann N (1979) Absence of the major dense line in myelin of the mutant mouse "shiverer". *Neurosci Lett* **12**:107-112.

Prossnitz ER, Sklar LA, Oprea TI and Arterburn JB (2008) GPR30: a novel therapeutic target in estrogen-related disease. *Trends Pharmacol Sci* **29**:116-123.

Quarles RH, Macklin WB and Morrell P (2006) Myelin Formation, Structure and Biochemistry, in *Basic Neurochemistry: Molecular, Cellular and Medical Aspects* (Siegel GJ ed) p 52, Elsevier, Amsterdam, Boston, Heidelberg, London, New York, Oxford, Paris, San Diego, San Francisco, Singapore, Sydney, Tokyo.

Rangaraju S, Madorsky I, Pileggi JG, Kamal A and Notterpek L (2008) Pharmacological induction of the heat shock response improves myelination in a neuropathic model. *Neurobiol Dis* **32**:105-115.

Ratcliffe CF, Westenbroek RE, Curtis R and Catterall WA (2001) Sodium channel beta1 and beta3 subunits associate with neurofascin through their extracellular immunoglobulin-like domain. *J Cell Biol* **154**:427-434.

Rathmann W and Ward J (2003) Socioeconomic Aspects, in *Textbook of Diabetic Neuropathy* (Ziegler FAGNECPALD ed) pp 361-372, Georg Thieme Verlag, Stuttgart.

Razandi M, Oh P, Pedram A, Schnitzer J and Levin ER (2002) ERs associate with and regulate the production of caveolin: implications for signaling and cellular actions. *Mol Endocrinol* **16**:100-115.

Razani B, Engelman JA, Wang XB, Schubert W, Zhang XL, Marks CB, Macaluso F, Russell RG, Li M, Pestell RG, Di Vizio D, Hou H, Jr., Kneitz B, Lagaud G, Christ GJ, Edelmann W and Lisanti MP (2001) Caveolin-1 null mice are viable but show evidence of hyperproliferative and vascular abnormalities. *J Biol Chem* **276**:38121-38138.

Rees JH, Gregson NA and Hughes RA (1995) Anti-ganglioside GM1 antibodies in Guillain-Barre syndrome and their relationship to Campylobacter jejuni infection. *Ann Neurol* **38**:809-816.

Revankar CM, Cimino DF, Sklar LA, Arterburn JB and Prossnitz ER (2005) A transmembrane intracellular estrogen receptor mediates rapid cell signaling. *Science* **307**:1625-1630.

Rieger F, Pincon-Raymond M, Lombet A, Ponzio G, Lazdunski M and Sidman RL (1984) Paranodal dysmyelination and increase in tetrodotoxin binding sites in the sciatic nerve of the motor end-plate disease (med/med) mouse during postnatal development. *Dev Biol* **101**:401-409.

Rios JC, Melendez-Vasquez CV, Einheber S, Lustig M, Grumet M, Hemperly J, Peles E and Salzer JL (2000) Contactin-associated protein (Caspr) and contactin form a complex that is targeted to the paranodal junctions during myelination. *J Neurosci* **20**:8354-8364.

Ritossa F (1962) A new puffing pattern induced by temperature shock and DNP in drosophila., pp 571-573, Cellular And Molecular Life Sciences.

Rosenbluth J (1976) Intramembranous particle distribution at the node of Ranvier and adjacent axolemma in myelinated axons of the frog brain. *J Neurocytol* **5**:731-745.

Rosenbluth J (1999) A brief history of myelinated nerve fibers: one hundred and fifty years of controversy. *J Neurocytol* **28**:251-262.

Saher G, Quintes S, Mobius W, Wehr MC, Kramer-Albers EM, Brugger B and Nave KA (2009) Cholesterol regulates the endoplasmic reticulum exit of the major membrane protein P0 required for peripheral myelin compaction. *J Neurosci* **29**:6094-6104.

Saher G, Quintes S and Nave KA (2011) Cholesterol: a novel regulatory role in myelin formation. *Neuroscientist* **17**:79-93.

Saher G and Simons M (2010) Cholesterol and myelin biogenesis. *Subcell Biochem* **51**:489-508.

Said G, Slama G and Selva J (1983) Progressive centripetal degeneration of axons in small fibre diabetic polyneuropathy. *Brain* **106 (Pt 4)**:791-807.

Saito F, Moore SA, Barresi R, Henry MD, Messing A, Ross-Barta SE, Cohn RD, Williamson RA, Sluka KA, Sherman DL, Brophy PJ, Schmelzer JD, Low PA, Wrabetz L, Feltri ML and Campbell KP (2003) Unique role of dystroglycan in peripheral nerve myelination, nodal structure, and sodium channel stabilization. *Neuron* **38**:747-758.

Sajjad MU, Samson B and Wyttenbach A (2010) Heat shock proteins: therapeutic drug targets for chronic neurodegeneration? *Current pharmaceutical biotechnology* **11**:198-215.

Salehi AH, Morris SJ, Ho WC, Dickson KM, Doucet G, Milutinovic S, Durkin J, Gillard JW and Barker PA (2006) AEG3482 is an antiapoptotic compound that inhibits Jun kinase activity and cell death through induced expression of heat shock protein 70. *Chemistry & biology* **13**:213-223.

Salzer JL (2003) Polarized domains of myelinated axons. *Neuron* **40**:297-318.

Salzer JL, Brophy PJ and Peles E (2008) Molecular domains of myelinated axons in the peripheral nervous system. *Glia* **56**:1532-1540.

Sancho S, Magyar JP, Aguzzi A and Suter U (1999) Distal axonopathy in peripheral nerves of PMP22-mutant mice. *Brain* **122 (Pt 8)**:1563-1577.

Scherer SS and Salzer J (2001) Axon-Schwann cell interactions in peripheral nerve degeneration and regeneration., in *Glial Cell Development* (Jessen KR and Richardson WD eds) pp 299-330, Oxford University Press, Oxford.

Schumacher M, Guennoun R, Robert F, Carelli C, Gago N, Ghoumari A, Gonzalez Deniselle MC, Gonzalez SL, Ibanez C, Labombarda F, Coirini H, Baulieu EE and De Nicola AF (2004) Local synthesis and dual actions of progesterone in the nervous system: neuroprotection and myelination. *Growth Horm IGF Res* **14 Suppl A**:S18-33.

Segars JH and Driggers PH (2002) Estrogen action and cytoplasmic signaling cascades. Part I: membrane-associated signaling complexes. *Trends Endocrinol Metab* **13**:349-354.

Shah NM, Marchionni MA, Isaacs I, Stroobant P and Anderson DJ (1994) Glial growth factor restricts mammalian neural crest stem cells to a glial fate. *Cell* **77**:349-360.

Sharma KR, Cross J, Farronay O, Ayyar DR, Shebert RT and Bradley WG (2002) Demyelinating neuropathy in diabetes mellitus. *Arch Neurol* **59**:758-765.

Sheikh KA, Nachamkin I, Ho TW, Willison HJ, Veitch J, Ung H, Nicholson M, Li CY, Wu HS, Shen BQ, Cornblath DR, Asbury AK, McKhann GM and Griffin JW (1998) Campylobacter jejuni lipopolysaccharides in Guillain-Barre syndrome: molecular mimicry and host susceptibility. *Neurology* **51**:371-378.

Sherman DL, Tait S, Melrose S, Johnson R, Zonta B, Court FA, Macklin WB, Meek S, Smith AJ, Cottrell DF and Brophy PJ (2005) Neurofascins are required to establish axonal domains for saltatory conduction. *Neuron* **48**:737-742.

Shimura H, Schwartz D, Gygi SP and Kosik KS (2004) CHIP-Hsc70 complex ubiquitinates phosphorylated tau and enhances cell survival. *J Biol Chem* **279**:4869-4876.

Shy ME, Jani A, Krajewski K, Grandis M, Lewis RA, Li J, Shy RR, Balsamo J, Lilien J, Garbern JY and Kamholz J (2004) Phenotypic clustering in MPZ mutations. *Brain* **127**:371-384.

Si J, Wang Q and Mei L (1999) Essential roles of c-JUN and c-JUN N-terminal kinase (JNK) in neuregulin-increased expression of the acetylcholine receptor epsilon-subunit. *J Neurosci* **19**:8498-8508.

Sivieri S, Ferrarini AM, Lolli F, Mata S, Pinto F, Tavolato B and Gallo P (1997) Cytokine pattern in the cerebrospinal fluid from patients with GBS and CIDP. *J Neurol Sci* **147**:93-95.

Snider WD and Wright DE (1996) Neurotrophins cause a new sensation. *Neuron* **16**:229-232.

Soldan SS, Alvarez Retuerto AI, Sicotte NL and Voskuhl RR (2003) Immune modulation in multiple sclerosis patients treated with the pregnancy hormone estriol. *J Immunol* **171**:6267-6274.

Soti C, Nagy E, Giricz Z, Vigh L, Csermely P and Ferdinandy P (2005) Heat shock proteins as emerging therapeutic targets. *British journal of pharmacology* **146**:769-780.

Soti C, Racz A and Csermely P (2002) A Nucleotide-dependent molecular switch controls ATP binding at the C-terminal domain of Hsp90. N-terminal nucleotide binding unmasks a C-terminal binding pocket. *J Biol Chem* **277**:7066-7075.

Spritz N, Singh H and Marinan B (1975) Metabolism of peripheral nerve myelin in experimental diabetes. *J Clin Invest* **55**:1049-1056.

Stankiewicz M, Nikolay R, Rybin V and Mayer MP (2010) CHIP participates in protein triage decisions by preferentially ubiquitinating Hsp70-bound substrates. *Febs J* **277**:3353-3367.

Strokov IA, Manukhina EB, Bakhtina LY, Malyshev IY, Zoloev GK, Kazikhanova SI and Ametov AS (2000) The function of endogenous protective systems in patients with insulin-dependent diabetes mellitus and polyneuropathy: effect of antioxidant therapy. *Bulletin of experimental biology and medicine* **130**:986-990.

Sugimoto K, Yasujima M and Yagihashi S (2008) Role of advanced glycation end products in diabetic neuropathy. *Curr Pharm Des* **14**:953-961.

Svaren J and Meijer D (2008) The molecular machinery of myelin gene transcription in Schwann cells. *Glia* **56**:1541-1551.

Syed N, Reddy K, Yang DP, Taveggia C, Salzer JL, Maurel P and Kim HA (2010) Soluble neuregulin-1 has bifunctional, concentration-dependent effects on Schwann cell myelination. *J Neurosci* **30**:6122-6131.

Tahrani AA, Askwith T and Stevens MJ (2010) Emerging drugs for diabetic neuropathy. *Expert opinion on emerging drugs* **15**:661-683.

Taleghany N, Sarajari S, DonCarlos LL, Gollapudi L and Oblinger MM (1999) Differential expression of estrogen receptor alpha and beta in rat dorsal root ganglion neurons. *J Neurosci Res* **57**:603-615.

Tan W, Rouen S, Barkus KM, Dremina YS, Hui D, Christianson JA, Wright DE, Yoon SO and Dobrowsky RT (2003) Nerve growth factor blocks the glucose-induced down-regulation of caveolin-1 expression in Schwann cells via p75 neurotrophin receptor signaling. *J Biol Chem* **278**:23151-23162.

Tang CK and Lippman ME (1998) EGF Family Receptors and Their Ligands in Human Cancer, in *Hormones and Signaling* (O'Malley BW ed) pp 113-166, ACADEMIC PRESS.

Tasaki I (1939) The electro-saltatory transmission of the nerve impulse and the effect of narcosis upon the nerve fiber. *Am J Physiol* **127**:211-227.

Taveggia C, Zanazzi G, Petrylak A, Yano H, Rosenbluth J, Einheber S, Xu X, Esper RM, Loeb JA, Shrager P, Chao MV, Falls DL, Role L and Salzer JL (2005) Neuregulin-1 type III determines the ensheathment fate of axons. *Neuron* **47**:681-694.

Thi AD, Jung-Testas I and Baulieu EE (1998) Neuronal signals are required for estrogen-mediated induction of progesterone receptor in cultured rat Schwann cells. *J Steroid Biochem Mol Biol* **67**:201-211.

Thomas P, Pang Y, Filardo EJ and Dong J (2005) Identity of an estrogen membrane receptor coupled to a G protein in human breast cancer cells. *Endocrinology* **146**:624-632.

Thomas PK and Lascelles RG (1965) Schwann-Cell Abnormalities in Diabetic Neuropathy. *Lancet* **1**:1355-1357.

Tiwari-Woodruff S, Morales LB, Lee R and Voskuhl RR (2007) Differential neuroprotective and antiinflammatory effects of estrogen receptor (ER)alpha and ERbeta ligand treatment. *Proc Natl Acad Sci U S A* **104**:14813-14818.

Tomlinson DR and Gardiner NJ (2008) Glucose neurotoxicity. *Nat Rev Neurosci* **9**:36-45.

Traka M, Goutebroze L, Denisenko N, Bessa M, Nifli A, Havaki S, Iwakura Y, Fukamauchi F, Watanabe K, Soliven B, Girault JA and Karagogeos D (2003) Association of TAG-1 with Caspr2 is essential for the molecular organization of juxtaparanodal regions of myelinated fibers. *J Cell Biol* **162**:1161-1172.

Trapp BD and Kidd GJ (2004) Structure of the Myelinated Axon, in *Myelin Biology and Disorders* (Lazzarini RA ed) pp 3-27, Elsevier.

Tsuji M, Inanami O and Kuwabara M (2000) Neuroprotective effect of alpha-phenyl-N-tert-butylnitrone in gerbil hippocampus is mediated by the mitogen-activated protein kinase pathway and heat shock proteins. *Neurosci Lett* **282**:41-44.

Urban MJ, Li C, Yu C, Lu Y, Krise JM, McIntosh MP, Rajewski RA, Blagg BS and Dobrowsky RT (2010) Inhibiting heat-shock protein 90 reverses sensory hypoalgesia in diabetic mice. *ASN neuro* **2**.

Urban MJ, Pan P, Farmer KL, Zhao H, Blagg BS and Dobrowsky RT (2012) Modulating molecular chaperones improves sensory fiber recovery and mitochondrial function in diabetic peripheral neuropathy. *Exp Neurol*.

Valls-Canals J, Povedano M, Montero J and Pradas J (2002) Diabetic polyneuropathy. Axonal or demyelinating? *Electromyogr Clin Neurophysiol* **42**:3-6.

Veiga S, Leonelli E, Beelke M, Garcia-Segura LM and Melcangi RC (2006) Neuroactive steroids prevent peripheral myelin alterations induced by diabetes. *Neurosci Lett* **402**:150-153.

Verheijen MH, Camargo N, Verdier V, Nadra K, de Preux Charles AS, Medard JJ, Luoma A, Crowther M, Inouye H, Shimano H, Chen S, Brouwers JF, Helms JB, Feltri ML, Wrabetz L, Kirschner D, Chrast R and Smit AB (2009) SCAP is required for timely and proper myelin membrane synthesis. *Proc Natl Acad Sci U S A* **106**:21383-21388.

Vigh L, Literati PN, Horvath I, Torok Z, Balogh G, Glatz A, Kovacs E, Boros I, Ferdinandy P, Farkas B, Jaszlits L, Jednakovits A, Koranyi L and Maresca B (1997) Bimoclomol: a nontoxic, hydroxylamine derivative with stress protein-inducing activity and cytoprotective effects. *Nat Med* **3**:1150-1154.

Virchow R (1854) Über das ausgebreitete Vorkommen einer dem Nervenmark analogen Substanz in den tierischen Geweben. *Virchows Arch Pathol Anat*:562–572.

Viswanath I, Bajpai HS and Katiyar BC (1974) Electrophysiological studies in diabetes mellitus. *Neurol India* **22**:122-130.

Vital A, Ferrer X, Lagueny A, Vandenberghe A, Latour P, Goizet C, Canron MH, Louiset P, Petry KG and Vital C (2001) Histopathological features of X-linked Charcot-Marie-Tooth disease in 8 patients from 6 families with different connexin32 mutations. *J Peripher Nerv Syst* **6**:79-84.

Voss AK, Thomas T and Gruss P (2000) Mice lacking HSP90beta fail to develop a placental labyrinth. *Development* **127**:1-11.

Wang H, Kunkel DD, Martin TM, Schwartzkroin PA and Tempel BL (1993) Heteromultimeric K+ channels in terminal and juxtaparanodal regions of neurons. *Nature* **365**:75-79.

Wang JY, Miller SJ and Falls DL (2001) The N-terminal region of neuregulin isoforms determines the accumulation of cell surface and released neuregulin ectodomain. *J Biol Chem* **276**:2841-2851.

Wang Z, Jin H, Li C, Hou Y, Mei Q and Fan D (2009) Heat shock protein 72 protects kidney proximal tubule cells from injury induced by triptolide by means of activation of the MEK/ERK pathway. *Int J Toxicol* **28**:177-189.

Waza M, Adachi H, Katsuno M, Minamiyama M, Sang C, Tanaka F, Inukai A, Doyu M and Sobue G (2005) 17-AAG, an Hsp90 inhibitor, ameliorates polyglutamine-mediated motor neuron degeneration. *Nat Med* **11**:1088-1095.

Whitacre CC, Reingold SC and O'Looney PA (1999) A gender gap in autoimmunity. *Science* **283**:1277-1278.

Wild S, Roglic G, Green A, Sicree R and King H (2004) Global prevalence of diabetes: estimates for the year 2000 and projections for 2030. *Diabetes Care* **27**:1047-1053.

Wrabetz L, Feltri ML, Kleopa KA and Scherer SS (2004a) Inherited Neuropathies: Clinical, Genetic, and Biological Features, in *Myelin Biology and Disorders* (Lazzarini RA ed) pp 905-951, Elsevier Academic Press.

Wrabetz L, Feltri ML and Suter U (2004b) Models of Charcot–Marie–Tooth Disease., in *Myelin biology and disorders* (Lazzarini RA ed) pp 1143–1168, Elsevier Academic Press, San Diego, CA.

Yagihashi S and Matsunaga M (1979) Ultrastructural pathology of peripheral nerves in patients with diabetic neuropathy. *Tohoku J Exp Med* **129**:357-366.

Yang Y, Lacas-Gervais S, Morest DK, Solimena M and Rasband MN (2004) BetaIV spectrins are essential for membrane stability and the molecular organization of nodes of Ranvier. *J Neurosci* **24**:7230-7240.

Yarden Y and Sliwkowski MX (2001) Untangling the ErbB signalling network. *Nat Rev Mol Cell Biol* **2**:127-137.

Yu C, Rouen S and Dobrowsky RT (2008) Hyperglycemia and downregulation of caveolin-1 enhance neuregulin-induced demyelination. *Glia* **56**:877-887.

Yun CH, Yoon SY, Nguyen TT, Cho HY, Kim TH, Kim ST, Kim BC, Hong YS, Kim SJ and Lee HJ (2010) Geldanamycin inhibits TGF-beta signaling through induction of Hsp70. *Arch Biochem Biophys* **495**:8-13.

Zanazzi G, Einheber S, Westreich R, Hannocks MJ, Bedell-Hogan D, Marchionni MA and Salzer JL (2001) Glial growth factor/neuregulin inhibits Schwann cell myelination and induces demyelination. *J Cell Biol* **152**:1289-1299.

Zhang L, Zhao H, Blagg BS and Dobrowsky RT (2012) C-Terminal Heat Shock Protein 90 Inhibitor Decreases Hyperglycemia-induced Oxidative Stress and Improves Mitochondrial Bioenergetics in Sensory Neurons. *J Proteome Res* **11**:2581-2593.

Zhou L, Messing A and Chiu SY (1999) Determinants of excitability at transition zones in Kv1.1-deficient myelinated nerves. *J Neurosci* **19**:5768-5781.

Zhu TS and Glaser M (2008) Neuroprotection and enhancement of remyelination by estradiol and dexamethasone in cocultures of rat DRG neurons and Schwann cells. *Brain Res* **1206**:20-32.

Zochodne DW, Ramji N and Toth C (2008) Neuronal targeting in diabetes mellitus: a story of sensory neurons and motor neurons. *Neuroscientist* **14**:311-318.

Zoupi L, Savvaki M and Karagogeos D (2011) Axons and myelinating glia: An intimate contact. *IUBMB Life*.